TÉCNICO LISBOA

Modeling, simulation, and altitude control of a weather meteorological balloon

Thaynara Caminhas Oliveira

Thesis to obtain the Master of Science Degree in

Mechanical Engineering

Supervisors: Prof. Alexandra Bento Moutinho
Prof. José Raul Carreira Azinheira

Examination Committee

Chairperson: Prof. Carlos Baptista Cardeira
Supervisor: Prof. José Raul Carreira Azinheira
Members of the Committee: Prof. Duarte Pedro Mata de Oliveira Valério

December 2021

To the ones who inspire me.

Acknowledgments

This work was partially financed by national funds through the FCT – Fundação para a Ciência e Tecnologia, I.P., through the IDMEC under the project SONDA (PTDC/EME-SIS/1960/2020), and through the IDMEC under LAETA, project UIDB/50022/2020.

I would like to thank my professors, Alexandra Moutinho and José Raul Azinheira, for all the help and assistance during the process of this final step of my master's course. A general thank you to all professors who are responsible for sharing their knowledge with not just me but with many students every year, you are vital to the world.

To all my friends who have been with me and who went through this journey by my side, facing the same hardships and growth. A special thanks to Solange Santos, for being a great help and support during this phase, to Inês Saraiva for being with me in work and life all these years, and to Raquel Ferreira who was my biggest company in this final race.

My family, my life teachers, who loves me more than anyone and allowed me to choose and do what I thought was right, thank you for being so brave and teaching me how to be as well.

Resumo

Os balões meteorológicos são ferramentas importantes para o estudo e previsões de diferentes características meteorológicas como a humidade, vento, temperaturas e a pressão atmosférica. Estes balões, geralmente feitos em latex, deslocam-se livremente pela atmosfera através da força de impulsão, resultante da diferença entre a densidades do ar e do gás de elevação do balão. Com base na proposta do projeto SONDA, a ideia de controlo de altitude para um balão meteorológico foi desenvolvida. O projeto SONDA sugere que o balão seja controlado de forma a utilizar as correntes de vento presentes na atmosfera para que se direcione para zonas de interesse para pesquisa. O controlo de altitude de balões é um tema de pesquisa comum para balões de grande altitude, contudo, este estudo para balões de latex ainda não é uma área muito explorada. Desta forma, esta tese apresenta duas partes principais. A primeira destina-se a modelar um balão meteorológico. A modelação inicia-se com a definição das componentes materiais do balão, passa pela definição de um modelo atmosférico e, em seguida, a criação do modelo hiper-elástico do balão que modela a sua elasticidade de forma não linear é feita. Além destes modelos, um modelo térmico, um modelo do vento e o modelo da dinâmica foram, também, desenvolvidos. A segunda parte do projeto foi o desenvolvimento do controlo de altitude. O controlo foi feito através duma estratégia de controlo em cascata para executar controlo de velocidade e altitude. Por fim, o controlo de altitude e dinâmica livre do balão modelado foram simulados.

Palavras-chave: Balões meteorológicos, Modelação de balões, Controlo de altitude, Controlo de velocidade

Abstract

Weather balloons are important tools for the study and prediction of different meteorological characteristics such as humidity, wind, temperatures and atmospheric pressure. These balloons, usually made of latex, fly freely in the atmosphere through a buoyant force, resulting from the difference between the densities of air and the lifting gas of the balloon. Based on the SONDA project proposal, the idea of altitude control for a weather balloon was developed. This project suggests that the balloon's altitude should be controlled so it can exploit the wind currents present in the atmosphere using them as guidance to interest research areas. Balloon altitude control is a common research topic for high altitude balloons, however, for latex balloons, this study is not a very explored area. Thus, this thesis has two main parts. The first is to model a weather balloon. The modelling starts with the description of the main components of the balloon, then, the definition of an atmospheric model to represent the atmospheric conditions the balloon would face and the study of the nonlinear model representing the balloon's elasticity is done. In addition to these models, a thermal model, a wind model and a dynamics model were also developed. The second part of the project was the development of altitude control. Control was done through a cascade control strategy to perform speed and altitude control. Finally, the control of altitude and free dynamics of the modelled balloon were simulated.

Keywords: Weather Balloon, Balloon Modelling, Altitude Control, Velocity Control

Contents

List of Tables

List of Figures

Nomenclature

Greek symbols

α	Solar absorptivity coefficient.
α_{IR}	Solar absorptivity coefficient in the infrared spectrum.
η	Shear modulus.
γ	Adiabatic expansion coefficient
κ	Thermal conductivity coefficient.
κ_a, κ_g	Thermal conductivity coefficients for air and gas.
λ	Longitude.
μ_a, μ_g	Dynamic viscosity coefficients for air and gas.
ϕ	Latitude.
ψ	Elevation angle of the sun.
ρ_a, ρ_g, ρ_b	Atmosphere, gas and latex densities.
ρ_{g0}	Initial gas density.
σ	Stefan-Boltzmann coefficient.
τ	Transmissivity coefficient.
τ_{atm}	Atmosphere transmissivity coefficient.
τ_{atmIR}	Atmosphere transmissivity coefficient in the infrared spectrum.
τ_{IR}	Transmissivity coefficient in the infrared spectrum.
ε	Emissivity.
ε_{ground}	Ground emissivity.

Roman symbols

$\mathbf{A}, \mathbf{B}, \mathbf{C}, \mathbf{D}$	State-space matrices of a linear model.

$\mathbf{K}$	Controller gain matrix.
$\mathbf{P}$	Solution of the Algebraic Riccati Equation for the Linear Quadratic Regulator controller.
$\mathbf{Q}, \mathbf{R}$	Weighting matrices for the Linear Quadratic Regulator controller.
$\mathbf{x}, \mathbf{u}, \mathbf{y}, \mathbf{w}, \mathbf{v}$	State, input, output, perturbation and noise vectors.
A_p	Projected area.
A_s	Surface area.
$AirMass$	Air mass factor.
$Albedo$	Albedo coefficient.
C_D	Drag coefficient.
c_f	Specific heat (rubber).
C_m	Virtual mass coefficient.
c_v	Specific heat (helium).
D	Balloon diameter.
Day_{number}	Days past since the beginning of the year.
$Days_{PerYear}$	Number of days per year.
E_{Sun}	Solar constant.
F_B	Buoyancy force.
F_{Dx}	Drag force in direction x.
F_{Dy}	Drag force in direction y.
F_{Dz}	Drag force in direction z.
F_D	Drag force.
F_G	Weight force.
Gr_a, Gr_g	Grashof numbers for air and gas.
He_{forced}	Convection coefficient for forced convection.
He_{free}	Convection coefficient for free convection.
H_e, H_i	Convection coefficients for external and internal convection.
I_{SunZ}	Solar irradiance flux at altitude z.
I_{Sun}	Solar irradiance flux.

J_m	Locking/Stiffening constant.
L	Lift.
m_b	Balloon film mass.
m_t	Total mass.
m_{cil}	Cylinder mass.
m_{g0}	Initial mass of gas.
m_g	Mass of gas.
M_{He}	Molar mass of helium.
m_p	Payload mass.
m_{valve}	Valve mass.
m_v	Virtual mass.
MA	Mean anomaly of the sun.
n	Number of moles.
Nu_{forced}	Nusselt number for forced convection.
Nu_{free}	Nusselt number for free convection.
Nu_i	Nusselt number for internal convection.
O_{NED}	Centrer of NED reference frame.
P_a, P_g	Atmospheric and gas pressures.
P_{in}	Inside pressure.
P_{out}	Outside pressure.
Pr_a, Pr_g	Prantdl numbers for air and gas.
Q_{Albedo}	Total heat from albedo.
q_{Albedo}	Albedo flux.
$Q_{ConvExt}$	Total heat from external convection.
$Q_{ConvInt}$	Total heat from internal convection.
$Q_{IREarth}$	Total heat from infrared radiation.
$q_{IREarth}$	Longwave radiation flux from ground at the balloon altitude z.
Q_{IRfilm}	Total heat from infrared self-glow.

Q_{IRout}	Total heat from film emissions.
Q_{Sun}	Total heat from direct solar radiation.
q_{Sun}	Direct solar flux.
R	Balloon radius.
r	Reflection coefficient.
R_0	Uninflated balloon radius.
R_g	Perfect gases constant.
R_i	Initial balloon radius at launch.
R_{Earth}	Earth radius.
r_{IR}	Reflection coefficient in the infrared spectrum.
R_{max}	Maximum balloon radius before it bursts.
Re	Reynolds number.
s_-, s_+	Elastic coefficients.
t_0	Thickness of the uninflated balloon.
T_a, T_f, T_g	Atmosphere, balloon film and gas temperatures.
T_{ground}	Ground temperature.
TA	True anomaly of the sun.
V	Balloon volume.
v	Velocity.
V_0	Initial volume.
v_z, v_{wx}, v_{wy}	Vertical, longitudinal and latitudinal velocities.
v_{ax}	Component x of the aerodynamic velocity.
v_{ay}	Component y of the aerodynamic velocity.
v_a	Aerodynamic velocity.
v_x	Component x of the absolute velocity of the balloon.
v_y	Component y of the absolute velocity of the balloon.
v_z	Component z of the absolute velocity of the balloon.
VF	View factor.

x, y, z	NED components.
z	Altitude.
k_h, k_v	Altitude and velocity gains, respectively.
a	Acceleration.
g	Acceleration of gravity.

Subscripts

0	At instant zero.
a	Atmospheric related parameters.
cil	Cylinder related parameters.
e	External.
$Earth$	Earth related parameters.
f	Balloon film related parameters.
$forced$	Forced component.
$free$	Free component.
g	Gas related parameters.
i	Internal.
IR	Infrared.
j	Instant j.
max	Maximum value.
p	Payload.
ref	Reference condition.
t	Total.
v	Virtual mass related parameters.
$valve$	Valve related parameters.
wx	Longitudinal component of the wind.
wy	Latitudinal component of the wind.
x, y, z	Cartesian components.

Superscripts

T	Transpose.

Glossary

ECEF	Earth-Centred Earth-Fixed reference frame.
GFS	Global Forecasting System.
GPS	Global Positioning System.
LLA	Latitude, Longitude and Altitude. Definition of the position in the Geodetic reference frame.
LQR	Linear Quadratic Regulator.
MIR	Montgolfier Infrared.
NED	North, East, Down reference frame.
NOAA	National Oceanic and Atmospheric Association.
NOMADS	NOAA Operational Model Archive and Distribution System.
SONDA	Synchronous Oceanic and Atmospheric Data Acquisition project.
SP	Super Pressure.
ZP	Zero Pressure.

1 Introduction

This work begins with an introduction to the theme, in which the motivation behind the work is explained, as well as some overview on the ballooning history, types and control altitude mechanisms. The main objectives, achievements and composition (outline) of this work are also presented in this chapter.

1.1 Motivation

Weather balloons are very useful and important tools for the meteorology field. They are launched from about 900 locations around the world, two times every day, to collect information on temperature, humidity, and winds at various levels in the atmosphere [1]. Remaining as an indispensable tool in atmospheric science, meteorology and other applications requiring stratospheric observations, they also became a low-cost alternative for meteorological research since maintenance and repair of satellites cannot be provided without extremely expensive equipment. Having their lift by buoyancy force, these balloons require much less power than traditional aircraft and satellites [2]. Despite its benefits, the weather balloon behaviour is dependent on the wind and atmospheric conditions, being difficult to accurately predict the trajectory and duration of the flight. Therefore, altitude control is a major area of interest within the weather balloon field for meteorological data acquisition. Controlling the flight, leading the weather balloon to a reference altitude, is a difficult task since the flight is highly disturbed by different aspects of the atmosphere.

In this context, the Synchronous Oceanic and Atmospheric Data Acquisition (SONDA) project, illustrated by Figure 1.1, intends to contribute to better atmospheric and oceanic monitoring by proposing the development of a complementary system to the existing observation means. This system brings innovation using probes to investigate the atmosphere and oceans and a weather balloon as the probes' carrier. This low-cost solution with high cargo capability travels passively through the atmosphere to reach targeted areas, but with low positional accuracy. The work through this thesis addresses the development of a control solution to allow the weather balloon to have some positioning capability, by controlling its altitude in agreement with the available wind currents. The development of this work intends to bring new perspectives to the ballooning field and solve different problems than just atmospheric data acquisition. One of the many creative ways to use controlled weather balloons is proposed by "Project SONDA".

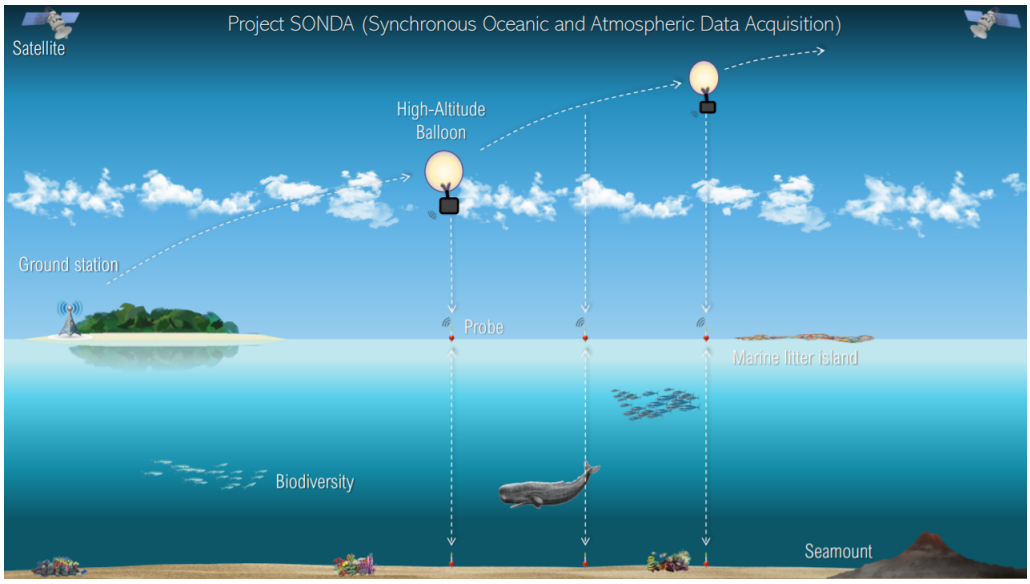

Figure 1.1: Illustration of the project SONDA. A project to study the atmosphere and the ocean using a probe coupled in a weather balloon (FCT funded project SONDA (PTDC/EME-SIS/1960/2020)).

1.2 Scientific Ballooning and its Applications

The scientific balloon has occupied a vital place in stratospheric flight. The stratospheric environment around the altitude of 20 km is quite complex [3]. In recent years, with the rapid development in mathematics or computer science, many studies have been carried out to survey the flight performance of scientific balloons. A meteorological balloon flight, as Figure 1.2 illustrates, usually carries a balloon envelope, a recovery parachute and a payload. The payload can contain different equipment, such as cameras, GPS receivers, radio transmitters and different sensors, such as thermometers or barometers, to carry out specific atmospheric measurements.

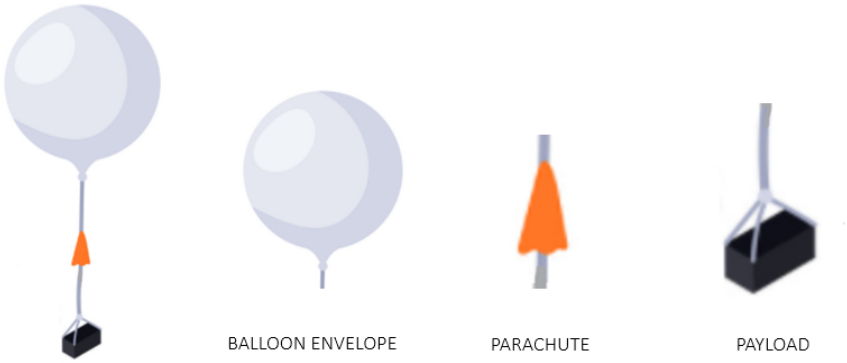

Figure 1.2: Weather balloon usual components.

1.2.1 Short History of Ballooning

Early Ballooning

In 1786 Etienne and Joseph Montgolfier started experiments with hydrogen-filled paper bags. Their first idea suggested that the buoyant force should cause the ascent of such bags if the lifting gas was lighter than the air. However, when the launch was made the bags fell due to the diffusion of the gas. After this attempt, they experimented with the particular 'gas' produced by the combustion of a mixture of moistened straw and wool so that a gas lighter than air could be produced. With a successful attempt of flying almost 2000 m, the hot-air balloon was created. The first experiment with a hydrogen filled balloon was made by the Robert brothers and Charles. To produce the required hydrogen, 540 kg of iron and 270 kg of sulphurous acid were consumed and the balloon inflation had a duration of four days. The balloon ascended quickly and soon disappeared into the clouds in a flight that endured approximately 45 minutes. The first instrumented, unmanned free balloon, which also carried a mercury barometer, was launched by Gustave Hermite and Besançon in 1892. Ten years later weather balloons enabled the discovery of tropopause and since then became a standard tool for atmospheric measurements and meteorological weather prediction widely used around the world [4].

Modern Ballooning

Until this day, hot air balloons are still used for travelling purposes. The vertical control of these balloons can be achieved manually by the pilot, pushing a valve that regulates the flow of gas, and therefore the vertical speed. However, for research purposes, high altitude balloons and weather balloons are the ones used. These balloons are filled in most of the cases with helium or hydrogen (in rare cases with methane). The main feature of these balloons is that they can reach the stratosphere to altitudes of 30 km for a weather balloon and even higher altitudes for high altitude balloons. For this reason, they are launched every day around the world for meteorological investigation purposes. Nowadays, in the ballooning field, the automatisation and control of unmanned balloon flights are in focus.

1.2.2 Existing Types of Weather Balloons

Zero-Pressure Balloons (ZP) [5]

These balloons are open at the bottom and have open ducts hanging from the sides to allow gas to escape and to prevent the pressure inside the balloon from building up during gas expansion as the balloon rises above Earth's surface. The duration of these balloons flight is long, the cycle through day and night can cause gas loss. This gas loss is what limits the time of flight. Figure 1.3 presents zero-pressure balloons before and during flight.

(a) Zero-pressure balloon before launch [6]

(b) Zero-pressure balloon at flight [7]

Figure 1.3: A demonstration of zero-pressure balloons before and after launching

Super-pressure Balloons (SP) [5]

These balloons do not have venting ducts and to contain the pressure inside the balloon, they have to be sealed tightly. They have a stronger envelope, made of a material that allows the balloon to always have a positive differential pressure (the pressure inside the balloon will always be greater than the pressure from the outside environment. Since gas loss is minimised in this balloon, super-pressure balloons can fly for longer periods than zero-pressure balloons. Figure 1.4 shows super-pressure balloons before and during a flight.

(a) Super-Pressure balloon before being launched [8].

(b) Super-Pressure high altitude balloon at flight [9].

Figure 1.4: Super-pressure balloons before and after launching.

Dual-Balloons [10]

These balloons, schematically represented in Figure 1.5, have been presented to increase lifetime and improve floating performance. Dual-balloon systems, are compound systems that combine a small super-pressure balloon and a large zero-pressure balloon. The small super-pressure balloon is used for controlling the altitude, while the large zero-pressure balloon is used for lifting the payload.

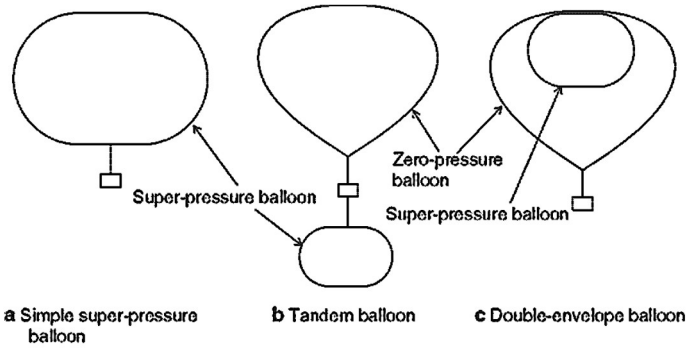

Figure 1.5: Representation of different dual-balloon types [10].

Infrared Montgolfier (MIR) [11]

These balloons are basically a zero-pressure hot-air balloon that takes great advantage of the Earth's thermal radiation (during the night) and of sunlight (during the day) in order to heat the lifting gas (air), thanks to a specifically conceived envelope made of different plastic materials. A representation of a MIR balloon before flight and a scheme are shown in Figure 1.6.

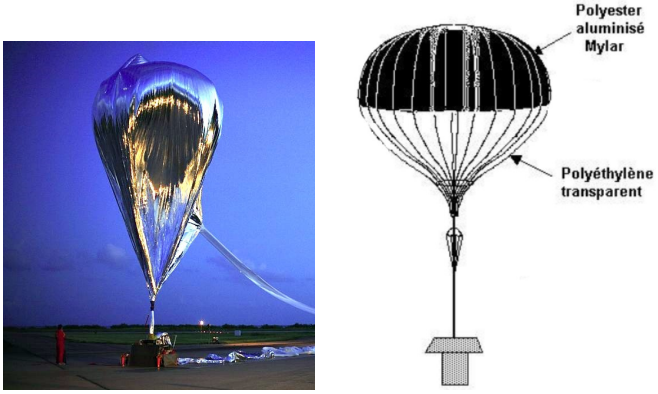

(a) MIR balloon before launch [12].

(b) Infrared Montgolfier scheme (adapted from [11]).

Figure 1.6: Representation of a MIR balloon at launch and a scheme of its features.

Latex Balloons [10]

Latex (or natural rubber) balloons, illustrated by Figure 1.7, are composed of elastic polymers that expand while ascending, maintaining a pressure difference (also defined as membrane pressure) between the internal pressure of the balloon and the external pressure until reaching the bursting altitude. These types of balloons are usually referred to as weather balloons.

Figure 1.7: Latex Weather Balloon flying [13].

1.2.3 Lifting Gas

Among the gases that present a lower density than the air and are used as lifting gases for weather balloons, helium and hydrogen are the most common ones.

Hydrogen is easy to manufacture and the lightest existing gas. Due to its easy production, it is also a cheaper option than helium. However, as some disasters such as the Hindenburg disaster [14] can justify, this is a highly flammable gas, which makes it far more dangerous than helium and demands training to work with.

Helium is the second lightest and is a byproduct of the radioactive decay of uranium [15]. Like with many other materials, there are two ways to obtain helium: either extract it from nature or synthesise it in a laboratory.

Since manufacturing is costly, the usual extraction of this gas is directly from nature. The earth has natural gas fields where large reserves of helium are placed [16].

1.2.4 Altitude Control Mechanisms and Solutions

Controlling a weather balloon flight is still a field to be explored and very few detailed investigations for rubber balloons in this area have been conducted. Although some traditional high altitude balloons can, theoretically, be controlled with minimal buoyancy changes, in practice, the influence of solar and infrared radiation or even atmospheric turbulence can disturb this equilibrium. To control the altitude of a weather balloon it is necessary to either change the buoyancy of the balloon or its mass. Buoyancy change is obtained by changing the volume of the balloon (which can be done with mass or temperature change). All this considered, throughout time, different approaches to adjust the altitude of a weather balloon were developed. Some of these methods focus on changing the mass (of the balloon itself or the lifting gas inside it), such as ballasting air or weights or even changing the mass of gas inside the balloon. Other methods were developed to change buoyancy by other means, for example, mechanical compression of the balloon itself or temperature control of the lifting gas. All the following existing mechanisms information was obtained from [17].

Existing Control Mechanisms

- **Ballast drop**

  One of the first systems for controlling buoyancy is the ballast drop which is commonly employed because it is simple to implement. In this system, ballast (for example, sand or other small weights) is added to the balloon payload. The ballast dropping process makes the balloon lighter and, as a result, the balloon rises.

- **Mechanical Compression**

  Changing the volume of the helium balloon through direct mechanical compression to adjust buoyancy is one of the existing ways to control it. In mechanical compression systems, a super-pressure balloon is compressed employing a winch or other constriction device. Proposed and tested by Solomon Andrews in the 1800s, mechanical compression has now become a real possibility because of the availability of strong synthetic materials and the development of the pumpkin balloon structure.

- **Pumped gas**

  Pumping helium between a non-pressurised zero-pressure balloon and a pressurised reservoir to adjust buoyancy. Differential-Expansion systems can be configured with the super-pressure vessel inside the zero-pressure envelope so that any lift gas that leaks from the high-pressure system is recovered. This type of configuration is ideal for long-duration flights.

- **Air Ballast**

  Air-ballast systems make use of the high molecular weight of air relative to the lift gas. To descend, ambient air is pumped into a bladder inside a super-pressure balloon. Since super-pressure balloons do not expand appreciably during the flight, the balloon's density increases with time. To rise, the process is reversed, and the air is released from the internal bladder into the surroundings.

- **Temperature Change**

  Hot Air Balloons: This is the oldest method of altitude control and involves changing the temperature of the lift gas. This category of altitude control includes hot-air balloons, dirigibles and blimps that use engine exhaust to heat their ballonets. Because heat loss across the balloon envelope is substantial, thermal altitude control is inefficient from an energy perspective.

  Insulation Method : This method is based on the advantages of solar radiation absorption by the balloon's envelope material. Half of the balloon's envelope is painted black and the other half is painted white. To increase its altitude, the balloon is rotated about its vertical axis and its black part is faced towards the sun, the lift gas expands resulting in a bigger lift force. To decrease the altitude, the balloon turns its white painted part towards the sun, resulting in a consequent reduction of the volume, and so a smaller lift force.

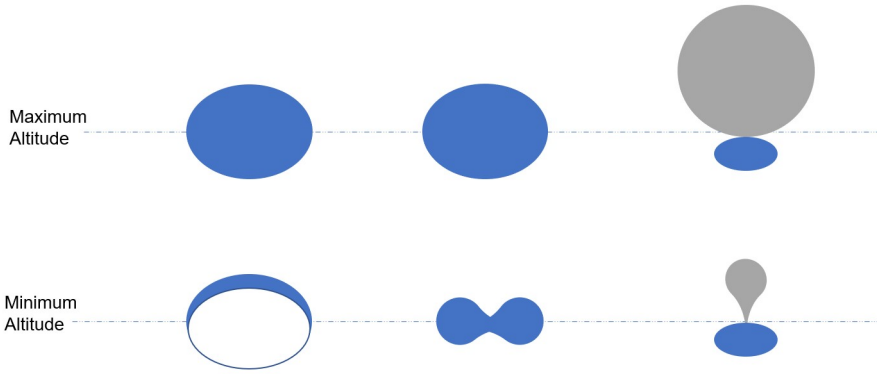

Figure 1.8: Air Ballast, Mechanical Compression and Pumped Gas representation (adapted from [17]).

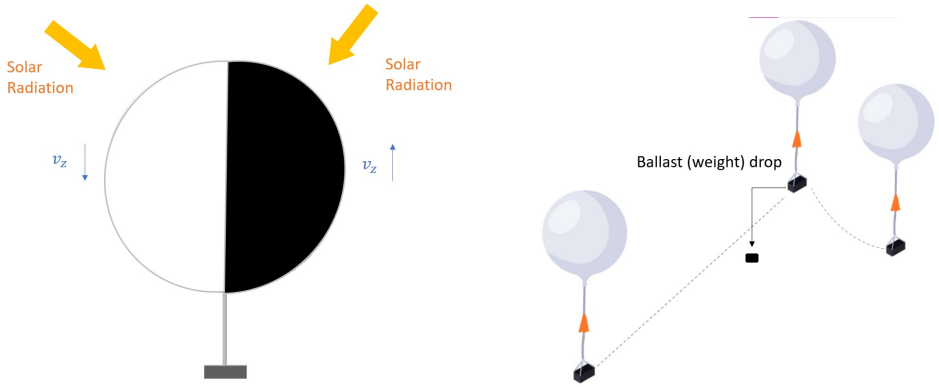

(a) Insulation method.

(b) Ballast drop/Weights ballasting.

Figure 1.9: Existing control mechanisms for a weather balloon.

Existing Control Strategies

Nowadays, in the balloon altitude control field, works have been developed for zero-pressure balloons such as [2], in which a PID control strategy with a compress–release mechanism was implemented. For a super super-pressure balloon, works such as [18], in which reinforcement learning was used to train a flight controller from simulations, were developed. Some work on station keeping considering that wind directions vary with altitude and exploring the natural wind field has been developed. An example of this work is [19], where the air ballast mechanism (consisting of a balloon with a helium bag and air ballonet that were separated by a membrane) was used and [3] that used a pumping-release mechanism. However, for latex (rubber) balloons very few works can be found focusing on the modelling and implementation of altitude control.

1.3 Objectives and Deliverables

The goal of this thesis is to develop a complete model for a latex weather balloon filled with helium and perform a simulation of its altitude control. After the model of the balloon is complete it is expected

to develop altitude control solutions to allow the weather balloon to find interest areas of research with wind currents as guidance. This thesis presented a latex balloon model in which a spherical shape was assumed. A nonlinear elasticity theory was used to represent the real elastic behaviour of latex. Two different nonlinear elastic theories were compared and one was chosen. Besides that, a complete thermal model was developed and implemented in which direct solar radiation, infrared radiation and convection components were accounted for. A gas cylinder and a valve were added to this balloon as the mechanism to perform the altitude control. Coupled with the idea of project SONDA of using the wind for horizontal movement, a wind model was also developed. Meteorological data from NOMADS servers were acquired and implemented. Two ways of implementing the wind data were compared and one was chosen. Finally, a control strategy was developed, in which cascade control was used to control not only the altitude but also the velocity in the weather balloon flight. In the end, tree simulations for different altitude references were performed and analysed.

1.4 Thesis Outline

This thesis is composed of four main chapters.

- **Chapter 1: Introduction**

  The first chapter corresponds to the state of the art and some information about weather balloons such as their history, their types and the kind of lifting gases generally used. Despite that, existing altitude control mechanisms and most recently developed solutions were presented.

- **Chapter 2: Balloon Modelling and Implementation**

  During this chapter, the modelling of the weather balloon is developed and implemented. This chapter is initiated with a brief description of reference frames and how they are approached in this thesis. Then the necessary equations to calculate basic but important parameters such as the initial necessary mass of gas and initial volume of the weather balloon are presented. After these parameters are presented, the following section exposes the hyperelastic theory and how it can be applied to a weather balloon as a better alternative to model the radius variation of natural rubber (latex). The atmospheric model used in most aircraft designs for different altitudes is shown in the following section. A thermal model is developed in which different heat contributions to the weather balloon are accounted for. Following this section, a section dedicated to the study and development of the dynamics is included in which the balance of forces is represented and a correlation adapted to the weather balloon for the drag coefficient is presented. Two model options for wind are shown next, one will be chosen after the implementation and comparison phase. The equations presented in all the developed models are put together in a state-space representation in the next section. Finally, the implementation of all models with the corresponding parameters is made.

- **Chapter 3: Altitude Control Design and Implementation**

  In this chapter, the altitude control strategy is presented. The theory behind the cascade control strategy, gain scheduling and LQR algorithm is briefly explained. And this designed control solu-

tion is implemented. The process of linearisation of the balloon model is explained and the used parameters to find the controller gains is shown.

- **Chapter 4: Simulation Results and Discussion**

  In this chapter four simulations are presented. The first one describes the free flight of the balloon with the model developed and implemented in this thesis, the second simulates the flight of the weather balloon for a constant altitude reference, the third simulation is for an increasing altitude reference and finally, the last simulation intends to couple the wind model and altitude control and having a start position in Lisbon the balloon receives an altitude reference that when following the modelled wind currents leads the weather balloon to land in Seville. All these simulations are analysed and discussed.

- **Chapter 5: Conclusions and Future Work**

  Finally, in this last chapter, conclusions about the work developed throughout this thesis and its results are presented. This chapter ends with some suggestions of ideas for future work in areas that could be improved or developed in this context.

2 Balloon Modelling and Implementation

This chapter initiates with the modelling of the weather balloon. Models for elastic behaviour, atmosphere, temperature evolution, wind and dynamics will be presented. In the last part of the chapter, the implementation of the developed models is made.

2.1 Coordinate Systems

A brief explanation of the coordinate system should be made, as a first step towards understanding how the weather balloon flies. These types of aircraft typically have their trajectory represented through "Latitude", "Longitude" and "Altitude" (LLA), while most vehicles present in aeronautics uses the "North", "East", "Down" (NED) system. These reference frames are illustrated by Figure 2.1.

- **NED (North, East, Down):** This reference frame is the usual choice in aeronautics and is fixed on the Earth's surface and is measured relative to the ECEF ("Earth-Centered Earth-Fixed") frame. Its center is O_{NED} as shown in Figure 2.1. However, this is a Cartesian reference frame and does not take into consideration the Earth's curvature. As a consequence, it is only useful for problems where the distances are short.

  For this project, in which the balloon's trajectory in the atmosphere is important, the Earth's curvature should be considered. The reference frame based on spherical coordinates, that can take into consideration the Earth's curvature and will be used through this work, is the **LLA**.

- **LLA (Latitude, Longitude, Altitude):** The geodetic grid for the planet is comprised of parallel East/West lines of latitude (ϕ) and North/South lines of longitude (λ) that intersect at the poles. Latitude and longitude lines are labelled by the angle they subtend concerning a reference. For latitude, that 0 reference is the Equator and for longitude that 0 reference is the Prime Meridian. The assumption of spherical Earth needs to be taken in order to transform the coordinates in the NED frame to latitude, longitude, altitude coordinates. With this assumption and with the radius being considered as the mean Earth radius, $R_{Earth} = 6371009$ m the conversion from LLA to the NED reference frame, if necessary, can be made with the following expressions:

$$x = (R_{Earth} + z)\cos\phi\cos\lambda \tag{2.1a}$$

$$y = (R_{Earth} + z)\cos\phi\sin\lambda \tag{2.1b}$$

$$z = (R_{Earth} + z)\sin\phi \tag{2.1c}$$

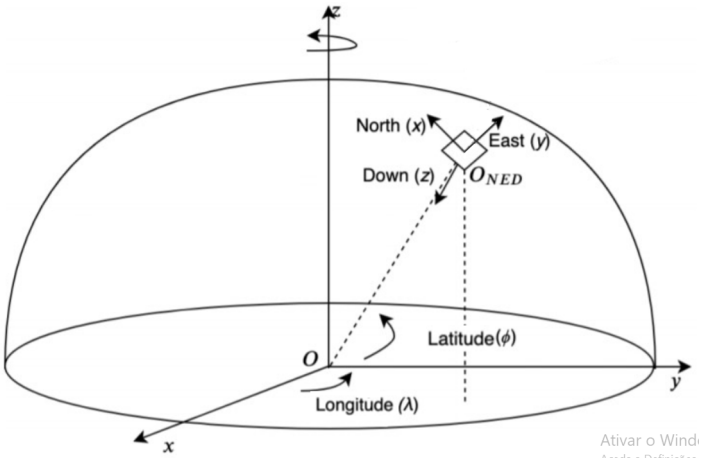

Figure 2.1: NED, Geodetic (LLA), and ECEF reference frames representation (adapted from [20]).

2.2 Balloon Characteristics and Launch Parameters

For this work, it is intended to firstly model a latex balloon filled with helium or hydrogen. For a usual weather balloon that only has a film mass and a payload, the following approach can be followed using the tabled values for a specific weather balloon. Knowing some specifications such as the balloon envelope mass (m_b), the payload mass (m_p), initial balloon radius at launch (R_i), its uninflated radius (R_0), latex density (ρ_b), neck size and maximum radius before it bursts (R_{max}) are known, posterior calculations of its dynamic behaviour at launch can be made. With all these balloon parameters as well as the lift gas density (ρ_{g0}), it is possible to calculate the values of the following variables at launching:

- **Thickness of the uninflated balloon:**

$$t_0 = \frac{m_b}{4\pi \cdot R_0^2 \cdot \rho_b} \tag{2.2}$$

- **Initial volume of the balloon at release:**

$$V_0 = \frac{4}{3}\pi \cdot R_i^3 \tag{2.3}$$

- **Initial mass of gas:**

$$m_{g0} = \rho_{g0} \cdot V_0 \tag{2.4}$$

However, the balloon will carry a gas cylinder of weight m_{cil} and a control valve (m_{valve}). And the

previous equations are only useful for a simple balloon without these added components. Different equations should be used when adding more weight to the weather balloon. Another way to analyse the initial necessary mass of helium is through lift. Lift is the difference between buoyancy and the weight of the balloon and it has to be positive when the balloon goes up and negative if it goes down. This method of evaluating the initial mass of helium will be the one used so these weights of the gas cylinder and control valve can be included. This method is represented by:

$$L = V_0 \cdot g \cdot (\rho_{a0} - \rho_{g0}) \tag{2.5}$$

The lift should compensate all weights in the weather balloon. Considering that the weather balloon will carry the balloon film mass, the payload, a gas cylinder and a control valve, the following expression can be used to find the initial necessary volume (and, therefore, the initial mass of gas) that allows the gas to compensate the weight the balloon carries:

$$m \cdot g = V_0 \cdot g \cdot (\rho_a - \rho_g) \Longleftrightarrow V_0 = \frac{m}{\rho_a - \rho_g} \tag{2.6}$$

Here, m represents the sum of all components of the weather balloon that does not include the mass gas.

$$m = m_b + m_p + m_{cil} + m_{valve} \tag{2.7}$$

The parameter ρ_a, represents the density of the air surrounding the balloon. Introducing this volume into Equation 2.4 the initial mass can be found and verified.

2.3 Hyperelastic Theory

Since rubber applies a restoring force inwards, the pressure inside any elastic balloon is always a little bit greater than the outside pressure. It could be useful to analyse whether this pressure difference affects the ascent of the balloon. This pressure variation is called the membrane pressure (ΔP) and it is the difference between the pressure inside the balloon (P_{in}) and the atmosphere pressure (P_{out}):

$$P_{in} = \Delta P + P_{out} \tag{2.8}$$

Knowing that a latex balloon will be deformed in a non-linear way, a non-linear model will be applied. Therefore, to derive the pressure-radius characteristic of a balloon, one must apply hyperelastic theory to a normal latex balloon for a more accurate representation of its behaviour.

The Mooney-Rivlin model is useful for rubber materials at small stretches, but it is not adequate for large strain subjection. Gent is able to model the stiffening that the rubber undergoes as it approaches its breaking point. However, the parameters are more laborious to measure precisely without destructing the balloon. The models here presented were the ones presented in [21].

- **Mooney-Rivlin Model:**

$$P_a(z) - \frac{nR_gT_g(z)}{\frac{4}{3}\pi R^3} + 2s_+\frac{t_0}{R_0}\left(\left(\frac{R_0}{R}\right) - \left(\frac{R_0}{R}\right)^7\right)\left(1 - \frac{s_-}{s_+}\left(\frac{R}{R_0}\right)^2\right) = 0 \tag{2.9}$$

- **Gent Model:**

$$P_a(z) - \frac{nR_gT_g(z)}{\frac{4}{3}\pi R^3} + 2\eta\frac{t_0}{R_0}\left(\left(\frac{R_0}{R}\right) - \left(\frac{R_0}{R}\right)^7\right)\left(\frac{J_m}{J_m - 2\left(\frac{R_0}{R}\right)^{-2} - \left(\frac{R_0}{R}\right)^4 - 3}\right) = 0 \tag{2.10}$$

The parameters found in these formulas are explained and can be consulted in detail in [21]. By rearranging (2.10) or (2.9), the radius can be obtained as a function of the mass and temperature of the weather balloon. The P_{in} component is derived from the perfect gas law as following:

$$P_{in}V = nR_gT_g \iff P_{in} = \frac{nR_gT_g}{\frac{4}{3}\pi R^3} \tag{2.11}$$

The number of moles, n, presented in this formula, is given by the division of the mass of gas inside the weather balloon and the molar mass of the gas ($M_{He} = 4 \cdot 10^{-3}$):

$$n = \frac{m_g}{M_{He}} \tag{2.12}$$

2.4 Atmospheric Model

The dynamics of the balloon are heavily influenced by the density, pressure and temperature of the air surrounding it. A typical weather balloon will reach altitudes of approximately 30-35 km (in the stratosphere) before it bursts [10]. To study the influence of atmosphere in the balloon the International Standard Atmosphere model [22] will be used. From this model, evolutions of the temperature (Figure 2.2(c)), pressure (Figure 2.2(a)) and density (Figure 2.2(b)) with altitude, can be obtained. The equations for the troposphere (0 to 11000 m), lower stratosphere (11000 to 25000 m) and upper stratosphere (above 25000 m) are the following:

$$T_a(z) = \begin{cases} 288.15 - 0.0065 \cdot z, & \text{if } 0 < z \leq 11000 \\ 216.65, & \text{if } 11000 < z \leq 25000 \\ 141.94 + 0.00299 \cdot z, & \text{if } 25000 < z \end{cases} \tag{2.13}$$

$$P_a(z) = \begin{cases} 101290 \cdot (\frac{288.15 - 0.0065 \cdot z}{288.15})^{5.256}, & \text{if } 0 < z \leq 11000 \\ 22650 \cdot \mathrm{e}^{(1.73 - 0.000157 \cdot z)}, & \text{if } 11000 < z \leq 25000 \\ 2488 \cdot (\frac{141.94 + 0.00299 \cdot z}{216.65})^{-11.388}, & \text{if } 25000 < z \end{cases} \tag{2.14}$$

Given the temperature and pressure information, it is possible to obtain the evolution of the density for the different altitudes using the perfect gas law. It can be observed that, as the altitude increases, the atmospheric pressure and the atmospheric density decreases substantially. As for the atmosphere temperature it decreases until 11 km, then it stays stationary at 216.65 K until 25 km.

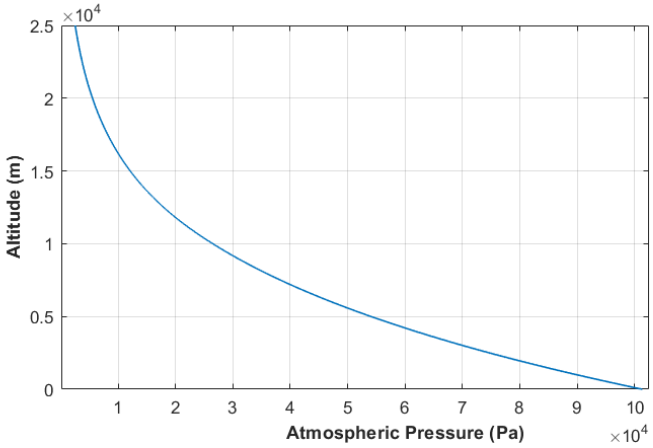

(a) Atmospheric Pressure evolution with altitude

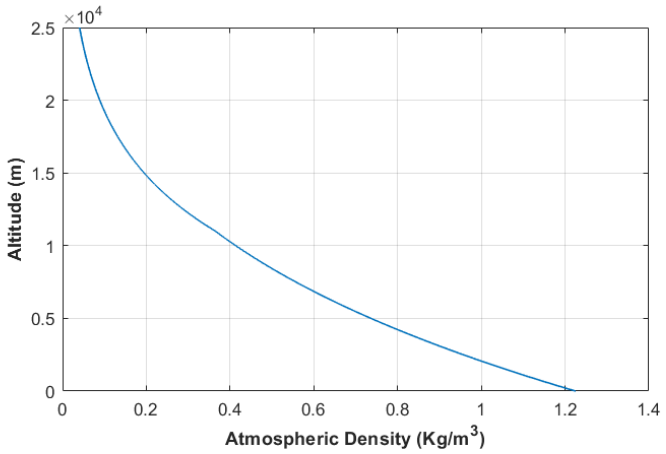

(b) Atmospheric Density evolution with altitude

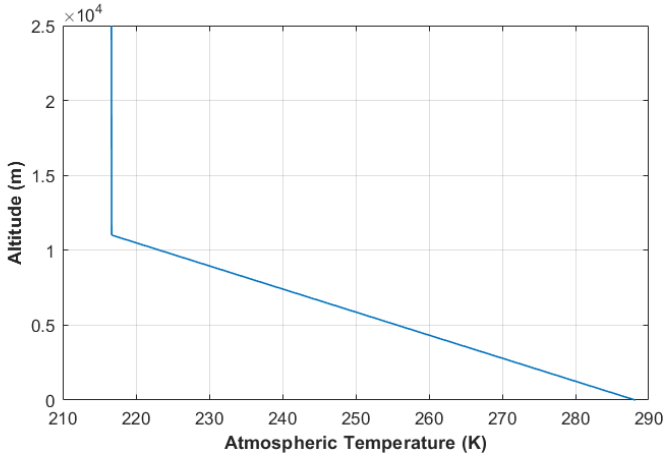

(c) Atmospheric Temperature evolution with altitude

Figure 2.2: Atmospheric properties variation with height

2.5 Thermal Model

The temperature inside the balloon changes during the different phases of the balloon flight. As a consequence of, mostly, direct solar radiation and infrared radiation from the Earth, the envelope heats the gas inside the balloon through convection and self glow and as a result, the gas inside the balloon expands, the balloon radius increases which leads the buoyancy to also increase. Due to this thermal phenomenon, the flying period of the balloon can reduce since the maximum radius is reached faster. Understanding the temperature variation of the weather balloon is important since the influence of temperature is an essential factor that conditions the density of the gas, therefore changing its volume and mass. To develop a thermal model, one should separate the thermal environment into two parts. The first one is the thermal influence of the external environment and the second one is the temperature influence caused by the internal environment. The model, illustrated in Figure 2.3 and followed in this thesis, is based on the one presented in [23].

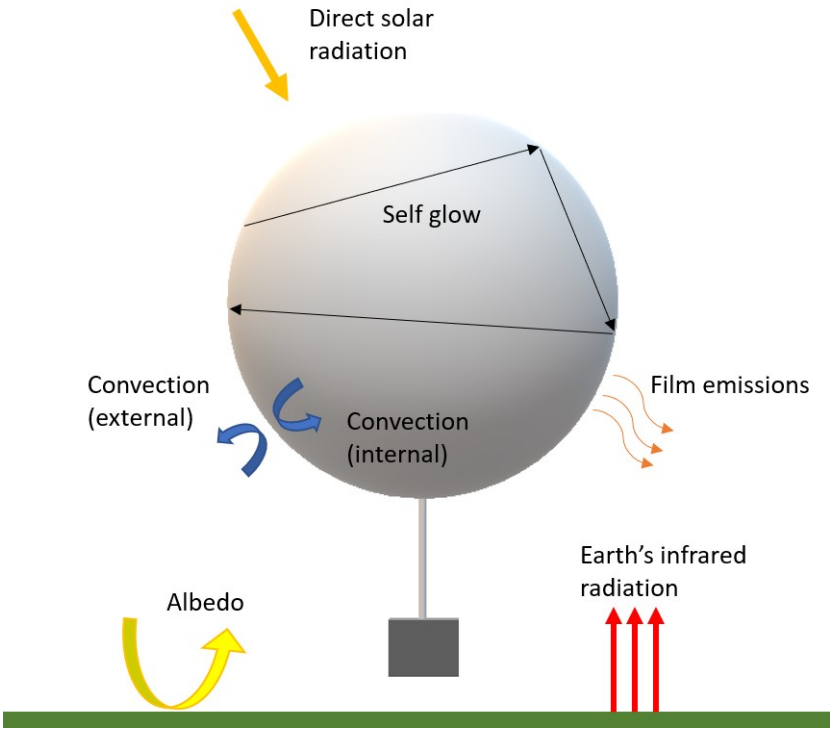

Figure 2.3: Thermal model of the weather balloon. The model is composed of radiation (solar or infrared), albedo, convection (internal and external), film emissions and self glow.

The external environment mainly comprises direct solar radiation, Earth reflected radiation, atmosphere infrared radiation, film emissions to the atmosphere and convection between the balloon and the external atmosphere while the internal thermal environment is composed of the internal natural convection and internal infrared radiation between the film and the gas.

2.5.1 External Environment

Direct solar radiation

The solar radiation depends only on the solar constant (which is here assumed to be $E_{Sun} = 1367.5$ W/m^2) and on the solar elevation angle (that is further explained in section 2.9.3). To compute the contribution of the solar environment, several orbital parameters are necessary. The following equations can be applied to any planet with a small orbital eccentricity and represents the process to compute the heat caused by direct solar radiation:

1. Mean Anomaly (MA)

$$MA = 2\pi \frac{Day_{number}}{Days_{PerYear}} \tag{2.15}$$

The mean anomaly depends on the variable Day_{number} that represents how many days have passed since the beginning of the year until the balloon date of launch and the parameter $Days_{PerYear}$, which is the total number of days in that year.

2. True Anomaly (TA)

$$TA \approx MA + 2e \sin(MA) + \frac{5}{4} e^2 \sin(2MA) \tag{2.16}$$

3. Solar irradiance flux at the top of the atmosphere

$$I_{Sun} = \frac{E_{Sun}}{R_{AU}^2} \cdot \left(\frac{1 + e\cos(TA)}{1 - e^2} \right)^2 \tag{2.17}$$

The parameters $e = 0.016708$ and $R_{AU} = 1$ are related to the planet (in this case, the values presented are for the Earth).

4. Direct solar irradiance at altitude Z

$$I_{SunZ} = I_{Sun} \tau_{atm} \tag{2.18}$$

The direct solar irradiance at a certain height depends on the transmissivity of the atmosphere, τ_{atm} (section 2.5.3), at such height.

5. Direct solar flux acting on the balloon

$$q_{Sun} = I_{SunZ} \tag{2.19}$$

The total heat from the direct solar influence is expressed by:

$$Q_{Sun} = \alpha \cdot A_p \cdot q_{Sun} \left(1 + \frac{\tau}{1 - r} \right) \tag{2.20}$$

where, A_p is the projected area, α is the solar absorptivity of the external surface, τ is the atmosphere transmissivity and the reflection coefficient is given by $r = 1 - \alpha - \tau$.

Infrared radiation

The longwave radiation flux from ground at the balloon altitude Z follows the Stefan-Boltzmann law (with $\sigma = 5.67 \times 10^{-8}$ W/m^{2}K^4) and is written as:

$$q_{IREarth} = q_{IRgroundZ} = q_{IRground} \cdot \tau_{atmIR} = \varepsilon_{ground} \cdot \sigma \cdot T_{ground}^4 \cdot \tau_{atmIR} \tag{2.21}$$

Ground emissivity is usually low in the hottest places while it is usually high in the coldest ones. However, it is possible to consider an average value ε_{ground}=0.95. The total heat resulted from the infrared radiation is given by:

$$Q_{IREarth} = \alpha_{IR} \cdot A_s \cdot q_{IREarth} \cdot VF\left(1 + \frac{\tau_{IR}}{1 - r_{IR}}\right) \tag{2.22}$$

where, A_s is the balloon surface area, α_{IR} is the absorptivity of the external surface in the infrared spectrum, τ_{IR} is the transmissivity of the atmosphere in the infrared spectrum (section 2.5.3) and $r_{IR} = 1 - \alpha_{IR} - \tau_{IR}$.

The VF component represents the "View Factor", which is the effective balloon area exposed to the planet surface. This component depends on the Earth radius R_{Earth} and the height z. The VF expression is given by:

$$HalfCone = \sin^{-1}\left[\frac{R_{Earth}}{R_{Earth+z}}\right] \tag{2.23}$$

$$VF = \frac{1 - \cos(HalfCone)}{2} \tag{2.24}$$

Albedo

The relationship between the surface albedo and albedo flux involves the solar flux, the albedo coefficient (that accounts for the fraction of solar radiation that is reflected by the planet surface and atmosphere) and the solar elevation angle, ψ (section 2.9.3).

$$q_{Albedo} = Albedo \cdot I_{Sun} \cdot \sin(\psi) \tag{2.25}$$

$$Q_{Albedo} = \alpha A_s q_{Albedo} VF\left[1 + \frac{\tau}{1 - r}\right] \tag{2.26}$$

Film emissions

The emitted energy from both the interior and exterior of the balloon skin depends on the film temperature itself, T_f, and the emissivity of the film ε.

$$Q_{IRout} = \sigma \varepsilon A_s T_f^4\left(1 + \frac{\tau_{IR}}{1 - r_{IR}}\right) \tag{2.27}$$

External Convection:

The weather balloon will be affected by external convection that will be considered forced or free convection depending on the velocity of the balloon. After computing all parameters to compare the convection coefficients, the bigger value is chosen. The Nusselt number for a sphere in free convection is:

$$Nu_{free} = 2 + 0.45 \cdot (Gr_a \cdot Pr_a)^{0.25} \tag{2.28}$$

The Nusselt number for forced convection is:

$$Nu_{forced} = 2 + 0.41 \cdot Re^{0.55} \tag{2.29}$$

The Grashof number is given by:

$$Gr_a = \frac{\rho_a^2 \cdot g \cdot |T_f - T_a| \cdot D^3}{T_a \cdot \mu_a^2} \tag{2.30}$$

Reynolds number is given by:

$$Re = \frac{v_z \cdot D \cdot \rho_a}{\mu_a} \tag{2.31}$$

- Free convection

$$H_{e_{free}} = \frac{Nu_{free} \cdot k_a}{D} \tag{2.32}$$

- Forced convection

$$H_{e_{forced}} = \frac{Nu_{forced} \cdot k_a}{D} \tag{2.33}$$

The heat transfer coefficient used for eternal convection should be the maximum value of the free and forced convection heat transfer coefficients:

$$H_e = max(H_{e_{free}}, H_{e_{forced}}) \tag{2.34}$$

And the heat through external convection is then:

$$Q_{ConvExt} = H_e \cdot A_s(T_a - T_f) \tag{2.35}$$

2.5.2 Internal Environment

Self-Glow

Absorbed infrared self-glow from the interior.

$$Q_{IRfilm} = \sigma \varepsilon \alpha_{IR} A_s T_f^4 \frac{1}{1 - r_{IR}} \tag{2.36}$$

Internal Convection:

The internal convection is only result of free convection. The Nussest number is obtained by the expression:

$$Nu_i = 2 + 0.45 \cdot (Gr_g \cdot Pr_g)^{0.25} \tag{2.37}$$

The Grashof number is given by:

$$Gr_g = \frac{\rho_g^2 \cdot g \cdot |T_f - T_g| \cdot D^3}{T_g \cdot \mu_g^2} \tag{2.38}$$

Once again, the heat transfer coefficient can be written as:

$$H_i = \frac{Nu_i \cdot k_g}{D} \tag{2.39}$$

Finally, the heat produced by internal and external convection are defined as follows:

$$Q_{ConvInt} = H_i \cdot A_s(T_f - T_g) \tag{2.40}$$

2.5.3 Atmosphere Transmissivity

The irradiance of both solar radiation and long-wave radiation is influenced by the presence of the atmosphere. The atmosphere transmissivity can be calculated for both the direct solar radiation and the ground infrared radiation as follows:

- Transmissivity of a solar beam through the atmosphere

$$\tau_{atm} = 0.5\left[e^{-0.65 \cdot AirMass} + e^{-0.095 \cdot AirMass}\right] \tag{2.41}$$

- Infrared transmissivity of the ground

$$\tau_{atmIR} = 1.716 - 0.5\left[e^{-0.65\frac{P_a}{P_0}} + e^{-0.095\frac{P_a}{P_0}}\right] \tag{2.42}$$

- Air Mass Factor:

$$AirMass = \left(\frac{P_a}{P_0}\right) \cdot \left(\sqrt{1229 + (614\sin(\psi))^2} - 614\sin(\psi)\right) \tag{2.43}$$

Note:
- P_a is ambient atmosphere pressure;
- P_0 is the Earth surface atmosphere pressure;

2.5.4 Heat Transfer Coefficient Parameters

The procedure to compute the internal and external convection requires the heat transfer coefficients. This coefficient depends on different air and gas properties that are represented by the following expres-

sions:

- Dynamic viscosity ($\frac{N \cdot s}{m^2}$)

$$\mu_a = \frac{1.458 \cdot 10^{-6}\ T_a^{1.5}}{T_a + 110.4} \tag{2.44}$$

$$\mu_g = 1.895 \cdot 10^{-5} \cdot \left(\frac{T_g}{273.15}\right)^{0.647} \tag{2.45}$$

- Conductivity ($\frac{W}{m \cdot K}$)

$$k_a = 0.0241 \cdot \left(\frac{T_a}{273.15}\right)^{0.9} \tag{2.46}$$

$$k_g = 0.144 \cdot \left(\frac{T_g}{273.15}\right)^{0.7} \tag{2.47}$$

- Prandtl number

$$Pr_a = 0.804 - 3.25 \cdot 10^{-4} \cdot T_a \tag{2.48}$$

$$Pr_g = 0.729 - 1.6 \cdot 10^{-4} \cdot T_g \tag{2.49}$$

2.5.5 Thermal Balance

Heat transfer on the film:

The thermal balance on the film is represented by the following equation:

$$\dot{T}_f = \frac{Q_f}{c_f \cdot m_b} \tag{2.50}$$

where the specific heat of the film, c_f, is obtained by the correlation presented in [24] given by

$$c_f = (1.947 + (43.7e-4)(T_f - 25) + (2.24e-6)(T_f - 25)^2) \times 10^3 \tag{2.51}$$

Note: This is the only situation where temperature T_f needs to represented in °C.

As shown in Figure 2.3, the balloon envelope is affected by the following heats:

$$Q_f = Q_{Sun} + Q_{IREarth} + Q_{Albedo} + Q_{IRfilm} + Q_{ConvExt} - Q_{IRout} - Q_{ConvInt} \tag{2.52}$$

Heat transfer on the lifting gas:

The thermal balance on the gas is represented by:

$$\dot{T}_g = \frac{Q_{ConvInt}}{\gamma \cdot c_v \cdot m_g} + (\gamma - 1) \cdot T_g \cdot \left(\frac{dm_g}{dt} \cdot \frac{1}{m_g} - \frac{dV}{dt} \cdot \frac{1}{V}\right) \tag{2.53}$$

Some geometric characteristics necessary to compute these heats are:

- Projected area: $A_p = \pi R^2$
- Surface area: $A_s = 4A_p$

2.6 Dynamics Model

The lifting force that allows a balloon to rise derives from Archimedes' Principle. This principle, states that any body completely or partially submerged in a fluid (gas or liquid) will be actuated by a vertical force with an intensity equal to the weight of the fluid displaced by the body. Besides the buoyancy responsible for lifting the balloon, forces such as gravity (due to the weight of the balloon structure) and drag (due to its movement), are also acting forces that define the balloon's trajectory and behaviour.

2.6.1 Mass Balance

An initial and important analysis to see the influence of the forces acting on the balloon is to understand the masses in the system. Expressing the initial mass of gas and the mass of the overall balloon structure separately, the total initial mass is given by:

$$m_{t0} = m + m_{g0} \tag{2.54}$$

where m is the sum of all components of the weather balloon that does not include gas (2.7). Being $\dot{m}_g$ the variation of gas mass on the weather balloon, and the total mass (including the gas), m_t, a varying parameter (or a state, as it will be seen in the next sections), the mass at instant j is obtained through the sum of mass at instant $j-1$ and the mass variation of instant j:

$$m_{t_j} = m_{t_{j-1}} + \dot{m}_{g_j} \tag{2.55}$$

In other words, assuming that the mass of gas is as a state of the system, the mass at a certain instant can be obtained by integrating the state derivative (that is $\dot{m}_g$), considering that the initial total mass of the balloon is given by Equation 2.54.

As for the volume at each instant, since the lift gas is assumed to behave as a perfect gas, can be determined using the perfect gas law. Considering that the gas temperature value is obtained employing the thermal equations described in section 2.5, the following happens:

$$P_g \cdot V = m_g \cdot R_g \cdot T_g \iff V = \frac{m_g \cdot R_g \cdot T_g}{P_g} \tag{2.56}$$

In this formula, P_g is the balloon pressure, V is the balloon volume, m_g is the mass of lifting gas, R_g is the gas constant ($R_g = 8.31$ J/mol·K), and T_g is the internal balloon temperature (in K).

An alternative way to calculate the volume is using the balloon radius (R) obtained from the hyperelastic theory equation. Since the latex balloon is assumed to be spherical, the expression $V = \frac{4\pi R^3}{3}$ is

valid.

2.6.2 Balance of Forces

To write the differential equations that describe the balloon dynamics, it is necessary to identify the forces (shown in Figure 2.4) that act on the system. The balloon is considered to be a point particle along the whole trajectory with a certain mass moving in the three-dimensional space under a known force. The balloon has three degrees of freedom, which means that three independent parameters are required to fully determine its position (LLA).

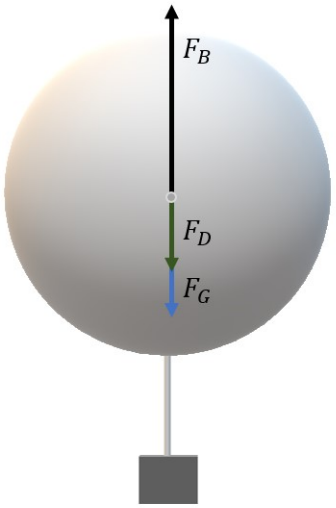

Figure 2.4: Acting forces on the weather balloon.

Weight: Representing the total weight of the weather balloon.

$$F_G = m_t \cdot g \tag{2.57}$$

Buoyancy: Force that follows the Archimedes' principle.

$$F_B = \rho_a \cdot V \cdot g \tag{2.58}$$

Drag: This force has a vertical component and is represented by:

$$F_{Dz} = \frac{1}{2} \cdot C_D \cdot A_b \cdot \rho_a v_z^2 \tag{2.59}$$

This component depends on the drag coefficient, C_D, which can be represented as a function of the Reynolds number, as explained in section 2.6.3.

- *Balance of Forces*

$$\sum F = m \cdot a \Longleftrightarrow m_t \cdot \ddot{z} = -F_G - F_{Dz} + F_B \tag{2.60}$$

- *Differential Equation*

The differential equation governing the vertical motion is then:

$$\ddot{z} = \frac{F_B - F_{Dz} - F_G}{m_t + m_v} \tag{2.61}$$

The m_v component added to the balloon's overall mass is the virtual mass determined by the direction of acceleration. The virtual mass equation is the following:

$$m_v = C_m \cdot \rho_a \cdot V \tag{2.62}$$

As explained in [10], the C_m coefficient varies for a zero pressure balloon, but for a sphere $C_m = 0.5$.

2.6.3 Drag Coefficient

The drag coefficient, C_D, denotes an important parameter that widely affects the ascent flight of the balloon. This coefficient depends on the balloon shape, and the Reynolds number, Re, as seen in the following expression:

$$Re = \frac{\rho_a D v_z}{\mu_a} \tag{2.63}$$

where D is the balloon's diameter, and μ_a is the coefficient of viscosity for air. The Reynolds number of the balloon, Re, is about $10^6 - 10^7$ on the ground and about $10^4 - 10^6$ at flying altitudes, depending on the magnitude of the buoyant force. For large balloons that are usually used in the Earth's stratosphere, C_D near the ground is of the order of 0.3 [10].

Correlation: Drag coefficient and Reynolds number

An extended literature survey on drag coefficient models for natural shape balloons was done and presented [25] and it is possible to conclude that, since the shape is inconstant, deformable and for dimensional reasoning, a variable drag coefficient should be considered while modelling the drag effect during a balloon flight. For this purpose, a correlation developed for spheres in [26], will be used with some adaptation to the weather balloon. Usually, the drag in balloons is slightly lower than in spheres. The correlation is developed for a spheric shape which could be a good approximation for a weather balloon, however as weather balloons differs slightly from spheres in shape (having a shape more similar to a drop of water, since there is more weight in its lower part), the curve will be slightly lowered to values in the order of 0.3 (as explained previously in this section to be the typical values for balloons) and the correlation used will be:

$$C_D = \frac{24}{Re} + \frac{2.6\left(\frac{Re}{5}\right)}{1 + \left(\frac{Re}{5}\right)^{1.52}} + \frac{0.411\left(\frac{Re}{2.63\times10^5}\right)^{-7.94}}{1 + \left(\frac{Re}{2.63\times10^5}\right)^{-8}} + \frac{0.25\left(\frac{Re}{10^6}\right)}{1 + \left(\frac{Re}{10^6}\right)} - 0.04 \tag{2.64}$$

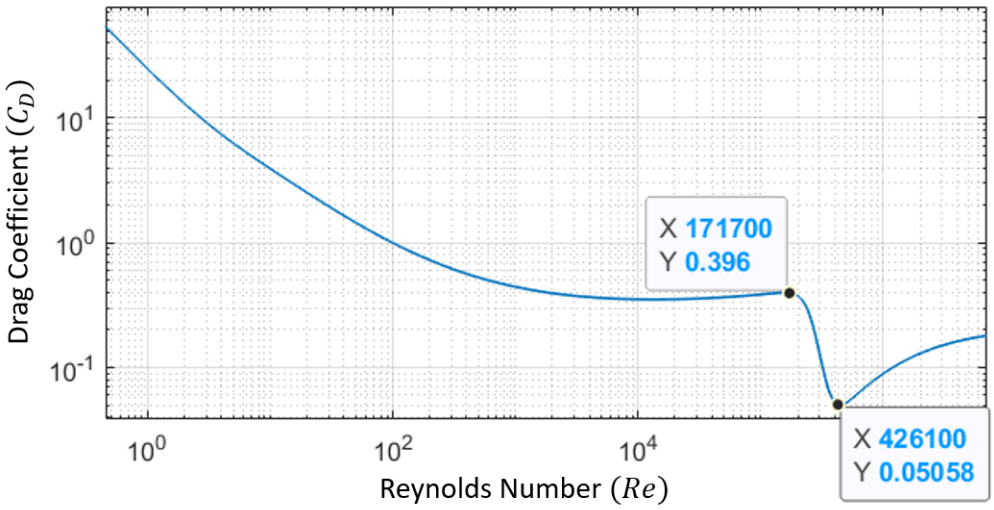

Figure 2.5: Drag coefficient and Reynolds number correlation for the weather balloon.

2.7 Wind Model and the Horizontal Movement of the Balloon

The wind is a very important contributor to the weather balloon flight. The balloon's trajectory is defined by the wind currents at a specified altitude. Therefore, it is responsible for the horizontal movement of the balloon. The wind can be interpreted and modelled as disturbance and to proceed to its implementation, two possibilities can be considered and compared.

2.7.1 Case 1: The Weather Balloon's velocity is the same as the wind

This case only happens if the horizontal motion can be simplified since the deformation and rotation of the balloon due to the incident wind are not considered. It is assumed that there is no horizontal slip between the balloon and the surrounding air mass, so the horizontal velocity of the balloon is equal to that of the incident wind itself. In this case, it is only necessary to convert the wind components v_{wx} and v_{wy} to the LLA coordinate system explained in section 2.1. Defining the mean Earth radius as $R_{Earth} = 6371009$ m, and with z being the current altitude of the balloon, the total distance to the centre of the Earth at each instant is given by $R_{total} = R_{Earth} + z$. The variations in latitude ($\frac{\delta\phi}{\delta t}$) and longitude ($\frac{\delta\lambda}{\delta t}$) in each instant can be obtained by:

$$\frac{\partial\phi}{\partial t} = \frac{180}{\pi}\frac{v_{wy}}{R_{total}} \tag{2.65a}$$

$$\frac{\partial\lambda}{\partial t} = \frac{180}{\pi}\frac{v_{wx}}{R_{total}\cdot cos(\phi\frac{\pi}{180})} \tag{2.65b}$$

where ϕ is the current latitude in degrees (°).

2.7.2 Case 2: Lateral Drag is considered

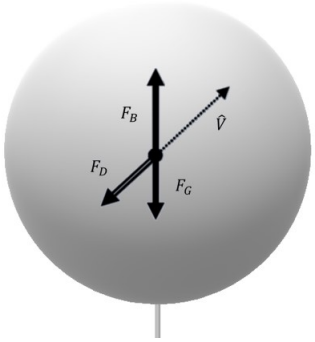

Figure 2.6: Acting forces with lateral drag considered.

If lateral drag is considered, the differential equations for the horizontal movement, since there are no forces acting horizontally except for the aerodynamic drag (in the presence of winds), are represented as:

$$\ddot{x} = \frac{F_{Dx}}{m_t + m_v} \tag{2.66}$$

$$\ddot{y} = \frac{F_{Dy}}{m_t + m_v} \tag{2.67}$$

The drag force components can be expressed by:

$$F_{Dx} = F_D \cdot \frac{v_{ax}}{v_a} \tag{2.68a}$$

$$F_{Dy} = F_D \cdot \frac{v_{ay}}{v_a} \tag{2.68b}$$

where,

$$F_D = \frac{1}{2} \cdot C_D \cdot A_p \cdot \rho_a v_a^2 \tag{2.69}$$

The component of velocity v_a represents the aerodynamic velocity which is the relative wind velocity with respect to the movement of the balloon and can be written as follows:

$$v_a = \sqrt{v_{ax}^2 + v_{ay}^2 + v_{az}^2} \tag{2.70}$$

$$\begin{cases} v_{ax} = v_{wx} - v_x \\ v_{ay} = v_{wy} - v_y \\ v_{az} = v_{wz} - v_z \end{cases} \tag{2.71}$$

The wind componets, v_{wx} and v_{wy} are obtained as explained in section 2.9.5 and the component v_{wz} is assumed to be zero. The variables v_x, v_y and v_z are the absolute velocities of the balloon.

2.8 State-Space Representation

In modern control theory, a methodology to study complex multiple-input multiple-output systems relies on a representation of such systems based on its states. The general state-space representation of a system is obtained through the state (2.72a) and output (2.72b) equations (both depending on the state vector $\boldsymbol{x}$, the input $\boldsymbol{u}$ and in some cases depending also on the perturbation $\boldsymbol{w}$ or the output noise $\boldsymbol{v}$).

$$\dot{\boldsymbol{x}}(t) = \boldsymbol{f}(\boldsymbol{x}, \boldsymbol{u}, \boldsymbol{w}) \tag{2.72a}$$

$$\boldsymbol{y}(t) = \boldsymbol{h}(\boldsymbol{x}, \boldsymbol{u}, \boldsymbol{v}) \tag{2.72b}$$

This general representation is useful for nonlinear systems since the relation of the state derivative, the state vector and the input is obtained by nonlinear functions. As explained in the previous sections, the weather balloon is a nonlinear system that will have the differential equations of velocity (vertical and lateral caused by the wind), vertical acceleration (2.61), temperature variation of the balloon film (2.50) and temperature variation of the gas (2.53). Despite that, the control strategy in this thesis will be developed based on the variation of mass in the system and, therefore, the system will have only one input named $\dot{m}_g$:

$$u = \dot{m}_g \tag{2.73}$$

If n variables are needed to completely describe the behaviour of a given system, then these n variables can be considered the n components of a vector x. Such a vector is called a state vector.

2.8.1 Balloon State-Space Model

In the balloon case, the state vector is composed of 7 states and is shown below:

$$\boldsymbol{x} = \begin{bmatrix} v_z & z & \phi & \lambda & T_f & T_g & m_g \end{bmatrix}^\top \tag{2.74}$$

The states that fully describe the system and composes the state vector (2.74) of the weather balloon are the following:

- v_z: Vertical velocity ($\frac{m}{s}$)
- z: Altitude (m)
- ϕ: Latitude ($^\circ$)
- λ: Longitude ($^\circ$)
- T_f: Temperature of the balloon film (K)
- T_g: Temperature of the gas (K)
- m_g: Mass of gas inside the balloon (Kg)

A disturbance, $\boldsymbol{w}$, caused by the presence of wind will also affect the system. As mentioned in section 2.7, v_{wy} is the latitudinal velocity of the wind and v_{wx} is the longitudinal velocity of the wind.

$$\boldsymbol{w} = \begin{bmatrix} v_{wy} & v_{wx} \end{bmatrix}^\top \tag{2.75}$$

The derivative of the states of the balloon system can be obtained from the differential equations previously exposed and represented in a state-space form such as:

$$\dot{\boldsymbol{x}} = \begin{bmatrix} \dot{v}_z \\ \dot{z} \\ \dot{\phi} \\ \dot{\lambda} \\ \dot{T}_g \\ \dot{T}_f \\ \dot{m}_g \end{bmatrix} = \begin{bmatrix} \frac{\rho_a \frac{4}{3}\pi R^3 g - \frac{1}{2} C_D \pi R^2 \rho_a v_z^2 - (m_{struc}+m_g)g}{m_{struc}+m_g+C_m \rho_a \frac{4}{3}\pi R^3} \\ v_z \\ \frac{180 v_{wy}}{\pi(r_{Earth}+z)} \\ \frac{180 v_{wx}}{\pi(r_{Earth}+z)\cos(\phi \frac{\pi}{180})} \\ \frac{H_i 2\pi R(T_f - T_g)}{\gamma c_v m_g} + (\gamma - 1) T_g (\frac{\dot{m}_g}{m_g} - \frac{dr^3}{r^3}) \\ (2.79) \\ k_v(k_h(z_r - z) - v_z) \end{bmatrix} \tag{2.76}$$

And the output will be:

$$\boldsymbol{y} = \begin{bmatrix} \phi & \lambda & z \end{bmatrix}^\top \tag{2.77}$$

The previous state equations are very complex and their representation can be difficult to read. For a better understanding of each component of these equations, their variables and what influences such variables will now be explained:

- R: Radius dependence of the temperature and mass of the gas inside the balloon $R(T_g, m_g)$. This value is obtained with the Mooney-Rivlin model presented in (2.9), where the roots of the polynomial expression give values in which the one real and positive value represents the balloon's current radius. Adding some detail to this variable, a more explicit formulation of the said polynomial equation of the model used to find the radius can be presented. Developing and multiplying the whole Equation (2.9) by R^7 it is possible to obtain:

$$\frac{p_0 k}{R_0} R^8 + P_a R^7 + p_0 R_0 R^6 - \frac{3 m_g R_g T_g}{4\pi M_{He}} R^4 - p_0 k R_0^5 R^2 - p_0 R_0^7 = 0 \tag{2.78}$$

  In this formula, p_0 represents $\frac{t_0}{R_0}$, which is the ratio between the thickness (t_0) and radius (R_0) of the balloon before inflation, k is the division of $\frac{s_-}{s_+} = \frac{-0.3}{3} = -0.1$ (the values of s_- and s_+ are presented in [21]) and R_g is the perfect gas constant ($R_g = 8.314 \frac{J}{K \cdot mol}$).

- ρ_a, P_a, T_a: The atmospheric parameters, that influence the balloon's dynamics, depend on the altitude. Then, they can be written as $\rho_a(z), P_a(z), T_a(z)$.

- C_D: The drag coefficient (that depends on the Reynolds number with correlation (2.6.3) depends on the vertical velocity (v_z), the balloon radius, $R(T_g, m_g)$, as well as on the atmosphere parameters that varies with the altitude (z). Therefore, $C_D(v_z, z, T_f, m_g)$.

- T_f equation: This equation is very long since is the sum of all heats contribution to the film,

therefore, to make the reading easier, considering $\beta = 1 + \frac{\tau}{1-r}$ and $\beta_{IR} = 1 + \frac{\tau_{IR}}{1-r_{IR}}$, this state equation can be presented as:

$$\begin{aligned}\dot{T}_f = &\frac{\alpha\pi R^2 q_{sun}\beta + \alpha_{IR}4\pi R^2 q_{IR_e} VF\beta_{IR} + \alpha 4\pi R^2 q_{alb} VF\beta + \sigma\varepsilon 4\pi R^2 T_g^4 \beta_{IR}}{m_b c_f} + \\ &\frac{H_e 4\pi R^2(T_a - T_g) - \sigma\varepsilon\alpha_{IR}4\pi R^2 T_g^4(\frac{1}{1-r_{IR}}) - H_i 2\pi R(T_f - T_g)}{m_b c_f}\end{aligned} \tag{2.79}$$

- H_i: This internal convection coefficient is a result of the following expression:

$$H_i = \frac{\left(2 + 0.45\left(\frac{\rho_g^2 g|T_f - T_g|(2R)^3}{T_g(1.895\times10^{-5}(\frac{T_g}{273.15})^{0.647})^2}(0.729 - 1.6\times10^{-4}T_g)\right)^{0.25}\right)0.144(\frac{T_g}{273.15})^{0.7}}{2R} \tag{2.80}$$

where ρ_g depends on the mass and the radius since $\rho_g = \frac{m_g}{V}$.

- H_e: This external convection coefficient depends on the maximum value between free and forced convection calculated.

$$H_{e_{free}} = \frac{\left(2 + 0.45\left(\frac{\rho_a^2 g|T_f - T_a|(2R)^3}{T_f\left(\frac{1.458\times10^{-6}T_a^{1.5}}{T_a+110.4}\right)^2}(0.804 - 3.25\times10^{-4}T_a)\right)^{0.25}\right)0.0241(\frac{T_a}{273.15})^{0.9}}{2R} \tag{2.81}$$

$$H_{e_{forced}} = \frac{\left(2 + 0.41\left(\frac{\rho_a^2 R v_z}{\frac{1.458\times10^{-6}T_a^{1.5}}{T_a+110.4}}\right)^{0.55}\right)0.0241(\frac{T_a}{273.15})^{0.9}}{2R} \tag{2.82}$$

And finally, H_e is the maximum value between these two values, that is, $max(H_{e_{free}}, H_{e_{forced}})$.

- $\dot{m}_g$: The mass only varies if the balloon is being controlled. Therefore, the equation of mass variation is obtained through Equation 3.4.

2.8.2 Linearisation

Nonlinear systems can be approximated by a linear set of equations. To obtain a linear mathematical model for a nonlinear system, one must assume that the variables deviate only slightly from some operating condition and, once the model is linearised, linear control strategies can be applied [27].

Considering a stationary flight (meaning that most derivatives of the states variables are zero), without disturbances or noise, the nonlinear state function at a working point $(\boldsymbol{x}, \boldsymbol{u}, w) = (\boldsymbol{x_o}, \boldsymbol{u_o}, 0)$ takes the form:

$$\dot{\boldsymbol{x}} = \boldsymbol{f}(\boldsymbol{x_o}, \boldsymbol{u_o}) \tag{2.83}$$

With the operation point set, the system can be locally linearised. The states $\boldsymbol{x}$ and inputs $\boldsymbol{u}$ will now represent now variations around the operating condition $(\boldsymbol{x_0}, \boldsymbol{u_0})$. To do that the first term of a Taylor Series expansion is used to obtain the matrices for the linear representation of the system.

$$\dot{\boldsymbol{x}} = \frac{\partial \boldsymbol{f}}{\partial \boldsymbol{x}}(\boldsymbol{x_o}, \boldsymbol{u_o}) * (\boldsymbol{x} - \boldsymbol{x_o}) + \frac{\partial \boldsymbol{f}}{\partial \boldsymbol{u}}(\boldsymbol{x_o}, \boldsymbol{u_o}) * (\boldsymbol{u} - \boldsymbol{u_o}) \tag{2.84}$$

$$\boldsymbol{y} - \boldsymbol{y_o} = \frac{\partial \boldsymbol{h}}{\partial \boldsymbol{x}}(\boldsymbol{x_o}, \boldsymbol{u_o}) * (\boldsymbol{x} - \boldsymbol{x_o}) + \frac{\partial \boldsymbol{h}}{\partial \boldsymbol{u}}(\boldsymbol{x_o}, \boldsymbol{u_o}) * (\boldsymbol{u} - \boldsymbol{u_o}) \tag{2.85}$$

Considering new state variables with deviations from the operating values, that is:

$$\tilde{\boldsymbol{x}} = \boldsymbol{x} - \boldsymbol{x_o} \tag{2.86a}$$

$$\tilde{\boldsymbol{u}} = \boldsymbol{u} - \boldsymbol{u_o} \tag{2.86b}$$

$$\tilde{\boldsymbol{y}} = \boldsymbol{y} - \boldsymbol{y_0} \tag{2.86c}$$

It is possible to obtain a linear system in state space with the following representation:

$$\dot{\tilde{\boldsymbol{x}}} = \boldsymbol{A}\tilde{\boldsymbol{x}} + \boldsymbol{B}\tilde{\boldsymbol{u}} \tag{2.87}$$

$$\tilde{\boldsymbol{y}} = \boldsymbol{C}\tilde{\boldsymbol{x}} + \boldsymbol{D}\tilde{\boldsymbol{u}} \tag{2.88}$$

The state matrix, $\boldsymbol{A}$ (with dimension $(n \times n)$), represents the relation between the states of the system and also defines the order of system n. Matrix $\boldsymbol{B}$ (with dimension $n \times m$) represents the influence of the inputs in the system. As for matrix $\boldsymbol{C}$ (with dimension $p \times n$), this matrix relates the output with the state variables. The last matrix is $\boldsymbol{D}$ (dimension $m \times p$), the $\boldsymbol{D}$ matrix is represents direct input to output action and its dimension is $m \times p$. These matrices $\boldsymbol{A}$, $\boldsymbol{B}$ and $\boldsymbol{C}$ and $\boldsymbol{D}$ (with a general formulation) are calculated for the operating condition as follows:

$$\begin{aligned} \boldsymbol{A} &= \begin{bmatrix} \frac{\partial f_1}{\partial x_1} & \cdots & \frac{\partial f_1}{\partial x_n} \\ \cdots & \cdots & \cdots \\ \frac{\partial f_n}{\partial x_1} & \cdots & \frac{\partial f_n}{\partial x_n} \end{bmatrix} \boldsymbol{B} = \begin{bmatrix} \frac{\partial f_1}{\partial u_1} & \cdots & \frac{\partial f_1}{\partial u_n} \\ \cdots & \cdots & \cdots \\ \frac{\partial f_n}{\partial u_1} & \cdots & \frac{\partial f_n}{\partial u_n} \end{bmatrix} \\ \boldsymbol{C} &= \begin{bmatrix} \frac{\partial h_1}{\partial x_1} & \cdots & \frac{\partial h_1}{\partial x_n} \\ \cdots & \cdots & \cdots \\ \frac{\partial h_n}{\partial x_1} & \cdots & \frac{\partial h_n}{\partial x_n} \end{bmatrix} \boldsymbol{D} = \begin{bmatrix} \frac{\partial h_1}{\partial u_1} & \cdots & \frac{\partial h_1}{\partial u_n} \\ \cdots & \cdots & \cdots \\ \frac{\partial h_n}{\partial u_1} & \cdots & \frac{\partial h_n}{\partial u_n} \end{bmatrix} \end{aligned} \tag{2.89}$$

2.9 Balloon Model Implementation

In this section, all the previously presented models will be implemented. Some models, such as wind and hyperelastic models, in which the model can be accomplished by two different methods will be implemented and compared. Finally, the altitude control design will be presented. To perform a simulation of the implemented model and altitude control, some specifications regarding the balloon's date and place of launching should be made. In Table 2.1, the information about the launching day, location and time is presented. It is assumed that the launching date of the TA450 balloon was scheduled to 25/03/2021, in Lisbon (with coordinates $(\phi, \lambda) = (38.730°, -9.140°)$), at 11h in the morning. Assuming that, at this location and time, the balloon will be released 4 times for different flight missions that endure for hours. The first launching intends to analyse how the balloon dynamics work and the others will be dedicated to flights where the altitude is controlled.

Table 2.1: TA450 date and location launching specifications

Date	25/03/2021
Location Coordinates	$(\phi, \lambda) = (38.730°, -9.140°)$

2.9.1 Balloon and Gas Parameters

The tabled parameters specified in [28] of the model TA450 is presented in Table 2.2. These are specifications made for a simple balloon with no additional structure. Only the payload, film, and initial gas mass.

Table 2.2: TA450 tabled parameters from [28]

Parameter	Symbol	Value	Units
Balloon mass	m_b	0.450	kg
Payload mass	m_p	0.250	kg
Uninflated radius	R_0	0.43	m
Radius at release	R_i	0.65	m
Burst radius	R_b	2.36	m
Latex (rubber) density	ρ_b	1100	kg/m^3

Additional weight is added to the payload the balloon carries. This weight is a product of the extra helium the balloon will need in order to adjust its altitude and velocity. For this purpose, having into consideration that a weather balloon should be light and since the TA450 model is a relatively small balloon, a lighter option for a gas cylinder with compressed gas was chosen. This cylinder will add a weight of 0.8 kg (which, as explained at the beginning of this chapter, will be named m_{cil}). The resulting values of initial mass and volume are presented in Table 2.3.

The atmosphere at launch will be considered the one at the altitude of 0 m. The values for these parameters are presented in Table 2.4.

Table 2.3: Balloon Launch Parameters

Parameter	Symbol	Value	Units
Initial Volume	V_0	1.5767	m^3
Initial Mass of Gas	m_{g0}	0.2814	kg

Table 2.4: Atmosphere parameters at launch

Parameter	Symbol	Value	Units
Temperature	T_0	288.15	K
Air pressure	P_{a0}	101325	Pa
Air density	ρ_{a0}	1.225	kg/m^3

As for helium, which is the gas considered in this simulation, the used parameters are the ones in Table 2.5.

Table 2.5: Gas parameters at launch

Parameter	Symbol	Value	Units
Molecular mass	M_{He}	$4.003 \cdot 10^{-3}$	Kg/mol
Perfect gas constant	R_g	8.315684	J/mol·K
Temperature	T_0	288.15	K
Gas pressure	P_{g0}	106913	Pa
Gas density	ρ_{g0}	0.1785	g/m^3

Note: Helium density is obtained using the perfect gas law.

2.9.2 Hyperelastic Theory Analysis

To analyse and compare both of the hyperelastic models presented in section 2.3, the parameters of the TA450 balloon model, presented in section 2.2, were implemented. Figure Figure 2.7 illustrates the behaviour for each model for radius, membrane pressure and ascent velocity evolution.

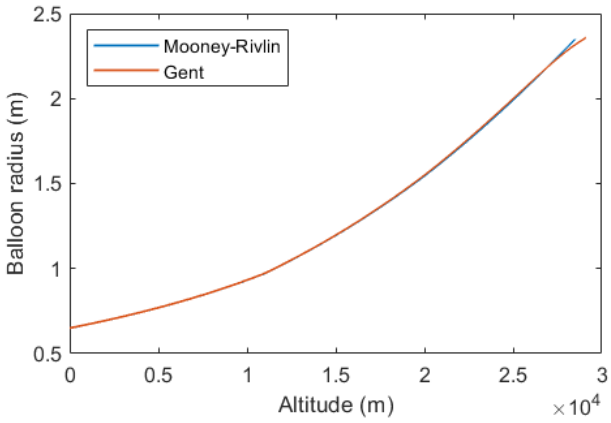

(a) Radius variation with height for both models

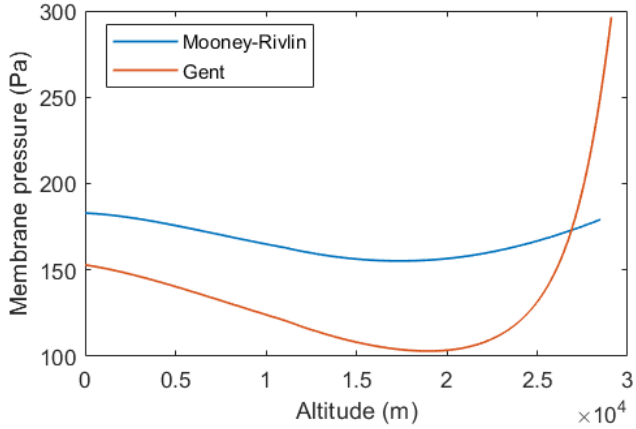

(b) Membrane Pressure variation with height for both models

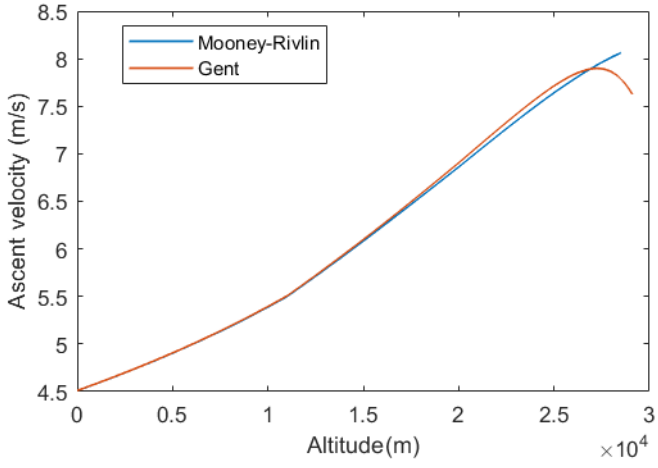

(c) Ascent Velocity variation with height for both models

Figure 2.7: Mooney-Rivlin and Gent models comparison of radius, membrane pressure and ascent velocity evolution.

Both of these models could be used as hyperelastic models that that better represent the balloon elastic behaviour than the typical non-elastic models. Since one of them should be chosen to model the

balloon system the following analysis was made:

- **Radius:** Comparing the radius curves it is possible to see they are very similar. The only small difference between them is at the end when the balloon is about to burst and it is shown that the Gent model presents the burst for an altitude value a little superior to the Mooney Rivlin model. However, it is not big enough to be relevant (only about 600 m). This similar behaviour is due to the pressure tendency balance between the helium inside the balloon and the air outside. Since the outside pressure is continuously decreasing, the helium that is inside the balloon tends to expand reducing the internal pressure.

- **Membrane pressure:** The membrane pressure (which is the difference between the inlet and outer pressure) presents very small values for both models when compared to the atmospheric pressure at sea level. For the Gent model, the membrane pressure reaches a minimum value slightly bigger than 100 Pa. In this model, as it represents the stiffening that the rubber undergoes when it is near the bursting point, at the highest altitude is seen that the membrane pressure increases up to 300 Pa. In the Mooney-Rivlin model, the membrane pressure value varies little during the balloon flight, and the values are near the value of 175 Pa. As was shown, depending on the model, some differences can be found. The Mooney-Rivlin model assumes a slightly bigger membrane pressure value (in average) throughout the whole range of altitudes, while the Gent model presents a big increase of membrane pressure when it is near the bursting point.

- **Ascent velocity:** The ascent velocity is very similar in both cases, presenting a bigger difference at the end of the flight where the Gent model, for taking into account the stiffening of the rubber, presents a decreasing velocity, while the Mooney-Rivlin model does not.

The models in the above analysis present a very similar behaviour when representing the radius evolution as well as the ascent velocity. Despite the membrane pressure being slightly different between these models, it is not enough to be what defines which model should represent the elastic behaviour of the balloon. However, the Mooney-Rivlin model was chosen in this thesis. This choice was influenced due to the fact that, as explained in section 2.3, Gent models parameters can be laborious to measure precisely and are very dependent on destructive testing.

2.9.3 Thermal Model Implementation

The process of this implementation begins with the calculation of each thermal component that influences the system's temperature and then the inclusion of these components in the differential equations of the film and the gas. The necessary and most important equations for this implementation can be consulted in section 2.5. The first step, that will lead to the beginning of the calculation of each thermal contribution, is the search for the elevation angle of the sun.

Solar elevation angle

The elevation angle, as shown in Figure 2.8, is defined as the angle between the direction of the sun and the horizon [29]. This angle is necessary since the position of the sun (that depends on the day of the year and the time of the day) will influence the intensity of the solar radiation. For this purpose, an algorithm that better demonstrates this step was developed and can be seen in algorithm 1.

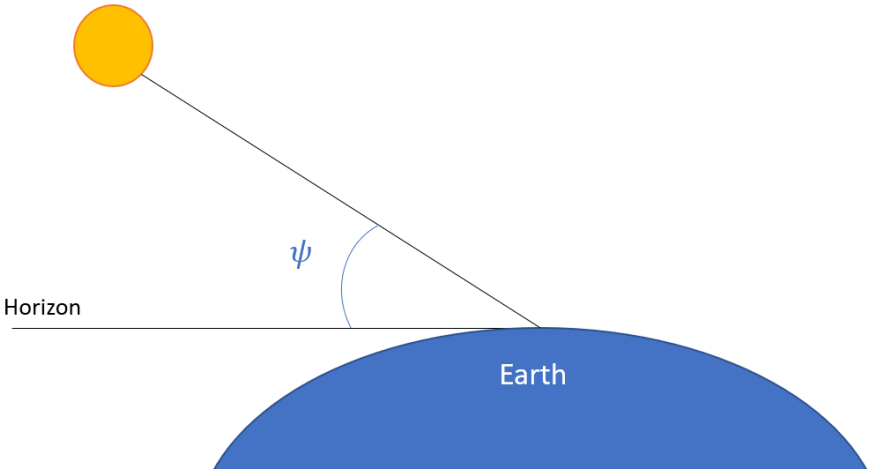

Figure 2.8: Elevation angle of the sun (ψ) and the horizon representation.

Algorithm 1 Elevation Angle of The Sun

function ELEVATION($lat, long, day, month, year, hour, min, sec$) ▷ The elevation angle of the sun for a specific time of year
  $g = g_1 + g_2 D$ ▷ Mean anomaly of the Sun
  $q = q_1 + q_2 D$ ▷ Mean longitude of the Sun
  $L = q + L_1 \sin(g) + L_2 \sin(2g)$ ▷ Ecliptic longitude of the Sun
  $b = 0$ ▷ Ecliptic latitude of the Sun
  $e = e_1 - e_2 D$ ▷ Mean obliquity of the ecliptic
  $RA = \arctan\left(\frac{\cos(e)\sin(L)}{\cos(L)}\right)$ ▷ Sun's right ascension
  $\delta = \arcsin(\sin(e)\sin(L))$ ▷ Sun's declination
  $T = \frac{D}{t}$; ▷ Julian centuries
  $\theta_0 = a_1 + a_2 D + a_3 T^2 - \frac{T^3}{a_4}$ ▷ Sidereal time at Greenwich
  $\theta = \theta_0 + long$ ▷ Local sidereal time
  $LHA = \theta - RA$ ▷ Local hour angle
  $\psi = \arcsin(\sin(lat)\sin(\delta) + \cos(lat)\cos(\delta)\cos(LHA))$
  return ψ ▷ The Elevation angle of the Sun
end function

While implementing this algorithm is important to know that the date should be converted to the Julian calendar (JD) (its calculation can be consulted in [30]) and to compute the number of Julian days and fractions (D) from a reference epoch (the expression $D = JD - 2451545.0$ can be used). All coefficients from this algorithm are in Table B.2.

After this first step is completed, all the components that contribute to the thermal balance of the system should be calculated. For this, the following procedure should be followed:

Algorithm 2 Thermal variation $(\dot{T}_f, \dot{T}_g)$ calculation.

procedure THERMAL VARIATION$(T_a, T_f, T_g, z, v_z, R, \rho_a, m_g)$ ▷ Corresponding equations
  Calculate A_p and A_s
  Find Q_{Sun} ▷ Eq. 2.15, 2.16, 2.17,2.18, 2.19, 2.20
  Find $Q_{IREarth}$ ▷ 2.21, 2.22
  Find Q_{Albedo} ▷ 2.25,2.26
  Find Q_{IRfilm} ▷ 2.36
  Find Q_{IRout} ▷ 2.27
  Calculate μ, k and Pr for gas and air ▷ 2.44,2.45,2.46,2.47,2.48,2.49
  Find $Q_{ConvInt}$ ▷ 2.37,2.38,2.39,2.40
  Find $Q_{ConvExt}$ ▷ 2.28,2.29,2.30,2.31,2.322.33,2.34,2.35
  $\dot{T}_f$ ▷ 2.50
  $\dot{T}_g$ ▷ 2.53
end procedure

2.9.4 Thermal Model Parameters

- *Film Radiative Properties*

Film radiative properties are vital to the correct prediction of the balloon flight performance. Yet the exact knowledge of these properties can be very challenging. Due to the large variety of film types and film coatings, thermal radiative properties can be completely different for different balloons, giving distinct ascent characteristics to balloons. As explained in section 2.5, α (which is the total solar absorptivity of the external surface) and τ (the atmosphere transmissivity) are necessary to compute the solar contribution to the thermal system. The information about the surface radiative properties shown in Table 2.6 and Table 2.7, is obtained from [31].

Table 2.6: Optical Properties of the film for direct solar radiation

Transmissivity	τ	0.61
Absorvity	α	0.35
Reflectivity	$r = 1 - \alpha - \tau$	0.04

Table 2.7: Optical Properties of the film for infrared radiation

Transmissivity	τ_{IR}	0.86
Absorvity	α_{IR}	0.1
Reflectivity	$r_{IR} = 1 - \alpha_{IR} - \tau_{IR}$	0.04

- *Albedo*

The Albedo coefficient varies depending on the type of surface below the balloon.

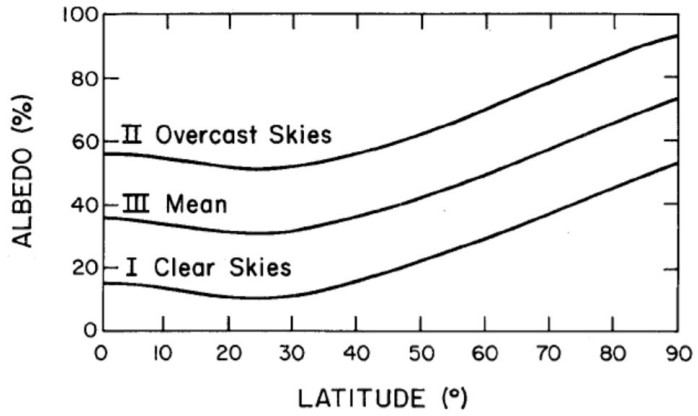

Figure 2.9: Albedo coefficient for different latitudes and meteorological conditions (from [31])

As shown in Figure 2.9 it is possible to see the different values of the albedo coefficient for different meteorological conditions and different latitude values. An average value was chosen to implement the thermal contribution of albedo. For this purpose, a value of $Albedo = 0.12$ is the chosen mean value to represent this contribution. Another important note is that since the heat the balloon receives from albedo depends on the elevation angle, when is nighttime and the elevation angle is negative, the albedo is 0.

- *Heat Transfer Parameters*

Table 2.8: Heat transfer parameters

Parameter	Symbol	Value	Units
Adiabatic expansion coefficient	γ	1.667	-
Specific heat (helium)	c_v	3115.89	$Jg^{-1}K^{-1}$

2.9.5 Wind Data and Model Analysis

Wind Data Acquisition

NOMADS servers:

The wind information required to represent the horizontal movement of the balloon is obtained from NOAA (National Oceanic and Atmospheric Association) servers. NOAA provides weather forecasts, ocean and coast data and the wind database can be found in NOMADS (NOAA Operational Model Archive and Distribution System), where global and regional models of statistical and forecast wind data are stored. For this work, the GFS (Global Forecast System) will be used. GFS output is posted to a maximum precision of 0.25 degrees (in longitude and latitude) with a temporal resolution of 1 hour out to 120 hours and data for various vertical standard pressure levels. NOMADS server provides a "grib" file that contains the global wind velocity data.

The "nctoolbox":

The wind data must be downloaded and stored in structures and matrices to be processed and used. Since the obtained data is in the "grib" format, one must access a useful MATLAB toolbox named "nctoolbox". This toolbox provides read-only access to GFS data model dataset in MATLAB. Using the "nctoolbox", it is possible to read the forecast data into a data structure from which 4D vectors for the longitudinal and latitudinal components for the wind velocity can be obtained. These vectors receive time, latitude, longitude and pressure as inputs. An example of the wind data acquired (with 0.25 degree precision) can be seen in Figure 2.10. In the presented image, v_{wx} (representing the longitudinal velocity) and v_{wy} (representing the latitudinal velocity) for a fixed latitude, longitude and time, is shown. The data obtained for different pressures is represented graphically as a function of height (until 25 km).

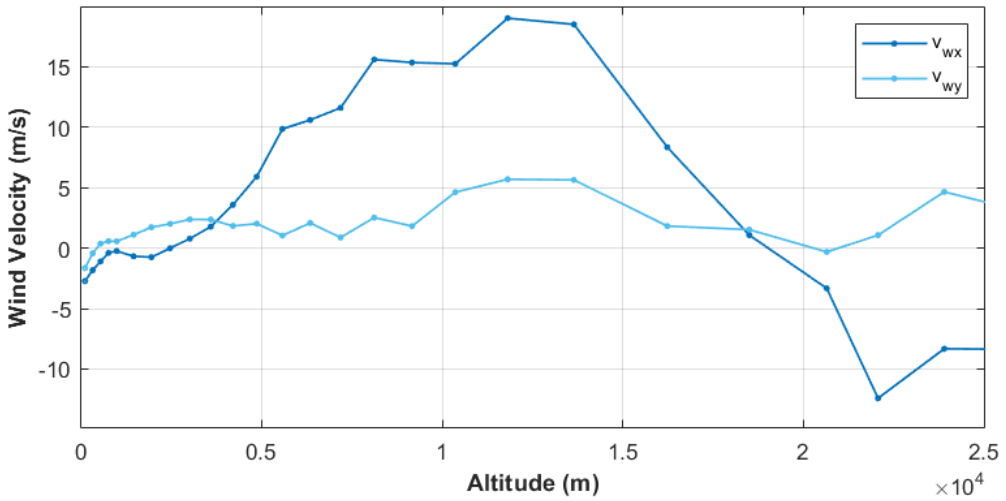

Figure 2.10: Wind data from the NOMADS server for a fixed latitude (53^{o}) and fixed longitude (350^{o}).

To interpolate wind velocity values for values different from the ones given by the NOMADS servers, a Simulink *lookup table* block was used.

Comparative Analysis of Wind Implementation

Given the two approaches the wind implementation in the model may have, once again, it is important to compare both and understand which one to choose for the TA450 model. For this purpose, both cases were implemented and compared. After the wind forecast data was obtained from the NOMADS servers, this data was used in the implementation and the models were analysed. In this analysis, it was considered that the initial point had the latitude and longitude at zero degrees.

The graph represent the degrees (of latitude and longitude) as a function of time for both of the previous cases and the error to evaluate if the difference between them is big enough to be considered.

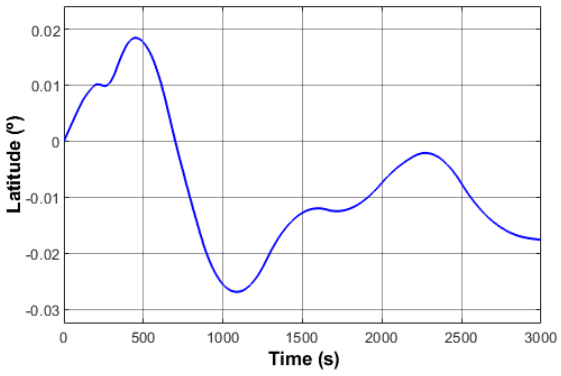

(a) Latitude variation with time.

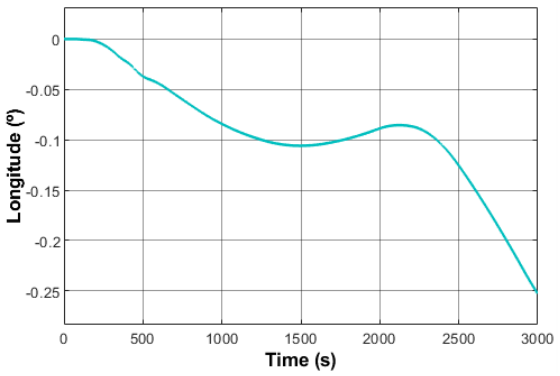

(b) Longitude variation with time.

Figure 2.11: Case 1: The weather balloon's velocity is the same as the wind.

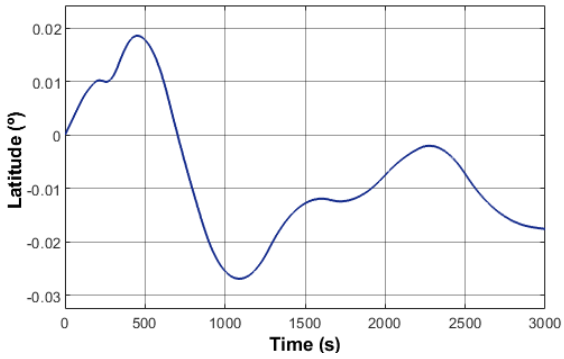

(a) Latitude variation with time.

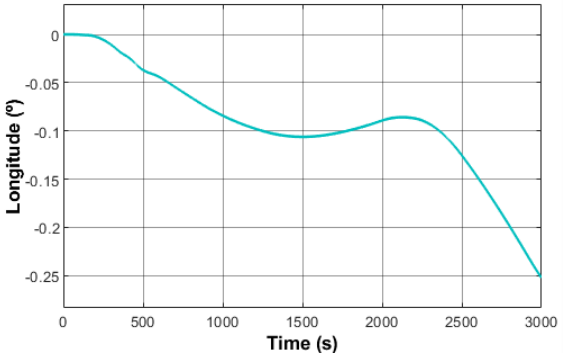

(b) Longitude variation with time.

Figure 2.12: Case 2: Lateral Drag is considered.

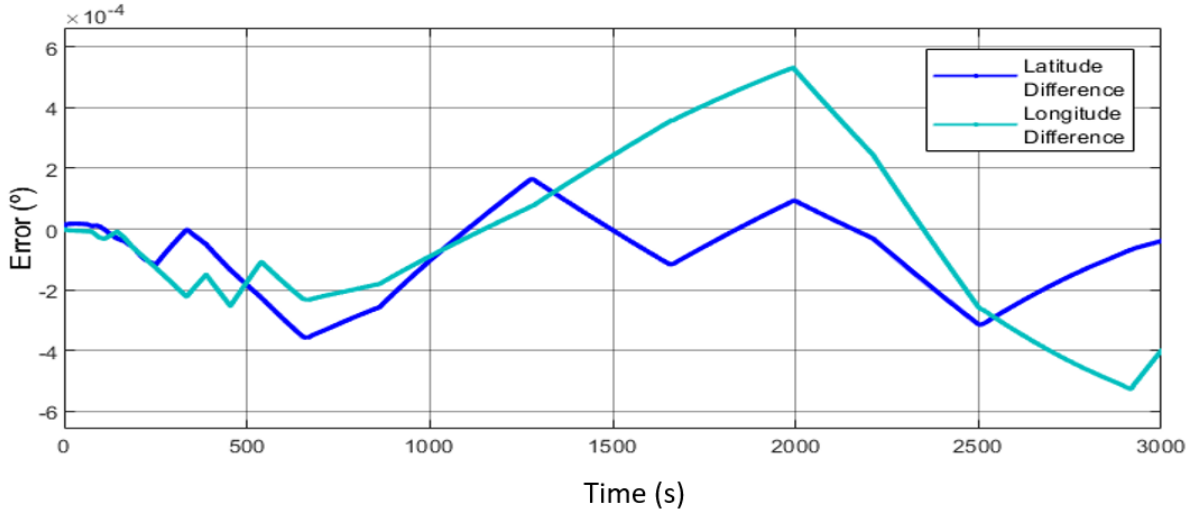

Figure 2.13: Evolution of the difference between latitude and longitude (in degrees) obtained in "Case 1" and "Case 2" with time (in seconds).

"Case 1" and "Case 2" Analysis: As one can see, in Figure 2.11 and Figure 2.13, there are very

few differences between these cases. It could either be difficult to understand that there are differences between them without numerical data to justify it. Therefore, by subtracting the latitude and longitude values of "Case 2" from "Case 1", the information from Figure 2.13 was obtained. Given that, as seen in Figure 2.13, there were no big differences between the two cases (as the maximum difference, in absolute value, was in the order of $5.31 \times 10^{-4\circ}$ for longitude and $3.56 \times 10^{-4\circ}$ for latitude), the assumption that there is no horizontal slip between the balloon and the surrounding air mass and that the deformation and rotation of the balloon due to the incident wind are not considered can be made. Since choosing one case or the other does not affect the overall system, the horizontal motion can be simplified to the simpler case. Therefore, after the shown results were obtained and analysed, it was decided to choose the first and simpler case as the one to continue in the implementation and to be included in the balloon model.

3 Altitude Control Design and Implementation

The theory behind the altitude control strategy designed in this thesis will be explained in this chapter. Then, in the last part of the chapter, the implementation of the control design is made.

3.1 Altitude Control

The control strategy proposed in section 3.2 will be performed in the first two states of the system, the altitude and the velocity, having the final objective of positioning the weather balloon in reference altitude.

This control strategy is based on the actuation of a valve, responsible for inflow and outflow of gas. The valve will be considered ideal. This means that it was assumed that the valve will supply the exact amount of gas that the control action commands to enter the weather balloon. This also means that the dynamic behaviour of the valve (if modelled and considering, for example, a first order transfer function to represent it) would have a time constant of 0 s. These were simplifications done to the valve model so the control could be easier to design. However, if for future work a more complete modelling of the valve is needed, in Appendix A, a linear valve model was presented and it can be used for future development.

The chosen control solution intends to be simple and yet accurate to achieve the mission objectives. In order to execute the control, it was chosen to use a cascade control strategy (section 3.1.1) with controller gains for velocity and altitude developed with the Linear Quadratic Regulator algorithm (section 3.1.3) implemented through Gain Scheduling (section 3.1.2). The Gain Scheduling technique allows the nonlinear system to be controlled in a simple and effective way. The theory coupled with the valve actuation and control technique will be exposed in the following sections presented in this chapter.

3.1.1 Altitude and Velocity Control

In order to control the altitude, it is necessary to remember that weather balloons are very unstable. Many external factors can influence the maintenance of the balloon at a defined altitude. Despite that, another factor to consider is the high influence the fast dynamics of vertical velocity has under altitude control. If the velocity is not considered while performing control, the amount of mass entering the weather balloon can cause the velocity to reach uncontrollable high values. Therefore, to avoid the

vertical velocity from being uncontrollable, one should have into consideration that controlling not only the altitude but also the balloon's vertical velocity, can result in a better overall altitude control. With this in mind, a cascade control strategy was chosen to solve the presented problem.

A typical configuration for cascade control is shown in Figure 3.1. The geometry of this block diagram defines an inner loop involving the secondary controller and an outer loop involving the primary controller. The inner loop functions like a traditional feedback control system with a set-point, a process variable, and a controller acting on a process employing an actuator. The outer loop is similar but uses the entire inner loop as its actuator. The inner loop is originated from the introduction of an additional sensor to separate, as much as possible, the fast (inner loop) and slow (outer loop) dynamics of the process [32].

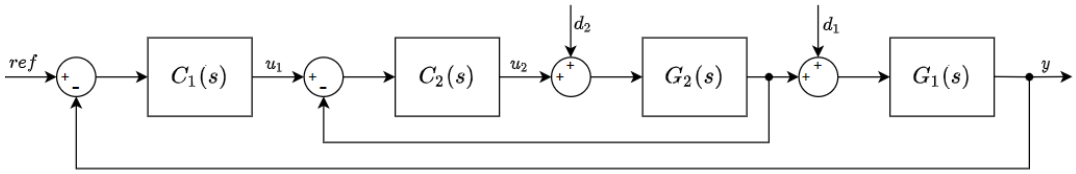

Figure 3.1: Cascade control general representation. The inner loop is composed of C_2 and G_2, while the outer loop is composed of C_1 and G_1.

3.1.2 Gain Scheduling

The weather balloon presents a highly nonlinear behaviour. Nonlinear systems can be controlled with nonlinear control or they can be lineasired so linear control strategies can be applied. While developing a controller, since there are many ways a system can be controlled, one must take into consideration the complexity of the proposed solution and the environment surrounding it. Nonlinear controllers are more complex to design than linear controllers and they can also be more sensitive to parameter variation [33]. For this and other limitations, nonlinear control brings, a linear control was chosen. Since the weather balloon presents different behaviour for different altitudes, a gain scheduling procedure was applied as a linear control strategy to the linearised model. Gain scheduling is an effective approach and a common technique for controlling nonlinear systems with dynamics changing from one operating condition to another. This method can be used when a single set of controller gains does not provide desired performance and stability throughout the entire range of operating conditions of the model [34]. This procedure is based on linear parameter-varying plant models and it can be developed through linearisation about an operation point.

The design of a gain scheduled controller for a nonlinear model follows a sequence of steps. The first one is to compute a linear parameter-varying model for the plant. The most common approach is based on Jacobian linearisation (which is explained in section 2.8.2) of the nonlinear model about a family of trim points, also called operating points. This yields a parametrised family of linearised models and forms the basis for what we call linearisation scheduling. Sequentially, the following step is to use linear design methods to design linear controllers for the linear parameter-varying plant model (which will be done with LQR). This design process may result directly in a family of linear controllers, or there may be an interpolation process to arrive at a family of linear controllers from a set of controller designs

at isolated values of the scheduling variables. Finally, the last step involves implementing the family of linear controllers such that the controller coefficients (gains) are varied (scheduled) according to the current value of the scheduling variables.

In the end, this process presents various advantages. Gain scheduling employs powerful linear design tools on difficult nonlinear problems, it does not require severe structural assumptions for the model. Finally, this method enables a controller to respond rapidly to changing operating conditions.

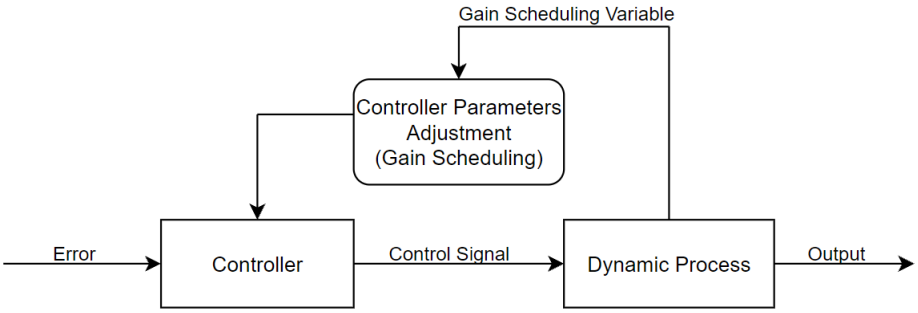

Figure 3.2: Gain Scheduling scheme.

3.1.3 Linear Quadratic Regulator

The Linear Quadratic Regulator algorithm consists on an optimisation problem in which the quadratic performance index (3.1) is minimised, subject to the system's dynamics $\dot{\boldsymbol{x}}(t) = \boldsymbol{A}\boldsymbol{x}(t) + \boldsymbol{B}\boldsymbol{u}(t)$, to determine the matrix of gains $\boldsymbol{K}$ of the optimal control vector (3.2).

$$J = \int_0^t \left(\boldsymbol{x}^\top(t)\boldsymbol{Q}\boldsymbol{x}(t) + \boldsymbol{u}^\top(t)\boldsymbol{R}\boldsymbol{u}(t)\right)dt \tag{3.1}$$

$$\boldsymbol{u}(t) = -\boldsymbol{K}\boldsymbol{x}(t) \tag{3.2}$$

If the pair of matrices $\boldsymbol{A}$ (dynamics matrix) and $\boldsymbol{B}$ (the input matrix associated with the state-space representation) is controllable (which means that the rank of the controllability matrix is equal to the system's dimension), the LQR problem can be solved following the next steps [27]:

- Define the cost matrices $\boldsymbol{Q}$ and $\boldsymbol{R}$:

  $\boldsymbol{Q}$, is the relative importance of energy associated with the state. The bigger the weight in the entries of this matrix, the more important is to bring that state to zero. This matrix is real and symmetric.

  $\boldsymbol{R}$, is the relative importance of energy associated with the control action. This matrix is real and symmetric.

- Solving the Algebraic Riccati Equation:

The Algebraic Riccati Equation (or ARE) is given by

$$\mathbf{0} = \boldsymbol{A}^\top + \boldsymbol{P}\boldsymbol{A} - \boldsymbol{P}\boldsymbol{B}\boldsymbol{R}^{-1}\boldsymbol{B}^\top\boldsymbol{P} + \boldsymbol{Q} \tag{3.3}$$

and the solution obtained is matrix $\boldsymbol{P}$.

- Obtaining the optimal gains $\boldsymbol{K}$: After the previous steps are completed, the gain vector can be obtained with $\boldsymbol{K} = \boldsymbol{R}^{-1}\boldsymbol{B}^\top\boldsymbol{P}$

The matrices Q, R and P are tuning parameters of the optimal control design.

3.2 Control Design Implementation

The general model of the weather balloon system coupled with the altitude control can be represented by the block diagram represented in Figure 3.3.

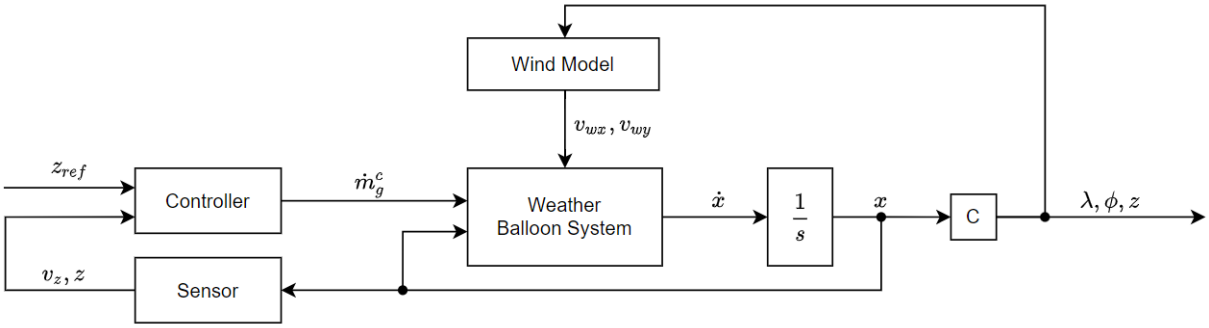

Figure 3.3: General block diagram for the developed weather balloon model and altitude control.

In this diagram it is possible to see that a reference altitude z_{ref} enters the controller, that also receives the signal of the actual vertical velocity and altitude of the weather balloon. Then the controller, through a cascade control strategy sends the control action (represented by the command variable, $\dot{m}_g^c$) to the weather balloon system. This system's output is $\dot{\boldsymbol{x}} = \begin{bmatrix} \dot{v}_z & \dot{z} & \dot{\phi} & \dot{\lambda} & \dot{T}_b & \dot{T}_f & \dot{m}_g \end{bmatrix}^\top$, the state derivatives, then, through the integrator, it is possible to obtain the state vector, $\boldsymbol{x}$, that feeds back the vertical velocity and altitude to the controller (with a sensor, which measures the values these two states). A block C appears to represent the output variables, ϕ, λ and z (representing the balloon position), that are selected from the vector $\boldsymbol{x}$ of states. These variables are not only the output of the system but also the variables that enter the "Wind Model" block, that is, they are entries of the wind model used, therefore, are responsible for the horizontal movement (caused by v_{wx} and v_{wy}) of the weather balloon.

3.2.1 Control Implementation

As explained in the Figure 3.1, the weather balloon presents two different dynamics regarding altitude and vertical velocity. One is faster than the other, and this led to the implementation of a cascade control

strategy to be applied. Bringing the general formulation of cascade control to the weather balloon, the inner loop will be formed by the faster dynamics which is the vertical velocity and the outer (and primary) loop the slower dynamics, the altitude.

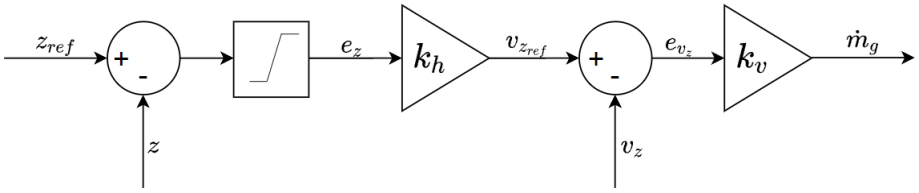

Figure 3.4: Cascade controller applied to the weather balloon.

$$\dot{m}_g = k_v(k_h(z_{ref} - z) - v_z) \tag{3.4}$$

$$z_{ref} - z \in [-500, 500] \tag{3.5}$$

This block diagram represents the inner loop containing the velocity control, and the outer loop containing the altitude control. In the first sum point, enters the reference altitude, z_{ref}, to which the variable z (the altitude) is subtracted, representing the altitude error. This error, e_z, is comprehended in a range of values, as Equation 3.5 suggests, through a saturation block. This error is then multiplied by the altitude gain k_h and is the representation of the reference velocity. This means that, as the weather balloon is closer to the reference altitude (tending to zero), the reference velocity tends to zero. The result is the velocity error, e_{v_z}, which is multiplied by the velocity gain, k_v. This control action will be assumed to be the mass variation needed by the weather balloon, $\dot{m}_g$.

Linearisation

As already mentioned in section 2.8.2, the initial step to linearise is to define the operation point (or, as some may call, trim point). The trim points corresponds to a set of values of the states, $\boldsymbol{x_o}$, and inputs, $\boldsymbol{u_o}$, that are expected to be operating conditions of the system. Due to the complexity of the modelling equations of the system, the trim points cannot be found analytically. Using the "Linear analysis tool" from MATLAB and introducing some restrictions to the velocity and altitude that were expected for the balloon a set of values that composes different operation points were obtained. It was decided to linearise the weather balloon model for a set of 9 operation points corresponding to different altitudes. These altitudes had a gap of 1 km between them and the points were prom 15 km to 23 km. The process of linearisation will now be demonstrated for one trim point (with an altitude of 15000 m) and other trim points can be consulted in section A.2:

$$u_o = 0 \tag{3.6}$$

This value of u_o was used for all cases of different trim states.

$$x_{o1} = \Big[0, 15000, 307, 307, 0.181\Big]^T \tag{3.7}$$

It can be observed that although the balloon system has 7 state variables, only 5 of them are included in the linearisation process. This happens since that the variables that correspond to the wind, which are 2 (ϕ and λ), are not included in the linearisation. These variables are perturbations in the system and they do not influence the vertical movement in any way, nor is influenced directly through the input of the system.

The linearisarion process (which was also made with the "Linear analysis tool"), was made in order to obtain the gains for velocity and altitude that will be controlled with a Gain Scheduling strategy. Therefore, although there was only one trim point shown, there were different trim points for different altitudes and there will also be many linearised models to find the necessary gains. For exemplification purposes in this part, only the linearisation for the first trim point (u_o, x_{o1}) will be shown. The linearisation of the nonlinear dynamics for this operatin condition resulted in:

$$\dot{\boldsymbol{x}} = \begin{bmatrix} \dot{v}_z \\ \dot{z} \\ \dot{T}_f \\ \dot{T}_g \\ \dot{m}_g \end{bmatrix} = \begin{bmatrix} -0.0001 & 0 & 0.0213 & 0 & 32.5815 \\ 1.0000 & 0 & 0 & 0 & 0 \\ 0 & 0.0043 & -0.4748 & 0.0104 & 154.2737 \\ 0 & 0.0002 & 0.0071 & -0.0761 & 0.9614 \\ 0 & 0 & 0 & 0 & 0 \end{bmatrix} \begin{bmatrix} v_z \\ z \\ T_g \\ T_f \\ m_g \end{bmatrix} + \begin{bmatrix} 0 \\ 0 \\ 1131.3 \\ 0 \\ 1.0 \end{bmatrix} \dot{m}_g \tag{3.8}$$

Controller Gains - LQR

With the linearisation done, it is possible to apply the LQR procedure. As already explained in section 3.1.3, to find the optimal LQR gains, it is necessary to apply the optimization procedure that is composed of three main steps. First, define the cost matrices Q and R, then find the matrix P obtained by the ARE equations and, finally, obtain the optimal gains.

1. Definition of the weights Q (relative importance of the energy associated with the state) and R (relative importance of the energy associated with the control action). Both of these matrices are real symmetric matrices. The weights that compose matrix Q must take into consideration the states that are important to be controlled to zero. In the weather balloon case, this weight will be bigger for the vertical velocity. With this in mind the following matrix Q was chosen:

$$Q = \begin{bmatrix} 5 & 0 & 0 & 0 & 0 \\ 0 & 0.007 & 0 & 0 & 0 \\ 0 & 0 & 0 & 0 & 0 \\ 0 & 0 & 0 & 0 & 0 \\ 0 & 0 & 0 & 0 & 0 \end{bmatrix} \tag{3.9}$$

As for the matrix R, this penalisation of the control action will be given by:

$$R = 100 \tag{3.10}$$

2. Resolution of the ARE (Riccati algebraic equation) given by $A^T P + PA - PBR^{-1}B^T P + Q = 0$, in order to P.

$$P = \begin{bmatrix} 2.0196 & 0.0750 & 0.0085 & 0 & 13.1293 \\ 0.0750 & 0.1899 & 0.0003 & 0 & 0.4838 \\ 0.0085 & 0.0003 & 0.0001 & 0 & 0.1022 \\ 0 & 0 & 0 & 0 & 0.0003 \\ 13.1293 & 0.4838 & 0.1022 & 0.0003 & 182.1691 \end{bmatrix} \tag{3.11}$$

3. Finally, knowing that $K = R^{-1}B^T P$, the gains K are found.

   The gains obtained with the shown data was:

$$K = \begin{bmatrix} 0.22692 & 0.00836 & 0.00173 & 0 & 2.97841 \end{bmatrix} \tag{3.12}$$

   in which the vertical velocity gain is $k_v = 0.22692$ kg/m and the altitude gain is $k_h = 0.00836$ s^{-1}.

This process is then repeated for the rest of the trim points. It is important to remember that Q, and R both allow the tuning of the controllers to obtain a better response of the system. So, if necessary, changes can be made in the process for better controller gains.

4 Simulation Results and Discussion

In this chapter, four different simulations for the implemented balloon model will be presented. One simulation is dedicated to the free dynamics of the weather balloon modelled. Three other simulations are presented in which the balloon is controlled.

4.1 Problem Definition

The project SONDA (presented in section 1.1), suggests that the wind currents direction can be used to determine the weather balloon trajectory to achieve a specified direction. As already explained in section 2.7, the wind presents different velocities and velocities directions for different altitudes in the atmosphere (as Figure 4.1 illustrates). To use these wind currents as guidance for the horizontal movement of the balloon, it is necessary to develop control solutions that allow the weather balloon to fly, in a stable way, through a reference altitude in which the wind current direction corresponds to the intended direction wanted for the balloon. In this thesis, as mentioned in section 3.1, it was implemented a cascade control strategy in the weather balloon that allowed the altitude and velocity to be controlled. In this chapter, the results of the balloon model and altitude control developed in the previous chapter will be presented and analysed.

Figure 4.1: Using the wind current directions as lateral movement guidance through altitude control of a weather balloon. Image from the discontinued Google project LOON [35].

4.2 Weather Balloon Model Simulation

After implementing the models developed in chapter 2, it is possible to obtain the evolution of temperature, LLA components, velocity and mass variation in the balloon through the flight. The simulation

of the TA450 weather balloon free flight had a duration of approximately 1 hour and 48 minutes (6585 s) and was done with the parameters shown in section 2.9.

The altitude and velocity evolution for the free weather balloon flight were the following:

As one can observe, for the vertical velocity, the simulation resulted in a velocity profile that initiates suddenly in the first seconds representing the ascension of the balloon from 0 m/s until approximately 1.5 m/s. Then a small (and sudden) change of velocity occurs near the 4000 s and after that, the curve continues to increase until the maximum vertical velocity value that was 6.182 m/s. As for the altitude evolution, the curve evolves until the maximum altitude of 24140 m with no unexpected changes in altitude.

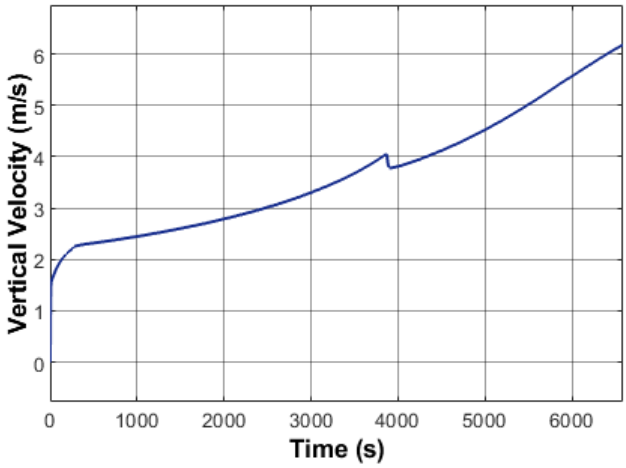

(a) Vertical velocity (m/s)

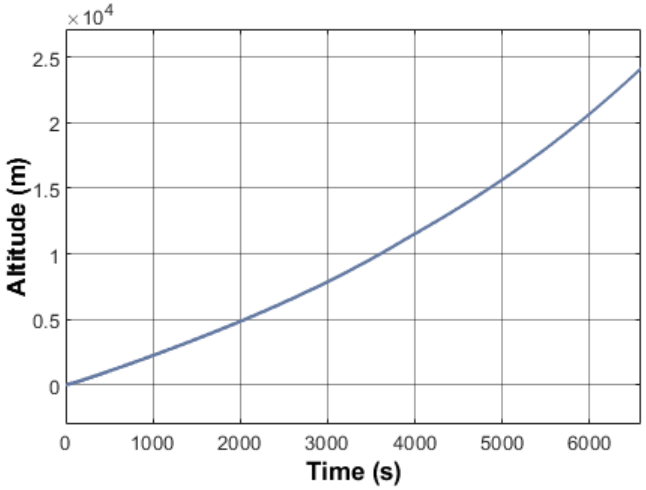

(b) Altitude (m)

Figure 4.2: Vertical velocity (v_z) and altitude (z) evolution with time for a free weather balloon flight.

As mentioned, there are two specific moments in velocity in which sudden changes in its profile occur. As the following figure shows, since the simulation is for 6585 s, some details might be lost when the graphic evolution is shown. For a better analysis Figure 4.3, with detailed views, was created.

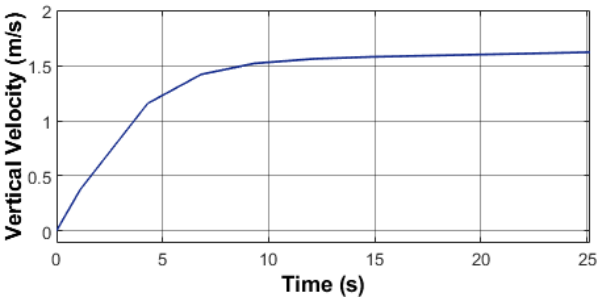

(a) Vertical velocity profile of the ascension phase of the weather balloon.

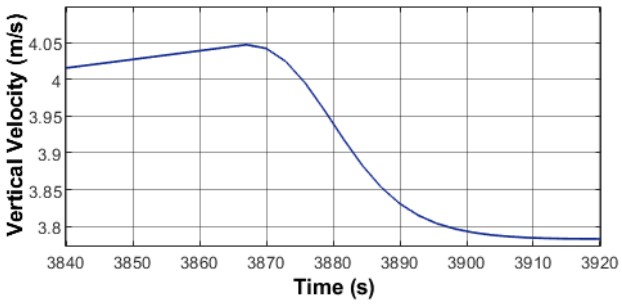

(b) Vertical velocity profile of the transition phase of the weather balloon.

Figure 4.3: Detailed view of sudden changes of vertical velocity evolution with time for a free weather balloon flight.

Weather balloons usually face a "drag crisis" that corresponds to a transition phase in the flight. This phase can be seen in Figure 4.3(b), when the velocity profile suddenly decreases when the simulation approximates to 4000 s. This simulation time corresponds to the altitudes where this transition occurs for weather balloons, as is shown in [36]. The Drag coefficient, C_D, evolution with Reynolds, Re, for this simulation is shown in Figure 4.4.

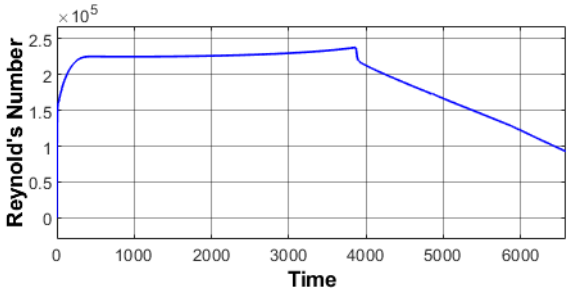

(a) Reynolds number, Re, variation with time.

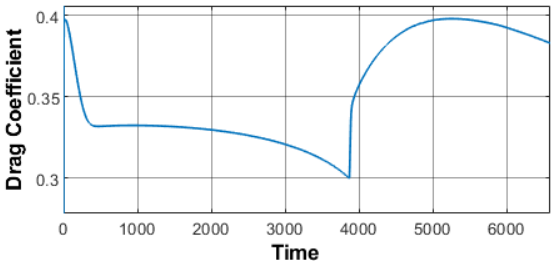

(b) Drag coefficient, C_D,variation with time.

Figure 4.4: Reynolds number (R_e) and drag coefficient (C_D) evolution with time for a free weather balloon flight.

The profile in Figure 4.3(b), results from a changing drag coefficient that depends on Reynolds number, therefore depending on the velocity itself. For a constant drag coefficient, such changes would not occur.

For the most part of the flight, the drag coefficient stays between 0.3 and 0.35. It is also possible to

see the low value in the drag coefficient occurring in the same area that the vertical velocity suffers a sudden change. After 4000 s, as Reynolds decreases, the drag coefficient increases having its maximum at 0.3982 (at t=5231 s).

The corresponding temperature evolution with time through this simulation, for both the gas and the balloon film, can be seen in Figure 4.5.

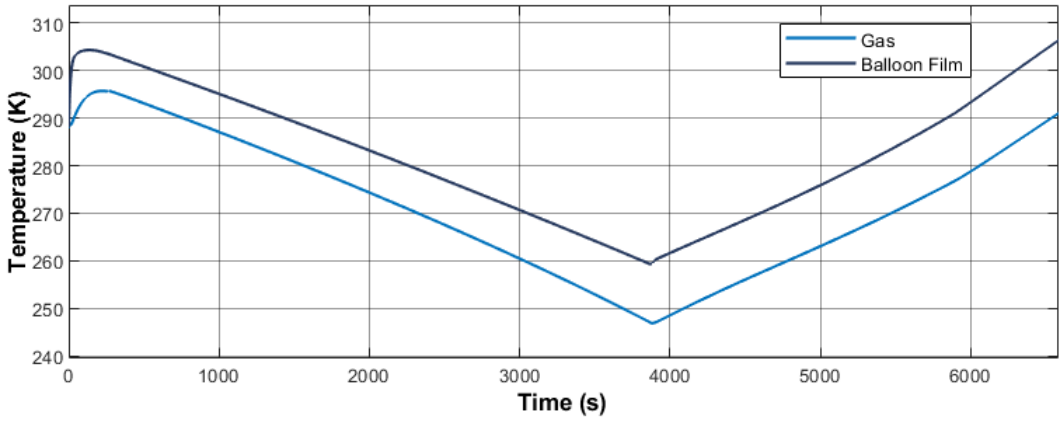

Figure 4.5: Film and gas temperature (K) evolution with time for a free weather balloon flight.

The temperature evolution will present similar profiles for both the gas and the balloon film since one (the balloon film) influences the other (the gas). As expected, since the atmosphere temperature decreases, until approximately 11000 m, the temperature evolution in the balloon is expected to decrease until this height and then, as the atmosphere temperature is constant until 25000 m, the weather balloon increases due to, mainly, the direct sun radiation and other thermal contributions.

The simulated wind velocity and influence on the horizontal movement of the weather balloon (Figure 4.6), presented the following profiles:

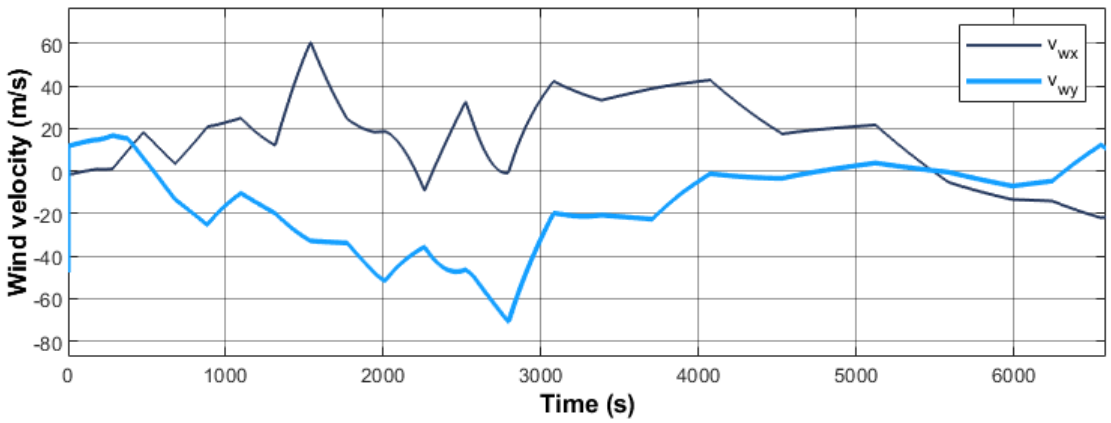

Figure 4.6: Longitudinal (v_{wx}) and latitudinal (v_{wy}) velocities evolution with time for a free weather balloon flight.

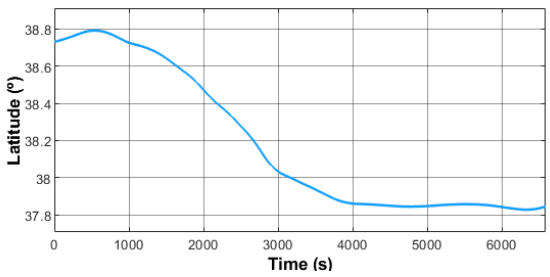

(a) Latitude (°) evolution with time for a free weather balloon flight.

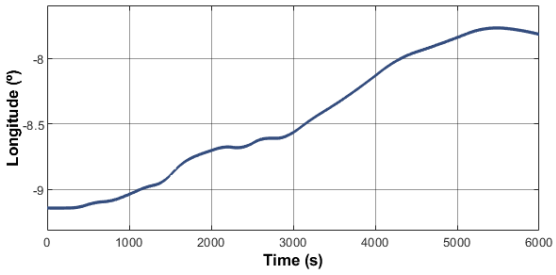

(b) Longitude (°) evolution with time for a free weather balloon flight.

Figure 4.7: Latitude and longitude evolution with time for a free weather balloon flight.

The resulted simulation for the wind data collected from the NOMADS servers resulted in a flight in which the latitudinal, velocities were mainly negative and the longitudinal velocities were mainly positive. This led to a latitude (seen in Figure 4.7(a)) decrease from $\phi = 38.73°$ to $\phi = 37.84°$ and a longitude (seen in Figure 4.7(b) increase from $\lambda = -9.140$ to $\lambda = -7.926$.

4.3 Altitude Control Simulation

The simulation results for altitude control will now be presented. To study the obtained results it is proposed an analysis of two different cases. The first one for a fixed altitude in which, if in the real world, the weather balloon would (ideally) follow similar wind currents to a specific direction (considering a general profile for the wind at a certain altitude that does not change drastically with longitude or latitude positions). The second case will approach different altitude references so a study on the balloon behaviour with the control strategy applied can be discussed. An important first note to make is that the flight simulation was divided into two phases. The first phase corresponds to the beginning of the ascension of the weather balloon. In this phase, as the weather balloon is naturally flying upwards, the balloon dynamics is free and not controlled during the first hour (the first 3600 seconds of simulation). This was decided since there were no constraints made to the time of the flight, therefore there is no urge to speed the flight process by adding gas at the beginning of the flight. Despite that, this would be useful in a real world flight, in which the amount of gas the balloon carries to inflate during flight could be limited or the inflation of the weather balloon at the beginning of the flight could cause some instability. To demonstrate the different dynamics the balloon presents while being controlled, tree references were generated. The first, named "Constant" reference, in which the balloon follows only one reference. The second, named "To the sky", in which the altitude references increase when a period of time passes until 23000 m, and then the balloon comes back to the ground. The third and last will be called "Lisbon to Seville" and in this reference, the wind currents were a part of the choice of the altitude references so the weather balloon could fly from Lisbon and land in Seville.

4.3.1 "Constant" Reference

A simulation for a constant altitude of 15000 m was be made and analysed (Figure 4.8). This simulation endured 10000 s (which corresponds to 2 hours and 46 minutes). Since the simulation values (when demonstrated graphically) are very compacted, some detailed views were added for a better result interpretation.

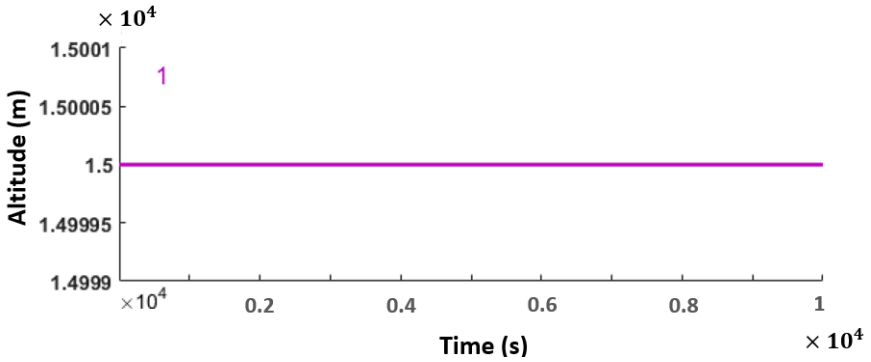

Figure 4.8: "Constant" altitude reference for an altitude of 15000 m

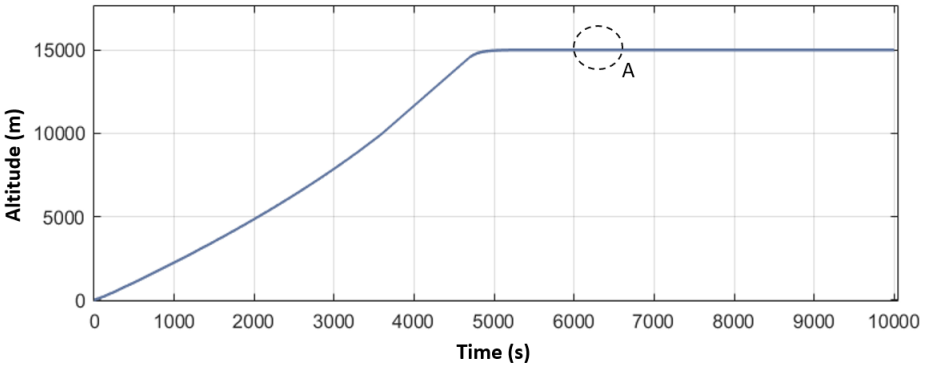

(a) Altitude (m) evolution with time for the "Constant" reference. A detail view "A" was included.

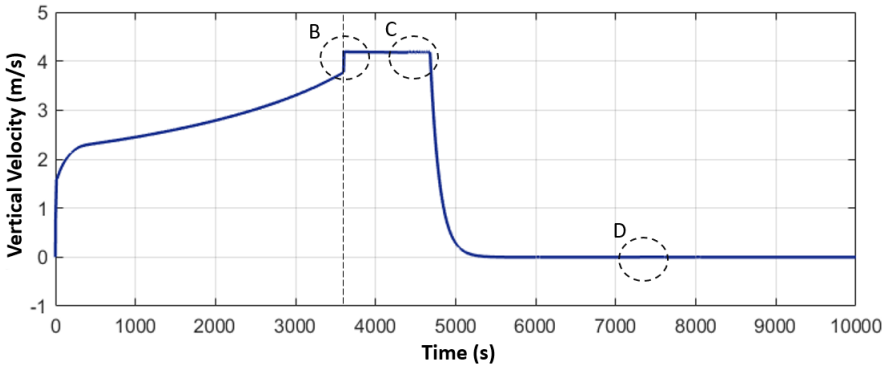

(b) Vertical Velocity (m/s) evolution with time for the "Constant" reference. A dashed line was included to indicate the beginning of the altitude control and the detail views "B","C", and "D" were also created.

Figure 4.9: Vertical velocity (m/s) and altitude (m) evolution with time for the "Constant" reference.

The altitude evolution, presented by Figure 4.9(a), suggests that the reference is not reached before 5000 s. That can be seen in detail "A" (Figure 4.10(a)) that shows that at 5500 s the balloon is 0.5 m distant from the reference. As for the velocity profile, it can be seen the moment when the velocity transitions from the first hour of uncontrolled flight in which its velocity was near 3.8 m/s to the control phase (Figure 4.10(b)) where this velocity is regulated to 4.2 m/s. Observing Figure 4.10(c), it is possible to see that this velocity is maintained as the maximum velocity that leads the weather balloon to the wanted position. After the balloon reaches a close altitude to the reference the velocity decreases and, as seen in Figure 4.10(d), it is reduced to almost zero. The mentioned detail views are the following:

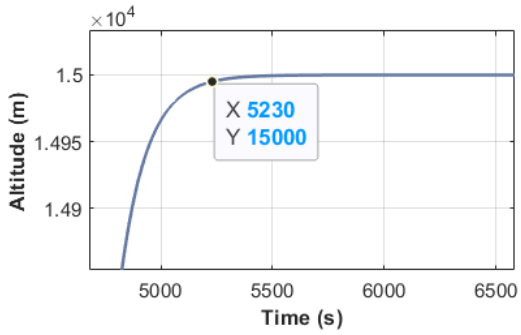

(a) Detailed view "A" of Altitude (m).

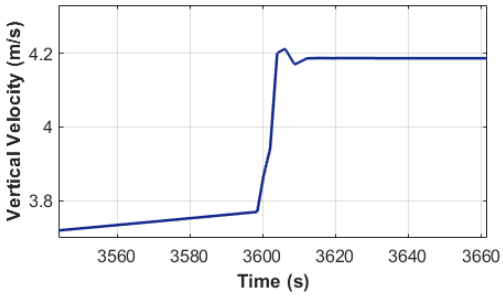

(b) Detailed view "B" of Vertical Velocity (m/s).

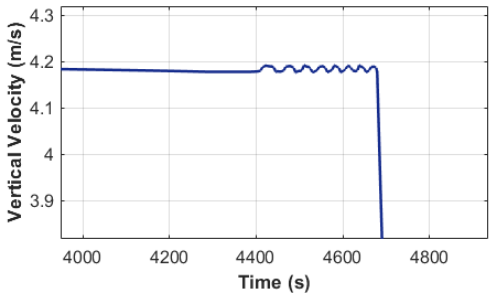

(c) Detailed view "C" of Vertical Velocity (m/s).

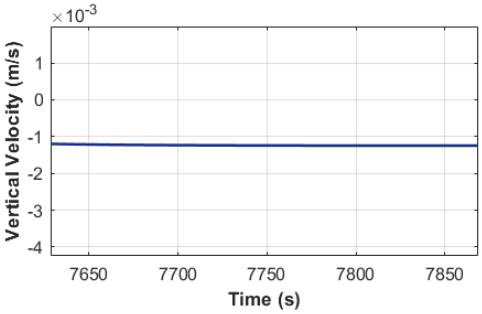

(d) Detailed view "D" of Vertical Velocity (m/s).

Figure 4.10: Detailed views "A", "B", "C" and "D" from vertical velocity (m/s) and altitude (m) evolution with time for the "Constant" reference.

The previously mentioned reference following is reinforced by the altitude error evolution. The view shown in Figure 4.11(a), with the evolution of the error, e_z, represents the difference between the altitude reference and the altitude of the balloon saturated to 500 m as maximum value and -500 m as minimum, as explained in section 3.1. Analysing view (b) (from the same figure) it is possible to see that the error is 0.2 then the simulation time is 5600 s converging to zero as the time passes. The altitude error evolution can be seen in Figure 4.11.

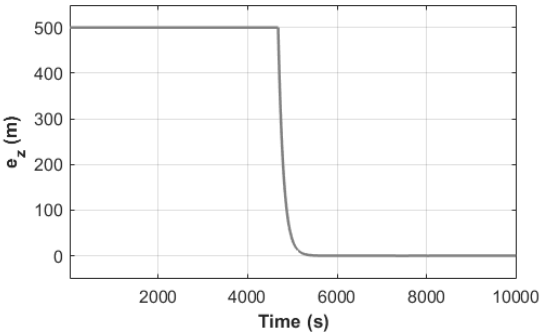

(a) Altitude error, e_z (m), evolution with time for the "Constant" reference.

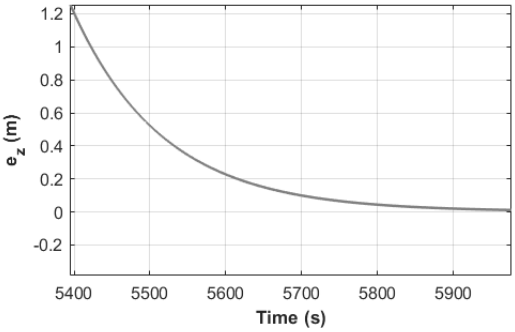

(b) Detailed altitude error, e_z (m), evolution with time for the "Constant" reference.

Figure 4.11: Altitude error, e_z (m), evolution with time for the "Constant" reference.

The wind model presented a varying profile until the weather balloon reached the constant value of 15000 m. At this point the wind longitudinal velocity, v_{wx}, was constant and has a value of 20 m/s and the latitudinal velocity was constant at 0 m/s (as can be seen in (a) from Figure 4.12).

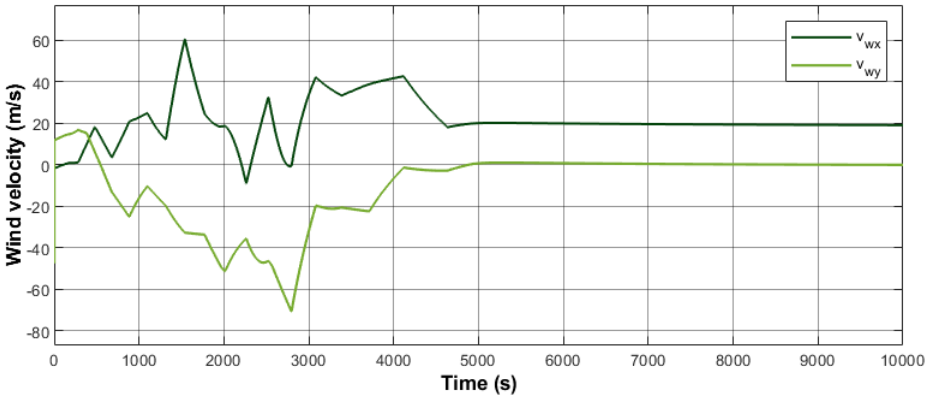

(a) Wind longitudinal(v_{wx}) and latitudinal (v_{wy}) velocities (m/s) with time for the "Constant" reference.

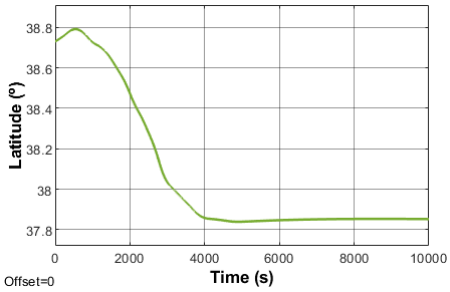

(b) Latitude evolution with time for the "Constant" reference.

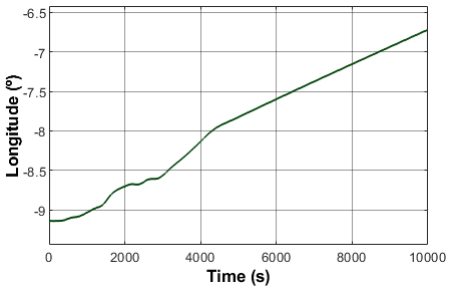

(c) Longitude evolution with time for the "Constant" reference.

Figure 4.12: Wind latitudinal/longitudinal velocities (m/s) and respective latitude/longitude (°) evolution with time, for the "Constant" reference.

As expected, this resulted in a constant increase of longitude that went from $-9.140°$ to $-6.750°$, while

latitude began at 38.730° and decreased to 37.854°. Since velocity was zero for this second component, this latitude value was maintained for a big part of the weather balloon flight.

The temperature values for this flight demonstrate the same evolution that the free model does for the initial hour since this corresponds to the non controlled phase of the flight. Then, in detail "E" of Figure 4.13(a), the change of temperature occurs since mass starts to enter the system and the velocity increases. The gas temperature becomes closer to the film temperature as the weather balloon altitude and velocities increase. When the constant value defined by the "Constant" reference is reached, the temperatures of the weather balloon film and the gas inside it maintain constant values with a small difference of 0.2 degrees. However, some adjustments in velocity during this phase cause some changes in the gas temperature as the detailed area shown in Figure 4.13(b). In these adjustments the difference between the balloon and the film temperatures are approximately 2 degrees. Temperature evolution:

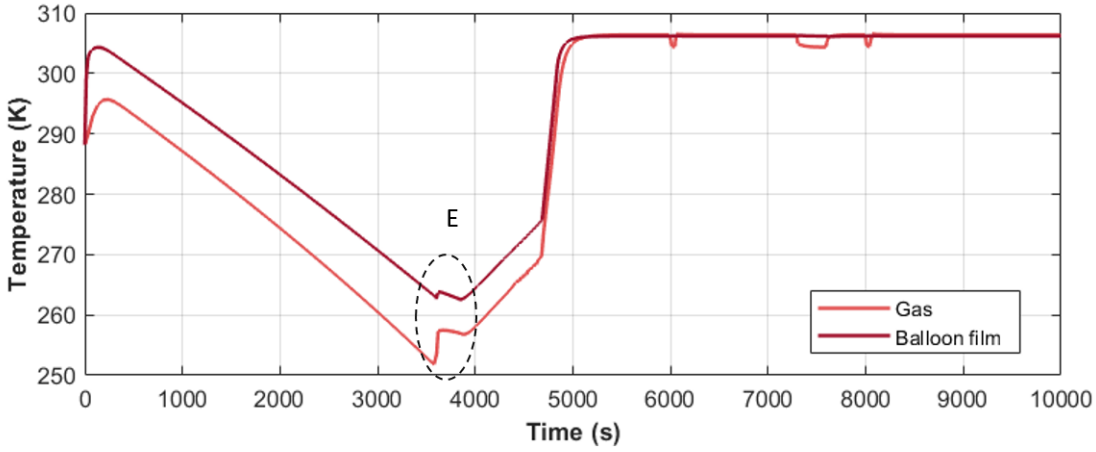

(a) Temperature(K) evolution with time of the weather balloon gas and film for the "Constant" reference.

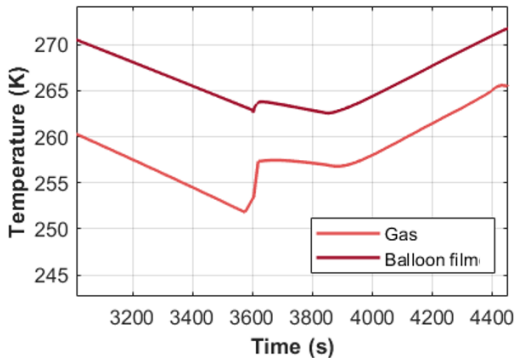

(b) Detailed view "E" of the temperatures (K).

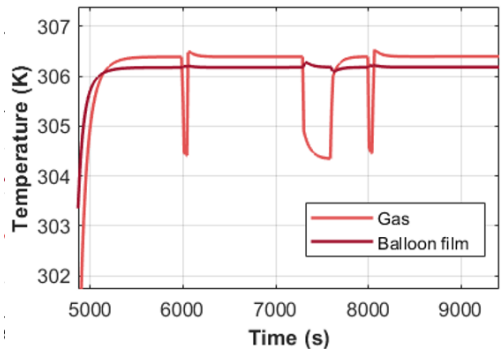

(c) Close view of of the temperatures (K) (4900s to 9700s).

Figure 4.13: Temperature (K) evolution with time and detailed views of the weather balloon gas and film for the "Constant" reference.

The mass of gas evolution can be seen in Figure 4.14. This mass is, initially, m_g=0.2814 kg and since the first hour is with no control, the mass does not change until the simulation reaches 3600 s. After that, an adjustment to increase velocity occurs (as can be seen closely in (b) from Figure 4.14) and then

the mass starts to decrease as the weather balloon gets closer to the reference altitude. The necessary mass to maintain the balloon in this altitude varies between 0.1812 kg and 0.1820 kg (as can be seen in (c) from Figure 4.14).

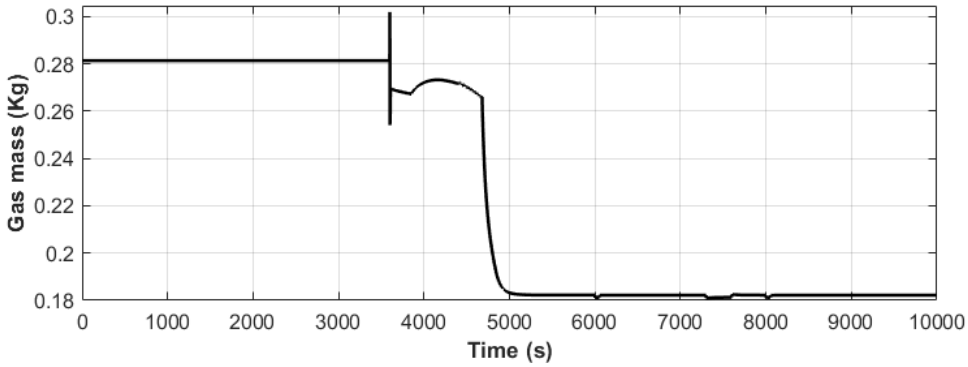

(a) Mass of gas (kg) evolution with time for the "Constant" reference.

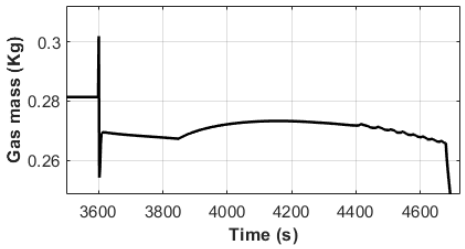

(b) Close view (3500s to 4700s) of the mass of gas (kg) evolution with time for the "Constant" reference.

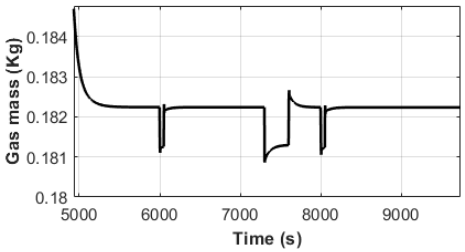

(c) Close view (5000s to 9600s) of the mass of gas (kg) evolution with time for the "Constant" reference.

Figure 4.14: Mass of gas, m_g, evolution with time for the "Constant" reference.

The control action and radius variation is shown in Figure 4.15. The control action reaches its maximum when the controlled flight begins to increase the weather balloon's velocity. The necessary radius for maintaining the wanted altitude reference has the value of 1.312 m (with come variations that occur in the same area the mass is regulated).

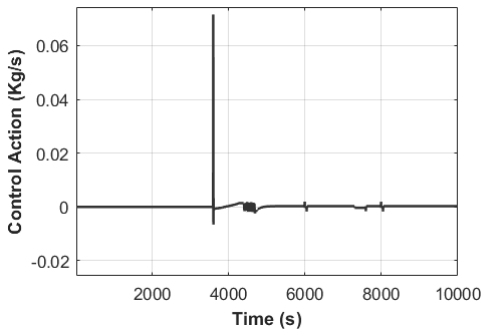

(a) Control action (kg/s) evolution with time for the "Constant" reference.

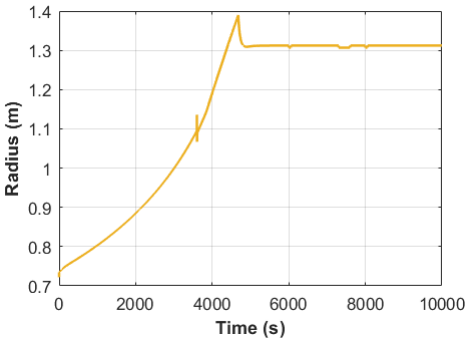

(b) Radius (m) evolution with time for the "Constant" reference.

Figure 4.15: Control action and radius evolution with time for the "Constant" reference.

4.3.2 "To the sky" Reference

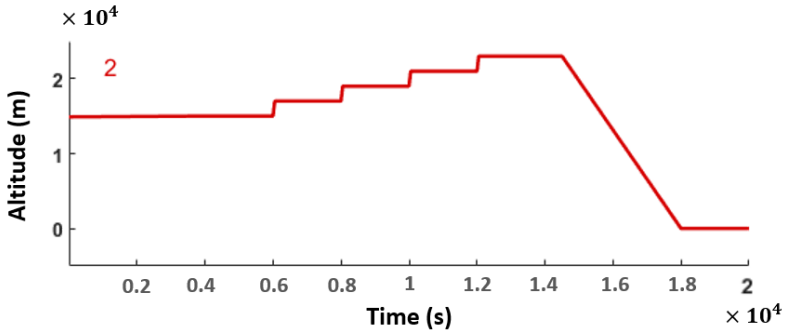

Figure 4.16: "To the sky" altitude reference.

Given an altitude reference (presented in Figure 4.16) in which the balloon rises through various altitudes, this simulation was done to analyse how the balloon behaves while getting higher to the sky. This second altitude reference begins in 15000 m until 6000 s, then it rises to 17000 m (from 6050 s until 8000 s), then it rises to 19000 m (from 8050 s until 10000 s), then it rises to 21000 m (from 10050 s until 12000 s), then it rises to 23000 m (from 12050 s until 14500 s and then finally comes back to the ground.

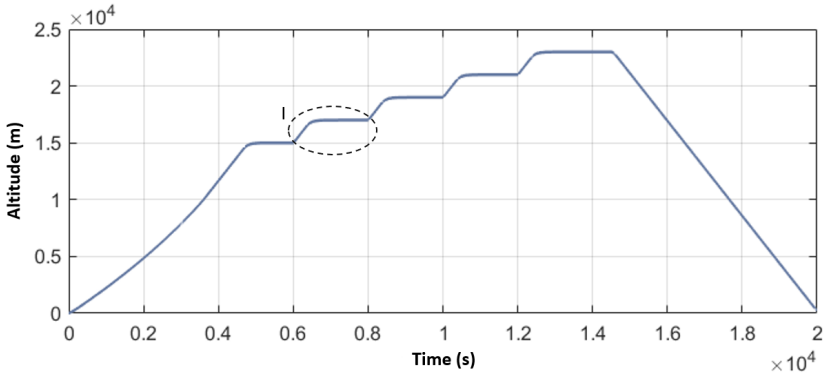

(a) Altitude (m) evolution with time for the "To the sky" reference. A detail view "I" was created.

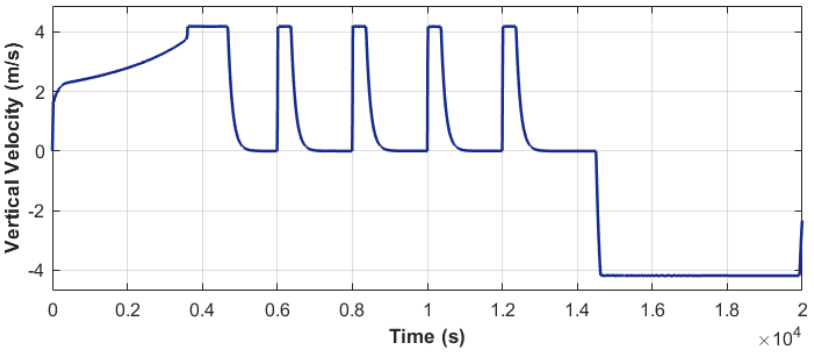

(b) Vertical Velocity (m/s) evolution with time for the "To the sky" reference.

Figure 4.17: Vertical velocity (m/s) and altitude (m) evolution with time for the "To the sky" reference.

Observing Figure 4.17, it can be seen that the velocity that leads the weather balloon to the wanted altitude is the same (and conditioned by the saturation of altitude error and controller gain) in every situation. This maximum velocity value for each increasing reference then decreases as the reference is reached and the velocity converges to 0 m/s. The close view (b) from Figure 4.18, shows that this "maximum velocity" has a value close to 4.19 m/s. As detail view "I" shows that it takes 916 s (approximately 15 minutes and 16 seconds) to place the weather balloon in the reference altitude (17000 m, in this case).

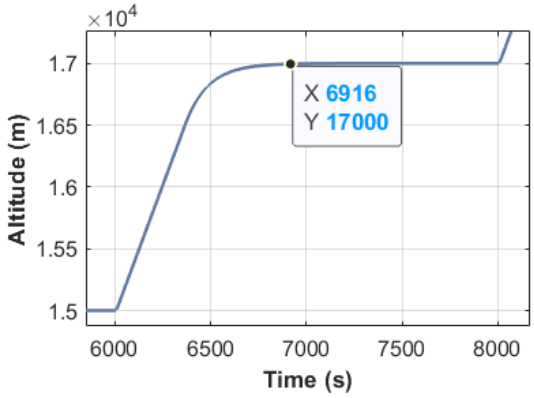

(a) Detailed view "I" of Altitude (m) for the "To the Sky" reference.

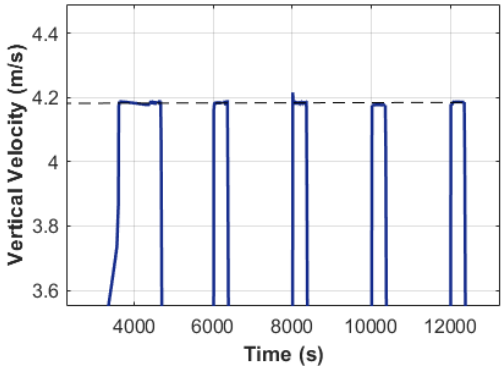

(b) Close view of Vertical Velocity (m/s) for the "To the Sky" reference.

Figure 4.18: Vertical velocity (m/s) and altitude (m) detailed views for the "To the Sky" reference.

The altitude error profile was the following:

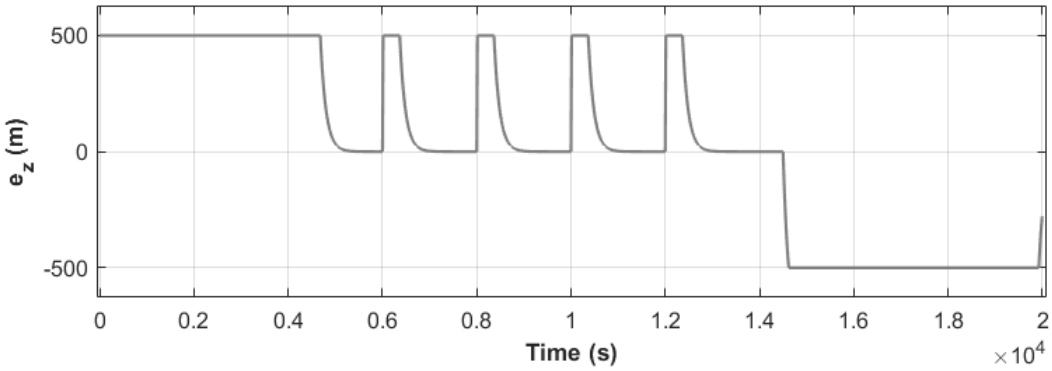

Figure 4.19: Altitude error, e_z (m), evolution with time for the "To the Sky" reference.

For this altitude and velocity adjustments the mass evolution can be seen in Figure 4.20.

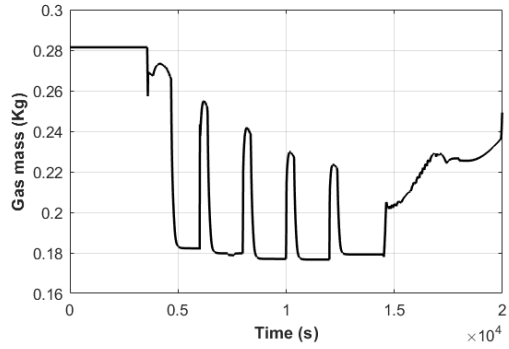

(a) Mass of gas (kg) evolution with time for the "To the Sky" reference. .

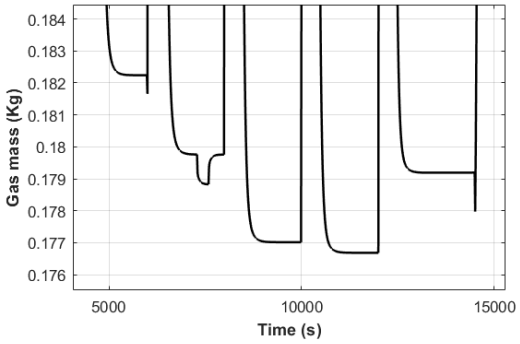

(b) Close view of the mass of gas for the "To the Sky" reference.

Figure 4.20: Vertical velocity (m/s) and altitude (m) evolution with time for the "To the Sky" reference.

Figure 4.20 shows which are the mass values that are necessary for maintaining the weather balloon in the reference altitudes. As the altitude increases it can be seen that the necessary amount of mass decreases from 15000 m to 23000 m and after that, it increases for the 23000 m reference. For 15000 m the necessary gas mass value is close to 0.1822 kg, as for 17000 m this value varies between 0.1788 kg and 0.1798 kg. This value then decreases to 0.177 kg at an altitude reference of 19000 m, decreases one more time at 21000 m for a value of 0.1767 kg and at the last constant reference of 23000 m it increases to 0.1792 kg.

The temperature evolution follows an increasing profile as the "To the Sky" reference demands higher values of altitude. The first phase of uncontrolled flight presents the expected values shown in the free flight simulation, but as the altitudes increase different and increasing values of temperature affects the gas inside the balloon. For 15000 m, the weather balloon film and gas present very similar values (as already seen in the "Constant" reference simulation) that are close to 306 K. To 17000 m these values are still similar but they both increase to a value surrounding 311 K. As for an altitude reference of 19000 m, the temperature of the gas and the balloon film differs and they have the values of 314 K and 316K respectively. For 21000 m there is still a two degree difference between these components being the gas temperature 319 K and the balloon film temperature constant at 321 K. The last constant altitude reference is for 23000 m and here the temperatures are similar and round the value of 326 K. This behaviour can be seen in (b) from Figure 4.21 and in (c) from the same figure the thermal consequence of the descent phase of the weather balloon flight can be observed. This profile is similar to the free flight temperature profile.

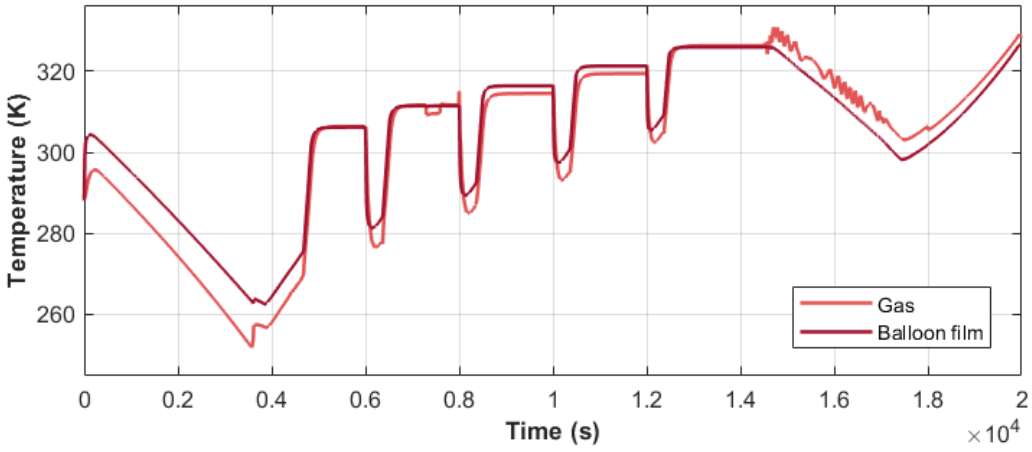

(a) Temperature (K) evolution of the weather balloon gas and film for the "To the sky" reference.

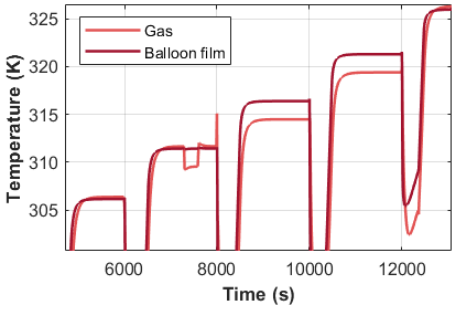

(b) Detailed view "E" of the temperatures (K) for the "To the sky" reference.

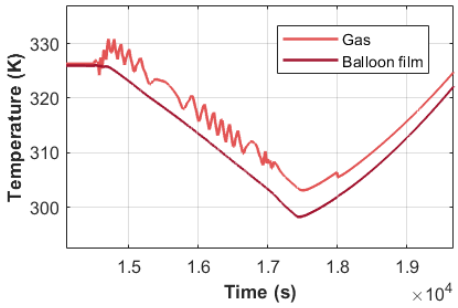

(c) Detailed view "F" of the temperatures (K) for the "To the sky" reference.

Figure 4.21: Vertical velocity (m/s) and altitude (m) evolution with time for the "To the sky" reference.

As a consequence of mass and temperature variation, the radius evolution (presented in Figure 4.22), follows a profile that increases as the altitude increase. Although the mass for the increasing constant altitude references tends to decrease, the radius is affected by the heating of this gas and, therefore, as the temperature increases for different increasing altitudes, the radius evolution presents increasing radius values for increasing constant altitude references.

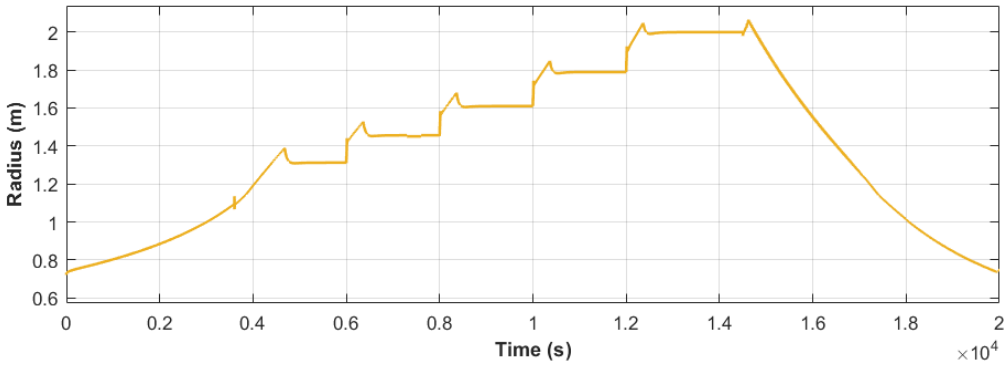

Figure 4.22: Radius (m) evolution with time for the "To the Sky" reference.

The control action evolution shows the areas of control that occur before the mass stabilisation. The control action presents very small values since small mass variation is enough to change quickly the dynamics of the weather balloon. This evolution can be seen in Figure 4.23.

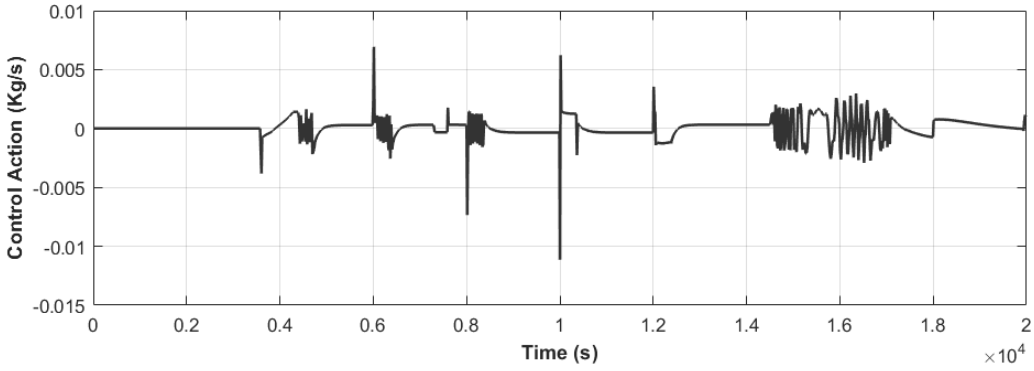

Figure 4.23: Control action (kg/s) evolution with time for the "To the Sky" reference.

The latitudinal and longitudinal evolution of the weather balloon can be seen in Figure 4.24. This profile led the final its latitude value to be 37.1642° and the longitude value to be −7.2759°.

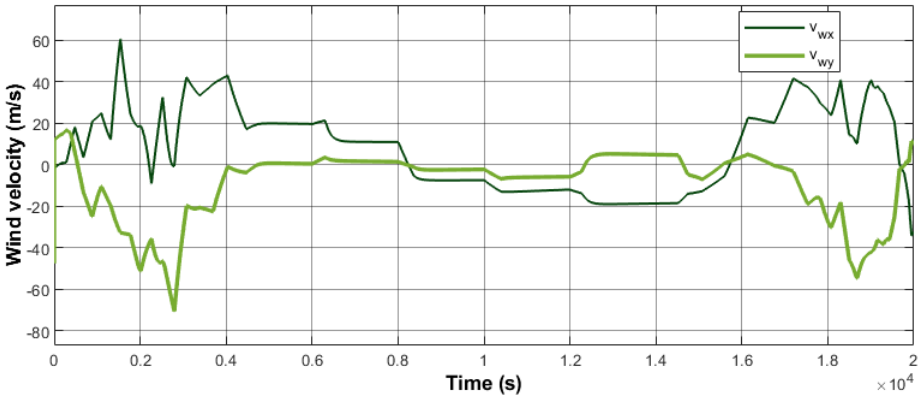

(a) Wind longitudinal(v_{wx}) and latitudinal (v_{wy}) velocities (m/s) with time for the "To the Sky" reference.

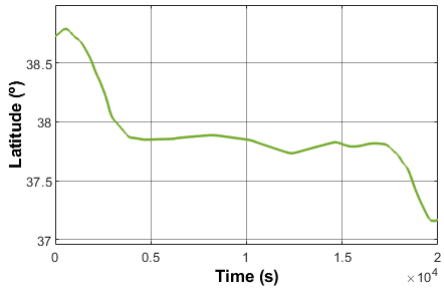

(b) Latitude (°) evolution with time for the "To the Sky" reference.

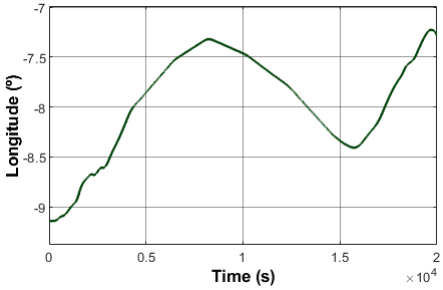

(c) Longitude (°) evolution with time for the "To the Sky" reference.

Figure 4.24: Wind latitudinal/longitudinal velocities (m/s) and respective latitude/longitude (°) evolution with time, for the "To the Sky" reference.

4.3.3 "Lisbon to Seville" Reference

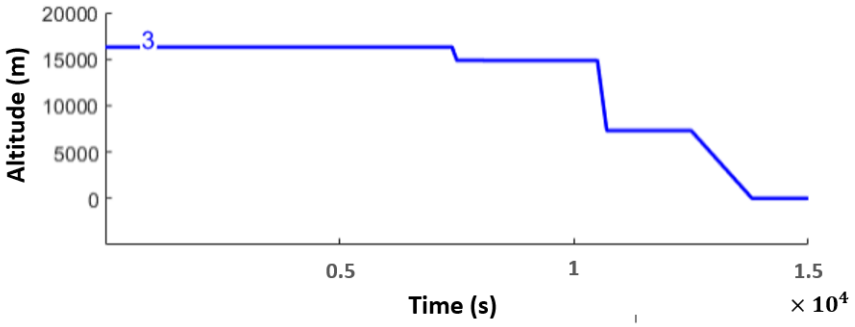

Figure 4.25: "Lisbon to Seville" altitude reference.

This last simulation intends to show how the altitude control could be combined with the study of the wind currents modelled so that the weather balloon could be led to specific areas of interest to the investigation. For this demonstration, the wind currents were studied and their corresponding altitude reference (presented in Figure 4.25) was manually chosen to see if the route would lead to the desired final destination.

This process of wind currents direction and intensity identification and simultaneous altitude reference change could be made autonomously if an algorithm for this purpose was applied. Some methods have been developed for this topic but since this thesis is focused on the altitude control strategy other than these wind algorithms, this ad hoc solution of manually defining the altitude reference was chosen. Nonetheless, these existing algorithms (and maybe new ones) could be implemented in the next phase of the development of this work.

This reference begins at 16300 m and this altitude is kept from the beginning of the flight until the simulation time is 7300 s. After that, the reference decreases linearly until 7400 s, where the reference altitude becomes 14870 m from that moment until 10500 s. from that point, the altitude decreases once again linearly for the next 200 s until 7300 m. That reference altitude is maintained until 12500 s where the reference falls linearly one last time for 1300 s until it reaches 0 m. The 0m reference is maintained to simulate the landing of the balloon until the end of the simulation (15000 s).

The velocity and altitude evolution with time for this flight are shown in Figure 4.26. The altitude profile presented for this reference shows that the first altitude reference of 16870 m is reached slightly after 5000 s of simulation. After the flight through this reference and the following reference of 14870 m, the weather balloon faces an almost linear descending, passing quickly through the 7300 m where the wind currents are faster.

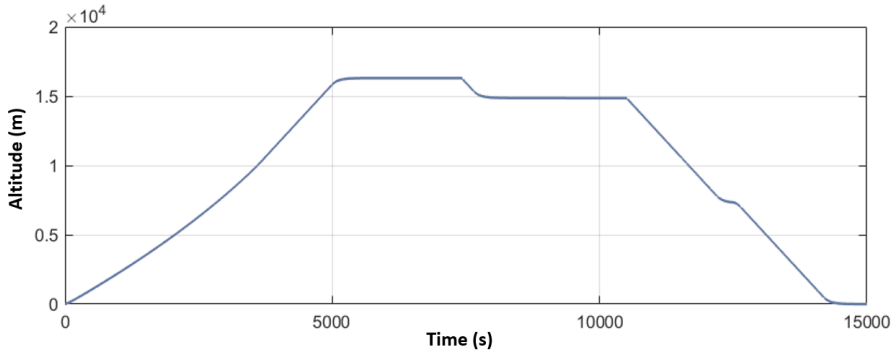

(a) Altitude (m) evolution with time for "Lisbon to Seville" reference.

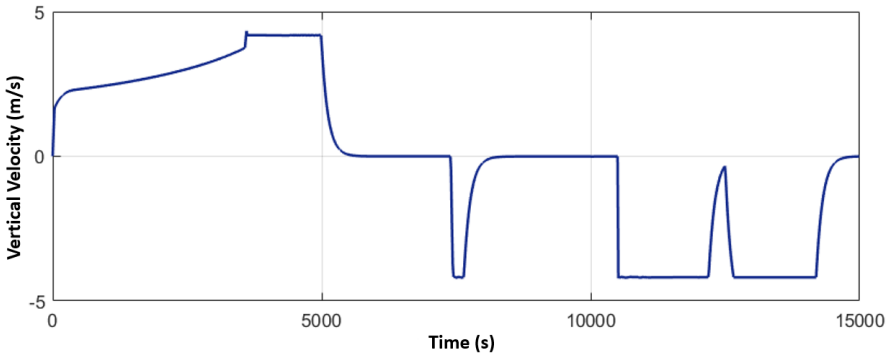

(b) Vertical Velocity (m/s) evolution with time for "Lisbon to Seville" reference.

Figure 4.26: Vertical velocity (m/s) and altitude (m) evolution with time for "Lisbon to Seville" reference.

The mass of gas inside the weather balloon and the radius variation during this flight can be seen in Figure 4.27.

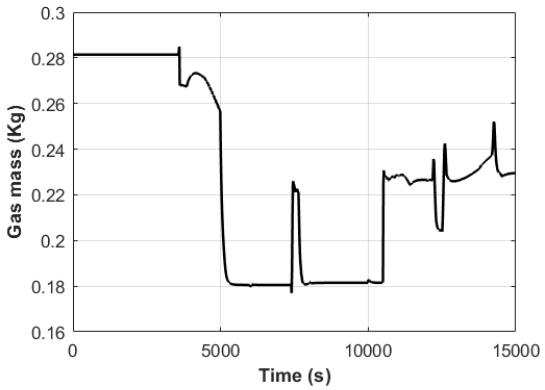

(a) Mass of gas (kg) evolution with time for the "Lisbon to Seville" reference.

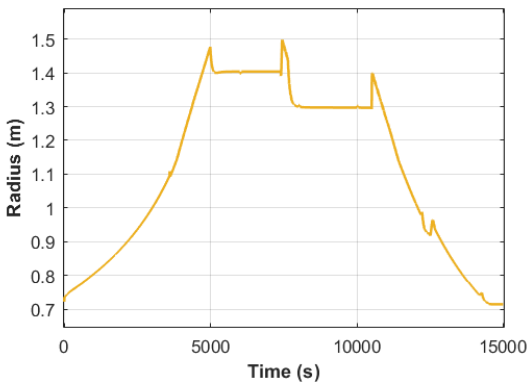

(b) Radius (m) evolution with time for the "Lisbon to Seville" reference.

Figure 4.27: Mass and radius evolution with time for the "Lisbon to Seville" reference.

From the balloon film and gas temperatures profiles presented in Figure 4.28, it can be seen that, after the first hour in which control isn't yet being applied, the temperatures maintain a similar value, since the altitudes given by the reference of 14870 m and 16300 m are relatively close (less than 2 km) and, therefore, the temperatures are also relatively close. After the 14870 m reference, the balloon

goes through a descending phase and, while the balloon approximates to the ground, the atmospheric temperature increases, causing the gas and balloon film temperatures to also increase.

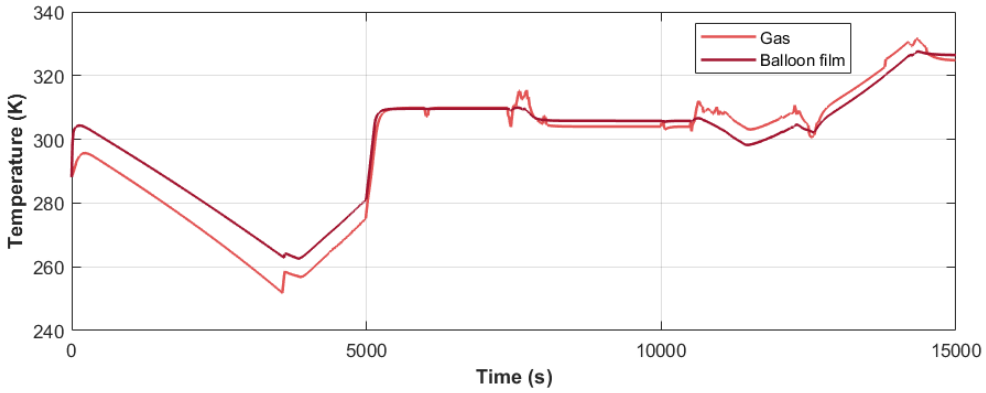

Figure 4.28: Temperature (K) evolution with time of the weather balloon gas and film for the "Lisbon to Seville" reference.

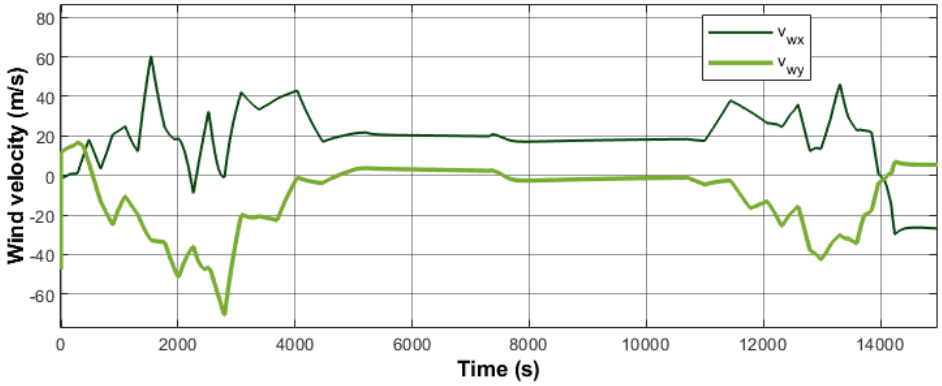

(a) Wind longitudinal(v_{wx}) and latitudinal (v_{wy}) velocities (m/s) with time for the "Lisbon to Seville" reference.

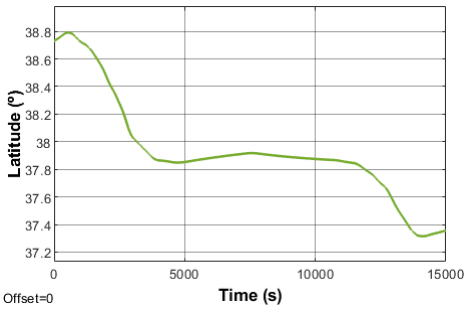

(b) Latitude evolution with time for the "Lisbon to Seville" reference.

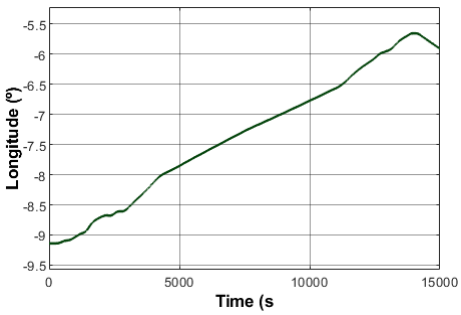

(c) Longitude evolution with time for the "Lisbon to Seville" reference.

Figure 4.29: Wind latitudinal/longitudinal velocities (m/s) and respective latitude/longitude (°) evolution with time, for the "Lisbon to Seville" reference.

The latitude and longitude, as well as the longitudinal and latitudinal velocities, can be seen in Figure 4.29. At the beginning of the flight, the first non controlled hour, the wind currents present a

positive profile for longitude velocity, while the latitudinal velocity presents negative values in this phase. This can be translated to an increasing longitude value and a decreasing latitude value. The next phase, when the weather balloon passes through 16300 m and 14870 m, is composed of a period where the longitudinal velocity is close to a constant 20 m/s value, while the latitudinal velocity is almost constant at 0 m/s. This means that during this phase the latitude will be almost constant for a period of time and longitude will increase almost linearly. After that, a fast passage of the weather balloon over the altitude reference of 7300 m occurs. At that altitude the wind currents are intense and this passage was intentionally fast so the latitude and longitude values could vary only the necessary amount. Finalising the flight, the weather balloon landing phase presents a negative value for longitudinal velocity and a small positive value for latitudinal velocity. This causes the latitude to increase slightly at the final part of the flight, and the longitude to decrease.

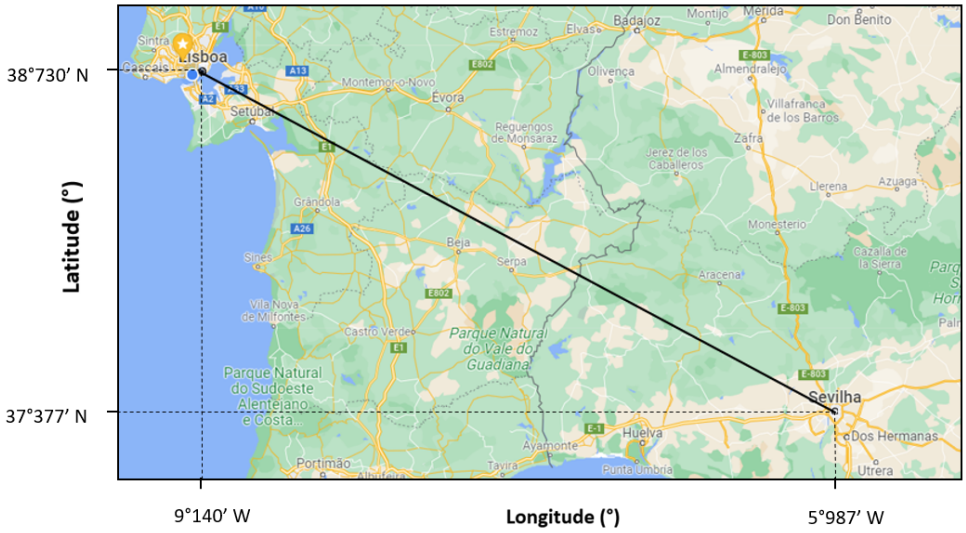

(a) Initial intended route "Lisbon to Seville" trajectory.

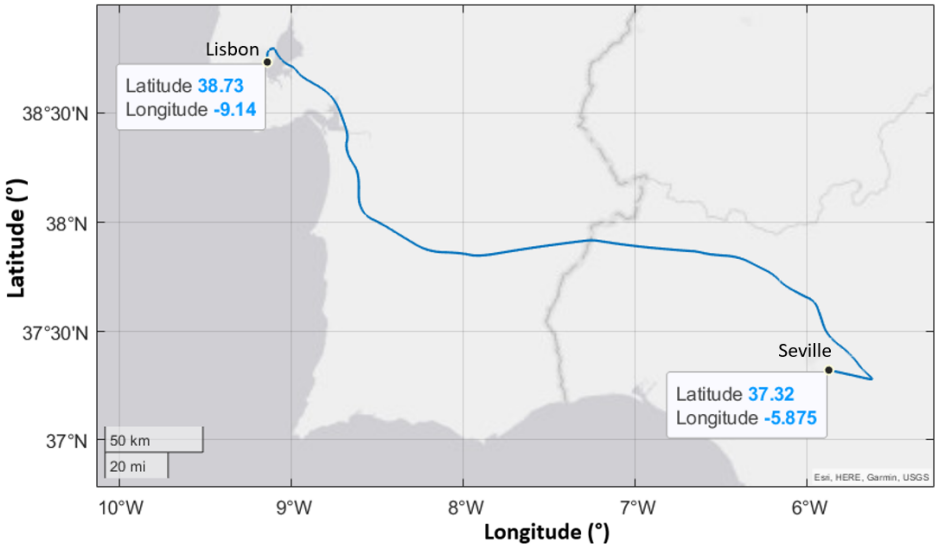

(b) Final result of "Lisbon to Seville" reference simulation.

Figure 4.30: Result of simulation for "Lisbon to Seville" reference.

Illustrating this intended trajectory is Figure 4.30. The first image shows the initial position of the weather balloon, in Lisbon, with geodetic coordinates $(\phi, \lambda) = (38.73°, -9.14°)$ (the negative value of longitude can also be read as a positive value into the west direction as shown in Figure 4.30). As for the final intended position, assuming that the balloon landing should be in "Plaza de España" with geodetic coordinates $(\phi, \lambda) = (37.377°, -5.987°)$.

The trajectory followed by the weather balloon resulted in a landing at the geodetic coordinates of $(\phi, \lambda) = (37.320°, -5.875°)$. There is an error of 0.057 degrees in latitude and a 0.112 degree error in longitude. This is equivalent to a error distance of 11.76 km. Considering the conditions in which this simulation was created, the wind uncertainty and the method in which the reference was chosen, this value can be considered good for a simulation and the following of wind currents through altitude control was successfully accomplished.

5 Conclusions and Future Work

In this chapter, a conclusion about all the developed work in this thesis regarding modelling and altitude control is done. Some suggestions of future work as an improvement to the work begun here is also made.

5.1 Achievements

5.1.1 Weather balloon model

A complete new model for a latex weather balloon resulted from this work. The TA450 model was assumed to carry, for control purposes, a gas cylinder and a control valve beyond the typical payload that weather balloons carry. For radius evolution modelling, since latex (natural rubber) is a hyperelastic material, a hyperelastic model, that could better represent the elasticity of latex, was implemented instead of a simple linear elastic model. The atmospheric model representing the atmosphere behaviour for different ranges of altitude was also implemented in the modelling process. A complete thermal model accounting for direct solar radiation, infrared radiation and internal and external convection was also implemented. A dynamics model was obtained and a correlation between the Reynolds number and the drag coefficient of the balloon was used and adapted from a sphere to the balloon (through a lowering of the curve). With the dynamics model, the nonlinear system's state-space representation was also presented. The wind currents were obtained from predictions made by GFS through the NOMADS servers and this data was implemented in two alternative ways to model the wind surrounding the balloon. The developed weather balloon model in this thesis considered possible different scenarios, such as wind and hyperelastic models, to compare and obtain better options so the model could be a good representation of the real situation a weather balloon could find. Concerning the approximations done in this thesis, it can be referred two major cases, the first being the control valve that was not modelled, and the second being the cylinder of gas which was assumed to be able to supply all the necessary amount of gas needed for the simulation. It is important to remember that this work was not validated in a real word environment, therefore the simulation only presents representative values that could happen given the models implemented and so are not the exact way the weather balloon would behave in a real environment. Even more, in a real word situation, the balloon would face many other complications such as different meteorologic conditions and different perturbations that could be taken into account in the following development of this work.

5.1.2 Altitude and velocity control

Another interesting result from this work was the altitude control strategy developed. The chosen control strategy was cascade control so not only the altitude but also the velocity could be controlled. This control strategy was implemented with gain scheduling in which the gains were found with the LQR algorithm and tuned after so the simulated curves could represent a normal behaviour for a weather balloon (trying to avoid drastic velocity or temperature changes). All simulations presented good results regarding altitude control and the references were properly followed. This control strategy was well implemented and is a good start for more investigation and development of other altitude control strategies for the weather balloon context.

5.2 Future Work

This work opens doors for many other developments in the latex balloon field, some of which are listed below.

- Laboratory model validation: A validation of the model and testing its behaviour in a real word environment would be a big step into improving. The used parameters would probably be changed and a final and more accurate to reality model could be obtained.
- Development of specific parameters for latex: Some parameters used in this thesis are an approximation of their real values. Testing to obtain accurate latex thermodynamic and hyperelastic parameters.
- Valve modelling: The valve modelling would influence how the control action works, this development could be an important evolution for a more accurate representation of the model.
- Wind algorithm implementation: In this work the wind currents were chosen manually, however, there are methods to identify wind currents intensity and direction while the weather balloon flies. Although some methods already exist, new and less complex solutions can be created and implemented.
- Other control strategies could be implemented and then be compared to look for the better possible solution for the weather balloon.
- Development of other control mechanisms. Since the weather balloon is a very simple and air dependent flying aircraft, it could be hard to think about effective mechanisms for its control. However, developing alternative ways of control could open doors to extraordinary future results.

Bibliography

[1] N. US Department of Commerce. Weather balloons NOAA, Oct 2020. URL `https://www.weather.gov/bmx/kidscorner_weatherballoons`. Accessed: 2021/07/20.

[2] Ö. Kayhan, Ö. Yücel, and M. A. Hastaoğlu. Simulation and control of serviceable stratospheric balloons traversing a region via transport phenomena and PID. *Aerospace Science and Technology*, 53:232–240, 2016.

[3] Y. Jiang, M. Lv, W. Zhu, H. Du, L. Zhang, and J. Li. A method of 3-D region controlling for scientific balloon long-endurance flight in the real wind. *Aerospace Science and Technology*, 97:105618, 2020.

[4] G. Pfotzer. History of the use of balloons in scientific experiments. *Space Science Reviews*, 13(2): 199–242, 1972.

[5] H. Zell. Types of balloons, Jul 2015. URL `https://www.nasa.gov/scientific-balloons/types-of-balloons`. Accessed: 2021/6/25.

[6] Balão a gás para projetos científicos. URL `https://www.aeroexpo.online/pt/prod/raven-aerostar/product-175129-64755.html`. Accessed: 2021/07/20.

[7] B. Brown. Tucson-based World View to offer balloon rides to space, Feb 2016. URL `https://eu.azcentral.com/story/news/local/arizona/2016/02/24/tucson-based-world-view-offer-balloon-rides-space/80851756/`. Accessed: 2021/07/20.

[8] NASA super pressure balloon. URL `https://www.tensys.com/nasa-super-pressure-balloon`. Accessed: 2021/07/20.

[9] Super pressure balloons, 2015. URL `https://stratocat.com.ar/fichas-e/2015/WNK-20150326.htm`. Accessed: 2021/07/20.

[10] N. Yajima, N. Izutsu, T. Imamura, and T. Abe. *Scientific Ballooning: Technology and applications of exploration balloons floating in the stratosphere and the atmospheres of other planets*, volume 112. Springer Science & Business Media, first edition, 2009. ISBN 9780387097275.

[11] MIR: The stratospheric balloon of the CNES, 2011. URL `https://ballonsolaire.pagesperso-orange.fr/en-historique3.htm`. Accessed: 2021/07/20.

[12] J. Glaisher. A brief history of solar ballooning and Aerocene, Jul 2020. URL https://aerocene.org/a-brief-solar-ballooning-and-aerocene/. Accessed: 2021/07/20.

[13] B. Belley and S. R. STEM. Weather balloon launch, Aug 2019. URL https://launchwithus.com/lwu-blog/tag/Weather+Balloon. Accessed: 2021/5/01.

[14] G. A. DiLisi. The Hindenburg disaster: Combining physics and history in the laboratory. *The Physics Teacher*, 55(5):268–273, 2017.

[15] C. A. Price. The Helium Conservation Program of the Department of the Interior. *Envtl. Aff.*, 1: 333, 1971.

[16] W. Al-Dahhan and E. Yousif. Hydrogen balloons: Bright colors but hidden fire hazard. *International Journal of Public Health & Safety*, 3(1):1–6, 2018.

[17] P. B. Voss, E. E. Riddle, and M. S. Smith. Altitude control of long-duration balloons. *Journal of Aircraft*, 42, 2005. ISSN 15333868. doi: 10.2514/1.7481.

[18] M. G. Bellemare, S. Candido, P. S. Castro, J. Gong, M. C. Machado, S. Moitra, S. S. Ponda, and Z. Wang. Autonomous navigation of stratospheric balloons using reinforcement learning. *Nature*, 588(7836):77–82, 2020.

[19] H. Du, M. Lv, J. Li, W. Zhu, L. Zhang, and Y. Wu. Station-keeping performance analysis for high altitude balloon with altitude control system. *Aerospace Science and Technology*, 92:644–652, 2019.

[20] J. F. F. Carreira. High-altitude Balloon Trajectory Prediction with Corrections based on Real-Time Observations. Master's thesis, Instituto Superior Técnico, Universidade de Lisboa, 2019.

[21] I. Müller and P. Strehlow. *Rubber and Rubber Balloons: Paradigms of Thermodynamics*. Lecture Notes in Physics. Springer Berlin Heidelberg, first edition, 2004. ISBN 9783540202448.

[22] Earth atmospheric model. URL https://www.grc.nasa.gov/www/k-12/airplane/atmosmet.html. Accessed: 2021/05/03.

[23] R. Farley. BalloonAscent: 3-D simulation tool for the ascent and float of high-altitude balloons. In *AIAA 5th ATIO and16th Lighter-Than-Air Sys Tech. and Balloon Systems Conferences*, page 7412, 2005.

[24] L. A. Wood and N. Bekkedahl. Specific heat of natural rubber and other elastomers aboved the glass transition temperature. *Journal of Polymer Science Part B: Polymer Letters*, 5(2):169–175, 1967.

[25] R. Palumbo, M. Russo, E. Filippone, and F. Corraro. ACHAB: Analysis code for high-altitude balloons. In *AIAA Atmospheric Flight Mechanics Conference and Exhibit*, page 6642, 2007.

[26] F. A. Morrison. Data correlation for drag coefficient for sphere. *Department of Chemical Engineering, Michigan Technological University, Houghton, MI*, 49931, 2013.

[27] K. Ogata. *Modern control engineering*. Prentice hall, 2010.

[28] Weather Balloons and Accessories (HOSKIN). URL http://www.myhoskin.com/Catalogs/Hoskin-Weather-Balloons-and-Accessories.pdf. Accessed: 2021/9/01.

[29] S. A. Kalogirou. Chapter 2 - Environmental Characteristics. In S. A. Kalogirou, editor, *Solar Energy Engineering (Second Edition)*, pages 51–123. Academic Press, Boston, 2014. ISBN 978-0-12-397270-5.

[30] Julian date. URL https://scienceworld.wolfram.com/astronomy/JulianDate.html. Accessed: 2021/05/30.

[31] A. L. Morris. *Scientific ballooning handbook*. Atmospheric Technology Division, National Center for Atmospheric Research, 1975.

[32] V. VanDoren. Fundamentals of cascade control: sometimes two controllers can do a better job of keeping one process variable where you want it. *Control Engineering*, 61(8):28–31, 2014.

[33] F. Behrooz, N. Mariun, M. Marhaban, M. A. Mohd Radzi, and A. Ramli. Review of Control Techniques for HVAC Systems—Nonlinearity Approaches Based on Fuzzy Cognitive Maps. *Energies*, 11:495, 02 2018. doi: 10.3390/en11030495.

[34] Gain scheduling. URL https://www.mathworks.com/discovery/gain-scheduling.html. Accessed: 2021/09/03.

[35] Loon Project. URL http://googleloon.blogspot.com/2013/06/googles-project-loon-balloon-powered.html. Accessed: 2021/9/20.

[36] A. Sóbester, I. P. Castro, H. Czerski, and N. Zapponi. Notes on meteorological balloon mission planning. In *AIAA Balloon Systems (BAL) Conference*, page 1295, 2013.

A | Model and Control design

In order to perform altitude control of the balloon, the actuation system must be modelled. Such control will be the result of the gas mass variation inside the balloon. To model this system one valve that allows inflow and outflow is needed. When actuated for inflow the gas will leave the gas cylinder an enter the weather balloon, as for outflow, the gas inside the balloon will be compressed into the cylinder. It will be assumed that the gas in the cylinder is not lost. The balloon has a tendency to increase its velocity (and, as a consequence, its altitude) if the flight is not controlled. As a result, most controlled balloons, as explained in 1.2.4, typically only uses the valve to release mass in order to reduce the balloon's velocity and extend the flight duration, preventing it to reach the burst radius for a longer period. However, these control techniques have a slow response. If a faster response is needed, introducing and releasing gas can be a better option to take into consideration. With that in mind, since the inflow and the outflow of gas in this case are required to change the altitude, the mass balance of the gas is:

$$\dot{m}_g = \dot{m}_{g_{in}} - \dot{m}_{g_{out}} \tag{A.1}$$

A.1 Linear Valve

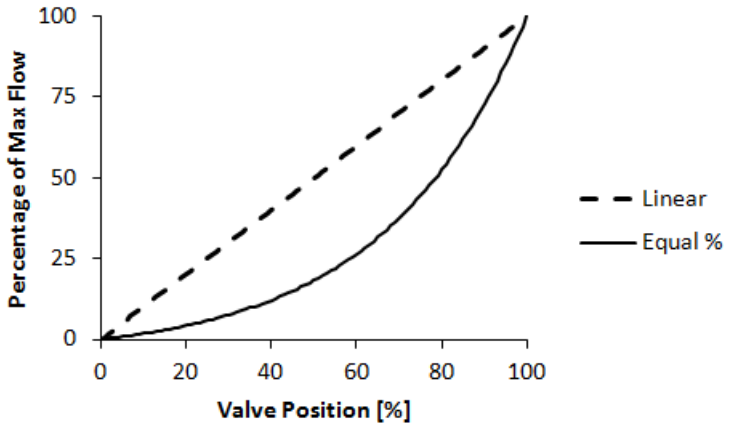

Figure A.1: Linear and equal percentage valves representation. In a linear valve, the percentage of maximum flow varies linearly with the percentage of the valve that is open.

The massic flow through a linear valve is represented by:

$$\dot{m} = C_d \cdot f(l) \cdot A_v \cdot \sqrt{2\Delta P_v \rho_g} \tag{A.2}$$

where $f(l)$ is linear and represents the flow as function of the opening of the valve.

- ΔP_v : Is the pressure drop. For inflow, this pressure drop is $P_v - P_b$ (the difference between the cylinder and the balloon pressures). For outflow it will change its direction (from the balloon to the gas cylinder) and $\Delta P_v = P_b - P_v$.
- A_v: Is the section area of the valve.
- C_d: Is the discharge coefficient of the valve.

Considering that the linear valve response to the opening or closing command, does not occur at the same instant the command is given. The following first order transfer function can be used as a representation of such dynamics.

$$G(s) = \frac{K}{Ts + 1} \tag{A.3}$$

Table A.1: Control Valve Parameters

Parameter	Symbol	Value	Units
Radius	r_v	0.015	m
Discharge Coefficient	C_{disch}	0.86	-
Pressure Drop	ΔP_v	$P_w - Pb$	Pa

A.2 Linearisation

The trim points found with "Linear Analysis Tool" were:

$$u_o = 0 \tag{A.4}$$

This value of u_o was used for all cases of different trim states.

$$x_{o1} = \Big[0, 15000, 37.83, -7.752, 265.0; 278.0; 0.2814\Big]^T \tag{A.5a}$$

$$x_{o2} = \Big[0, 16000, 37.83, -7.752, 265.0; 278.0; 0.2814\Big]^T \tag{A.5b}$$

$$x_{o3} = \Big[0, 17000, 37.83, -7.752, 265.0; 278.0; 0.2814\Big]^T \tag{A.5c}$$

$$x_{o4} = \Big[0, 18000, 37.83, -7.752, 265.0; 278.0; 0.2814\Big]^T \tag{A.5d}$$

$$x_{o5} = \Big[0, 19000, 37.83, -7.752, 265.0; 278.0; 0.2814\Big]^T \tag{A.5e}$$

$$x_{o6} = \Big[0, 20000, 37.83, -7.752, 265.0; 278.0; 0.2814\Big]^T \tag{A.5f}$$

$$x_{o7} = \Big[0, 21000, 37.83, -7.752, 265.0; 278.0; 0.2814\Big]^T \tag{A.5g}$$

$$x_{o8} = \Big[0, 22000, 37.83, -7.752, 265.0; 278.0; 0.2814\Big]^T \tag{A.5h}$$

$$x_{o9} = \Big[0, 23000, 37.83, -7.752, 265.0; 278.0; 0.2814\Big]^T \tag{A.5i}$$

A.3 Nonlinear Control

Control Method	Advantage	Disadvantage
Nonlinear control	(1) This method offers a completely different approach for dealing with the nonlinear model and the slowly time-varying or uncertain parameters of the system.	(1) Difficulty in finding the Lyapunov functions. (2) Complexity in integration of nonlinear observer with HVAC. (3) Sensitivity to parameter variation. (4) Limited operating range in state feedback. (5) Proof of stability is difficult. (6) Need for measuring all state variables or additional measurement. (7) Possibility only on stable processes. (8) Nonlinear observer is required if the all state variables were not measurable.

Figure A.2: Nonlinear control advantages and disadvantages.

B | Tables

B.1 Elevation angle coefficients

The necessary coefficients to implement algorithm 1 are the following:

Table B.1: Elevation angle algorithm coefficients

g_1	357.529
g_2	0.98560028
q_1	280.459
q_2	0.98564736
L_1	1.915
L_2	0.020
e_1	23.439
e_2	0.00000036
t	36525
a_1	280.46061837
a_2	360.98564736629
a_3	0.000387933
a_4	38710000

B.2 Radiative properties

Table B.2: Radiative properties of several different balloon coatings [31]

Material	**IR Emissivity,** ε	**Solar Absorption,**α
Silver (polished)	0.02	0.07
Platinum	0.05	0.1
Aluminum	0.08	0.15
Nickel	0.12	0.15
Aluminum paint	0.55	0.55
White lead paint	0.95	0.25
Zinc oxide paint	0.95	0.3
Gray paint	0.95	0.75
Black paint	0.95	0.95
Lamp black	0.95	0.97
Silver sulfide	0.03	0.6
Nickel black	0.1	0.9
Cupric oxide	0.15	0.9

B.3 Gas Cylinder

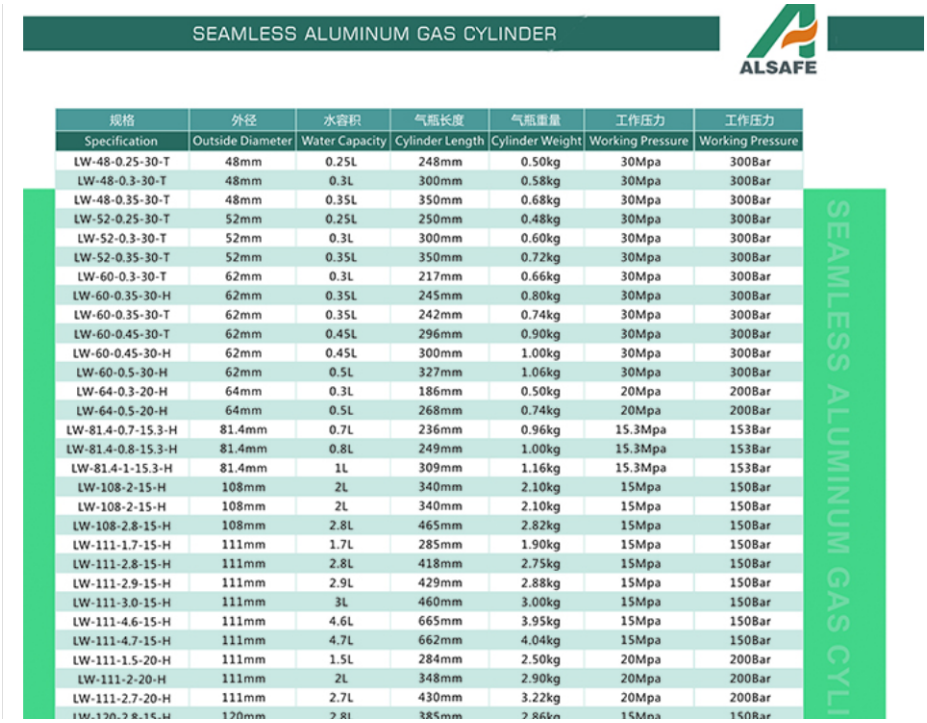

规格 Specification	外径 Outside Diameter	水容积 Water Capacity	气瓶长度 Cylinder Length	气瓶重量 Cylinder Weight	工作压力 Working Pressure	工作压力 Working Pressure
LW-48-0.25-30-T	48mm	0.25L	248mm	0.50kg	30Mpa	300Bar
LW-48-0.3-30-T	48mm	0.3L	300mm	0.58kg	30Mpa	300Bar
LW-48-0.35-30-T	48mm	0.35L	350mm	0.68kg	30Mpa	300Bar
LW-52-0.25-30-T	52mm	0.25L	250mm	0.48kg	30Mpa	300Bar
LW-52-0.3-30-T	52mm	0.3L	300mm	0.60kg	30Mpa	300Bar
LW-52-0.35-30-T	52mm	0.35L	350mm	0.72kg	30Mpa	300Bar
LW-60-0.3-30-T	62mm	0.3L	217mm	0.66kg	30Mpa	300Bar
LW-60-0.35-30-H	62mm	0.35L	245mm	0.80kg	30Mpa	300Bar
LW-60-0.35-30-T	62mm	0.35L	242mm	0.74kg	30Mpa	300Bar
LW-60-0.45-30-T	62mm	0.45L	296mm	0.90kg	30Mpa	300Bar
LW-60-0.45-30-H	62mm	0.45L	300mm	1.00kg	30Mpa	300Bar
LW-60-0.5-30-H	62mm	0.5L	327mm	1.06kg	30Mpa	300Bar
LW-64-0.3-20-H	64mm	0.3L	186mm	0.50kg	20Mpa	200Bar
LW-64-0.5-20-H	64mm	0.5L	268mm	0.74kg	20Mpa	200Bar
LW-81.4-0.7-15.3-H	81.4mm	0.7L	236mm	0.96kg	15.3Mpa	153Bar
LW-81.4-0.8-15.3-H	81.4mm	0.8L	249mm	1.00kg	15.3Mpa	153Bar
LW-81.4-1-15.3-H	81.4mm	1L	309mm	1.16kg	15.3Mpa	153Bar
LW-108-2-15-H	108mm	2L	340mm	2.10kg	15Mpa	150Bar
LW-108-2-15-H	108mm	2L	340mm	2.10kg	15Mpa	150Bar
LW-108-2.8-15-H	108mm	2.8L	465mm	2.82kg	15Mpa	150Bar
LW-111-1.7-15-H	111mm	1.7L	285mm	1.90kg	15Mpa	150Bar
LW-111-2.8-15-H	111mm	2.8L	418mm	2.75kg	15Mpa	150Bar
LW-111-2.9-15-H	111mm	2.9L	429mm	2.88kg	15Mpa	150Bar
LW-111-3.0-15-H	111mm	3L	460mm	3.00kg	15Mpa	150Bar
LW-111-4.6-15-H	111mm	4.6L	665mm	3.95kg	15Mpa	150Bar
LW-111-4.7-15-H	111mm	4.7L	662mm	4.04kg	15Mpa	150Bar
LW-111-1.5-20-H	111mm	1.5L	284mm	2.50kg	20Mpa	200Bar
LW-111-2-20-H	111mm	2L	348mm	2.90kg	20Mpa	200Bar
LW-111-2.7-20-H	111mm	2.7L	430mm	3.22kg	20Mpa	200Bar
LW-120-2.8-15-H	120mm	2.8L	385mm	2.86kg	15Mpa	150Bar

Figure B.1: Gas cylinders specifications and weights

$https://www.alibaba.com/product-detail/New-high-pressure-150bar-aluminum-5L_60741454312.html.$